On vibrational relaxations in carbon dioxide

ON VIBRATIONAL RELAXATIONS IN CARBON DIOXIDE

PROEFSCHRIFT

TER VERKRIJGING VAN DE GRAAD VAN DOCTOR IN DE TECHNISCHE WETENSCHAP AAN DE TECHNISCHE HOGESCHOOL TE EINDHOVEN, OP GEZAG VAN DE RECTOR MAGNIFICUS Dr. K. POSTHUMUS, HOOGLERAAR IN DE AFDELING DER SCHEIKUNDIGE TECHNOLOGIE, VOOR EEN COMMISSIE UIT DE SENAAT TE VERDEDIGEN OP DINSDAG 5 MAART 1963, DES NAMIDDAGS TE 4 UUR

door

WILHELMUS JACOBUS WITTEMAN

WERKTUIGKUNDIG INGENIEUR

geboren te Monster

DIT PROEFSCHRIFT IS GOEDGEKEURD DOOR DE PROMOTOR
PROF. DR. L. J. F. BROER

Aan mijn vrouw

Aan mijn ouders

The research described in this thesis was started at the Institute for Fluid Dynamics and Applied Mathematics of the University of Maryland (U.S.A.). The experiments were performed there, being supported by the United States Air Force through the Air Force Office of Scientific Research and Development Command.

My sincere thanks are due to Prof. Dr. J. M. Burgers for his valuable advice and encouragement, and to Dr. P. C. T. de Boer for stimulating discussions concerning the density measurements with the integrated Schlieren method.

The theoretical studies here described were carried out at the Philips Research Laboratories, Eindhoven, Netherlands. I feel greatly indebted to the management of the Philips Research Laboratories for affording me the opportunity to publish this work as a thesis.

CONTENTS

Summary

The vibrational excitation of carbon dioxide gas is investigated. This excitation process takes place during molecular collisions. Therefore we have studied in detail the thermal collision between two carbon dioxide molecules. A derivation of the cross-sections, obtained by means of the method of the distorted waves, and of the total number of effective collisions per unit time is presented. We find direct excitation for the bending vibration and indirect excitation for both symmetrical and asymmetrical valence vibration.

The energy-exchange process of the indirect excitations possibly occurs not only within the molecules but also among the vibrational modes of different molecules. There then exist ten possibilities of exciting the symmetrical valence vibration and eight possibilities of exciting the asymmetrical valence vibration.

From the excitation processes we arrive at the relaxation equations. The corresponding relaxation times have been calculated. For temperatures below 600 °K the calculated relaxation times for the bending vibration are less than twice the experimental values, which may be considered a fair agreement in view of the uncertainty involved in the interaction potential and in other approximations which had to be introduced into the calculations.

Experimentally, the rate at which the energy approaches thermal equilibrium in suddenly heated carbon dioxide gas has been studied by using shock waves and the integrated Schlieren method for density measurements. An optical method for the qualitative study of the density distribution behind shock waves has been developed. The method, which uses photo-electric recording, is based upon the Schlieren method originally devised by Resler and Scheibe.

The experimental results agree fairly well with the predicted direct excitation of the bending modes and the indirect excitation of the valence mode in the temperature range of 440-816 °K. The measured relaxation times for the direct excitation process range from 3.75 μ sec at 440 °K to 0.64 μ sec at 816 °K. The effect of impurities that are introduced through leakage in the tube can be considered negligible. The temperatures of the measured bending energies are slightly higher than the corresponding temperatures of the valence energies, which indicates that the time constant of the indirect excitation process is at least one order of magnitude smaller than that of the direct excitation process.

Résumé

Examen de l'excitation vibratoire du gaz d'anhydride carbonique. Le processus d'excitation se déroule au cours des collisions moléculaires. Pour cette raison, nous avons effectué une étude détaillée de la collision thermique entre deux molécules d'anhydride carbonique. Présentation d'une dérivation des sections droites, obtenue par la méthode des ondes déformées, ainsi que du nombre total de collisions effectives par temps unitaire. Nous observons une excitation directe pour la vibration de flexion et une excitation indirecte pour la vibration de valence tant symétrique qu'asymétrique.

Le processus d'échange énergétique des excitations indirectes se produit non seulement au sein des molécules mais aussi parmi les modes vibratoires de différentes molécules. Il existe alors dix possibilités d'exciter les vibrations de valence symétriques et huit possibilités d'exciter les vibrations de valence asymétriques.

A partir du processus d'excitation, nous obtenons les équations de relâchement. Les temps de relâchement correspondants ont été calculés. A des températures au dessous de 600 °K, les temps de relâchement calculés pour la vibration de flexion sont inférieures au double des valeurs expérimentales, ce qui peut être considéré comme assez conforme, étant donné les aléas du potentiel d'interaction et autres approximations qui durent être englobées dans les calculs.

Expérimentalement, la vitesse à laquelle l'énergie tend vers l'équilibre thermique dans le gaz d'anhydride carbonique subitement chauffé a été étudiée en utilisant des ondes de choc ainsi que par la méthode densimétrique intégrée de Schlieren. On a conçu une méthode optique pour l'étude qualitative de la répartition énergétique en arrière des ondes de chocs. Cette méthode, utilisant l'enregistrement photoélectrique, est basée sur le système de Schlieren, laquelle fut çoncue à l'origine par Resler et Scheibe.

Les résultats expérimentaux s'accordent assez bien avec les prévisions en matière d'excitation directe des mbdes de flexion et d'excitation indirecte du mode de valence pour des températures comprises entre 440 et 816 °K. Les temps de relachement relevés pour le processus d'excitation directe s'échelonnent de 3,75 μsec à 440 °K à 0,64 μsec à 816 °K. On peut considérer comme négligeable l'effet des impuretés introduites par les fuites dans le tube. Les températures des énergies de flexion mesurées sont légèrement supérieures aux températures correspondantes des énergies de valence. Ceci montre que la constante de temps du processus d'excitation indirecte est plus petite d'au moins un ordre de grandeur que celle du processus d'excitation indirecte.

Zusammenfassung

Es werden die Schwingungen in gasförmigem Kohlendioxyd untersucht, die durch Aufeinanderprallen der Moleküle hervorgerufen werden. Der durch Wärmebewegung verursachte Aufeinanderprall zweier Kohlendioxydmoleküle wird daher einer genaueren Untersuchung unterzogen. Die mit der Methode der verzerrten Wellen abgeleiteten Querschnitte und die Gesamtzahl der tatsächlichen Zusammenstöße je Zeiteinheit werden mathematisch abgeleitet. Es werden Biegeschwingungen direkt und symmetrische und asymmetrische Valenzschwingungen indirekt hervorgerufen.

Bei der indirekten Schwingungserregung kommt es möglicherweise nicht nur zwischen den Molekülen, sondern auch zwischen den Schwingungsarten der verschiedenen Moleküle zu einem Energieaustausch. Es gibt dann zehn Möglichkeiten für die Erzeugung von symmetrischen Valenzschwingungen und acht für die Erzeugung von asymmetrischen Valenzschwingungen.

Aus den Schwingungsvorgängen werden die Gleichungen für das Abklingen gefunden. Die entsprechenden Relaxationszeiten werden errechnet. Bei Temperaturen unter 600 °K sind die errechneten Relaxationszeiten für die Biegeschwingungen kleiner als die zweifachen Versuchswerte, was wegen der Unbestimmtheit des Wechselwirkungspotentials und anderer in den Berechnungen eingeführter Näherungen als ziemlich gute Übereinstimmung betrachtet werden kann.

Mit Stoßwellen und der integrierten Schlierenmethode für Dichtemessungen wurde experimentell untersucht, wie schnell sich die Energie in plötzlich erhitztem Kohlendioxydgas dem Wärmegleichgewicht nähert.

Es wurde eine optische Methode zur qualitativen Untersuchung der hinter Stoßwellen auftretenden Dichteverteilung entwickelt. Das auf einer photoelektrische Aufzeichnung fußende Verfahren beruht auf der Schlierenmethode, die ursprünglich von Resler und Scheibe erdacht wurde.

Die Versuchswerte stimmen sowohl mit den vorausgesagten direkten Biegeschwingungen als auch mit den indirekten Valenzschwingungen im Temperaturbereich von 440-816 °K ziemlich gut überein. Die gemessenen Relaxationszeiten liegen bei der direkten Schwingung zwischen 3,75 μs bei 440 °K und 0,64 μs bei 816 °K. Die Wirkung der durch Undichtheit der Röhre hervorgerufenen Verunreinigung kann vernachlässigt werden. Die Temperaturen für die gemessenen Biegeschwingungsenergien liegen etwas höher als die entsprechenden Temperaturen für die Valenzschwingungsenergien. Dies zeigt, daß die Zeitkonstante für die indirekte Schwingungserregung zumindest um eine Größenordnung kleiner ist als die Zeitkonstante für die direkte.

CHAPTER 1

INTRODUCTORY REMARKS

1.1. What does vibrational relaxation mean?

Relaxation phenomena are found in many types of physical processes, e.g. in dielectric polarization, in paramagnetism and in molecular rotation and vibration. These processes are generally characterized by the change of a physical quantity, followed by a slower process of equilibration of other quantities. The relaxation time is a characteristic time of such a process, so that it gives an indication of the time in which essentially stationary conditions will be reached after the initiation of a particular change of a physical quantity. In order to get a physical understanding of the behaviour of the process one often studies the periodic changes of the variables. This can be done by varying the amplitude and frequency of an independent variable and seeing what happens to the dependent variables. In this way the relaxation phenomena do not produce anything that would not have occurred anyway in a more static process, but may prevent the production of something that would have happened in a static process. For example, if one slowly supplies energy to a gas, this energy will be distributed among all its degrees of freedom. However, if this is done at a sufficiently high frequency there is no time to transfer the energy to all its degrees of freedom. The energy will then only be found in the translational degrees of freedom. This result is well known in sound absorption and dispersion techniques.

Normally, during these periodic changes one has to deal with very small amplitudes, so that in an elementary study the relaxation process can be described approximately by a linear differential equation in which only the first and zero order terms are present. Fortunately, extensive theoretical analysis of the vibrational relaxation equation for diatomic gases shows that the process is fully described by this equation, irrespective of the magnitude of both amplitude and frequency.

The mechanism of vibrational relaxation can be physically understood as follows. Let us supply energy to a gas. This energy will be taken up by its translational degrees of freedom, thus giving rise to a higher temperature. At this instant the new, increased translational energy is not in equilibrium with the internal degrees of freedom. Energy must therefore flow from the translational to the internal degrees of freedom. This goes on until all degrees of freedom (translational, rotational and vibrational) are in thermal equilibrium. This process of equilibration will occur during the molecular collisions. Now, it has been shown both theoretically and experimentally that the rotational degrees of freedom adjust themselves very rapidly, as compared to the vibrational degrees of freedom, so that when studying the vibrational relaxation

we may consider both translation and rotation as external degrees of freedom having no time delay for their adjustment to energy variation. The slower process of energy exchange, by which the molecular vibrations obtain their share of the energy, is called the vibrational relaxation.

Although the theoretical treatment of this slow energy exchange process is complicated, Landau and Teller [1]) were able to show that, by assuming harmonic oscillations, the vibrational relaxation of a diatomic gas could be represented by the simple relation

$$\frac{dE}{dt} = \frac{1}{\tau}\{E(T) - E\},$$

where τ is a time constant, usually called the relaxation time, E is the momentary value of the vibrational energy, and $E(T)$ the value it would have in equilibrium with the external degrees of freedom. We see that the rate of restoring the energy balance for the internal motion is proportional to the extent of the imbalance.

The theory of vibrational relaxation is also very important for understanding the molecular background of the so-called bulk viscosity. It is well known that in many cases the motion of a mass element of a polyatomic gas cannot be completely described by the Navier-Stokes equations that assume that shear viscosity stress is due to shear flow along the considered element. This problem arises especially in motion with strong density variations per unit time, such as the Kantrowitz effect, and also in the acoustical studies of sound absorption and dispersion. Tisza [2]) has pointed out that in order to understand the absorption and dispersion phenomena of polyatomic gases it is desirable to introduce also a scalar viscosity called bulk viscosity, proportional to the time differential of the density. Since in the hydrodynamic equation there is no physical distinction between the stresses due to the pressure and to the bulk viscosity it is clear that one can replace pressure and bulk viscosity by one term called the effective pressure, which is smaller than the pressure found by neglecting the bulk viscosity. It has been shown by Broer [3]) that this decrease of the pressure can be fully described by the irreversible process of vibrational relaxation.

1.2. Historical development of the slow-collision problem

The problem of vibrational excitation by means of inelastic molecular collisions has been studied by some authors in connexion with the structure, temperature and density dependence of the vibrational relaxation. The main difficulty in this study of inelastic collisions is how to obtain a solution of the problem concerning the relative motion of two colliding molecules. It is not so much the approximate solution of the Schrödinger wave equation, but rather the restricted knowledge of the shape of the curve for the interaction potential of two molecules that makes the calculations inaccurate. The transition pro-

bability turns out to be very sensitive to small changes in the steepness of the interaction potential.

The Born approximation in the treatment of systems involving a time-dependent perturbation has been successfully applied to the study of high velocity collisions such as electron scattering. Similar success has not attended the study of slow molecular collisions. The Born approximation considers the incident and outgoing waves as simple plane waves and does not take into account the distortion of the waves at the point of closest approach, where transitions are most effective. At this point the Born approximation breaks down.

Zener [4]) successfully treated the relative motion of the centre of mass of two molecules by describing this motion approximately with classical equations. He found that energy exchange in a slow collision depended in a relatively simple manner on three factors: the magnitude of the change in total energy; the matrix elements with respect to the internal and final states of the interaction energy at the closest distance of approach; and the duration of the collision. He found that collisions were quite effective in the transfer of rotational energy and ineffective in the transfer of vibrational energy.

Landau and Teller [1]) tried to approach the problem of excitation by using Ehrenfest's adiabatic principle. This principle states that if initially a periodic motion of a system is in a certain quantum state and if the external conditions, e.g. the strength of the external force, are changed very slowly, so that the relative change of the external condition is small compared with the motion of the system, the system must remain in an allowed quantum state under the new conditions, just as if the new conditions has persisted for a long time. In particular, if the external force is restored to the initial condition, the system will be in the same state as if the external conditions had not been changed. Transitions can only occur if the external conditions change rapidly during the motion of the system. If we now revert to the molecular collisions, Landau and Teller concluded that the efficiency of vibrational excitation increased with the ratio of the period of vibration to the duration of interaction. If this principle is applied also to the rotational excitation, this ratio is found to be much larger than for vibrational excitation. Consequently, the rotational excitation is much more effective. This is in accordance with experimental results [5]) showing the very small relaxation time for rotational excitation *). The work of Landau and Teller established the temperature dependence of the relaxation time.

Herzfeld and his co-workers [6–7]) took a great step forward when they showed how a qualitatively good quantum-mechanical treatment of the relative motion could be obtained in closed form. They used the one-dimensional solution

*) Herzfeld and Litovitz in their book [5]), chapter VI, pp. 236-241 give an excellent review of rotational relaxation times in gases.

obtained by Jackson and Mott [8]) in which an exponential, repulsive potential was selected for mathematical reasons. However, the calculations were always made for the collisions between an atom and a molecule and not for the collision of a molecule with another molecule, which actually happens in a relaxation process.

This relaxation process can be complicated when more vibrations, which may also be degenerated, are available for the energy exchange.

In this field the calculations for the linear CO_2-molecule are especially interesting because it happens that the energy quanta of the bending modes are approximately half the quanta of the valence mode. Therefore it is possible, during collisions, for two quanta of the bending modes to be transferred into the valence mode. This case of exact resonance has been indicated by Slawsky, Schwartz and Herzfeld [6]). But these authors did not consider the various possibilities in which the energy can be exchanged. There is the possibility that one quantum of the valence mode may be transferred in the collision not only as two quanta of one of the degenerated bending modes, but also as one quantum to each of two independent bending modes. Moreover it may happen that the energy is exchanged between the valence mode of one molecule and the bending modes of the other.

1.3. The existence of more than one relaxation time

Since carbon dioxide has three normal modes of vibration, of which the bending mode is degenerated, it has been suggested that there might be more than one relaxation process, with different relaxation times. Each vibration may be excited differently. In this connexion it is necessary to distinguish between two excitation processes different in principle: It is possible that the vibrations obtain their energy independently from translation, in which case a set of independent equations is obtained. This is called parallel excitation. The other possibility is that the vibrational energy enters the molecule via one mode and is redistributed from this mode to the others. This type of excitation is called excitation in series.

Many experiments have been performed to try to establish whether carbon dioxide has more than one relaxation time. These experiments were concerned largely with the measurements of absorption and dispersion in the ultrasonic region. However, the conclusions on the data are conflicting. Fricke [9]), Pielemeier [10]) and Vigoureux [11]) found two relaxation times, while Shields [12]), Gutowski [13]), Henderson and Klose [14]) found that the experimental results fitted the assumption of one relaxation time and one corresponding specific heat.

According to the results of chapter 3 of the present work the valence vibration is excited in series and the relaxation time is much smaller than that of the bending vibration. If this process, in which a single mode is slowly activated

by translation, followed by a rapid energy transfer to other modes, occurs in nature, the whole excitation process appears to the observer as if described by one relaxation process. Therefore, from the theoretical point of view it is rather improbable that any further information concerning the existence of more than one relaxation process can be obtained from ultrasonic results unless one is dealing with parallel excitation having widely differing relaxation times.

We shall try to obtain information experimentally by measuring the density pattern behind a shock wave. This density pattern depends on the relaxation process. Therefore, the rate at which the internal energy tends towards the achieving of equilibrium and the absolute magnitude of this energy is found as a function of the translational temperature. The result can be compared directly to the relaxation equations.

1.4. Introduction to the present work

When the motion of the molecules is not disturbed, the translational, rotational and vibrational degrees of freedom are to a good approximation independent. The thermodynamic properties of a gas can then be calculated by summing the separate contributions of these degrees of freedom. Quantum mechanically, the motion of the molecule is described by the product of wave functions associated with each degree of freedom.

Chapter 2 discusses the quantum theory of the rotation and vibration of the CO_2-molecule, which is considered to be free and not subject to intermolecular interaction. The rotation is treated as if one were dealing with a rigid rotator. Further, since the vibrational amplitudes are small we may consider all vibrations to behave in accordance with the laws of simple harmonic motion, which description is an excellent approximation of the thermal energy levels. The corresponding energy is then obtained from the Einstein formula for a harmonic oscillator.

It has been established experimentally that the energies associated with the various degrees of freedom are in thermal equilibrium. Therefore there must be some link between these degrees of freedom, otherwise it would never be possible to find such an equilibrium after distortion. It is generally accepted that the mechanism for transferring energy comes into play when the molecules are perturbed by a force field that interacts with various degrees of freedom. In other words, the molecular collisions are essential to the energy transfer process.

In chapter 3 we treat the motion of the molecules in the presence of an intermolecular force field. It is our purpose to study the molecular energy transfer from motion as a whole to internal modes of the molecules. We shall consider molecular collisions and not the simplified model of a collision between an atom and a molecule. By doing this we shall be able to derive a full set of equations of vibrational energy transfer according the various intermolecular exchange probabilities. Particular attention is given to the nature of the interaction

potential, the assumption being made that its repulsive part is built up of the sum of all repulsive potentials between atoms of different molecules. This interaction potential, which excites the vibrations, must also somehow depend on the interatomic distances in a molecule, because otherwise the exernal force could never bring about a vibration within it. For example, during the interaction the repulsive force exerted by a CO_2-molecule on the nearer O-atom of another molecule can be much greater than that exerted on the farther O-atom. The overall force on the valence bonds of the molecule then tends to compress it. The force field interacts directly with the vibration.

The quanta of translational and rotational energy are very small. This means that in effect any translational and rotational energy is accessible, so that the energy can be considered to have a classical distribution. This does not hold for the vibrational energy, where the spacing between the energy levels is large. The energy quanta of the bending mode, which has the smallest quanta, are greater than $3kT$ at room temperature and therefore cannot be treated classically. Since these energy quanta are so large the vibrational excitation is thermally accessible for only a relatively small number of molecules at room temperature. This mainly accounts for the slow process of vibrational relaxation.

Throughout chapter 3 we have used the assumptions that

a) the rotation of the molecules plays no role on the energy exchange, and
b) since we consider small gas densities, triple collisions may be neglected.

The last two chapters are devoted to the experimental part of the study. Chapter 4 deals with the shock-tube technique and a method to measure the density profile. In chapter 5 the energy profiles and relaxation times from the experimental data are given.

CHAPTER 2

ROTATION AND VIBRATION OF A FREE CO_2-MOLECULE

2.1. Introduction

The exact solution of the wave equation describing the motion of the individual atoms of a molecule (relative to the centre of mass) is a difficult problem, because molecules have as a rule a rather complex structure. However, the empirical results of molecular spectroscopy on CO_2, as obtained by Dennison [15]), show that the energy values bear a simple relationship to one another, so that the energy of the molecule can be conveniently considered to be made up of two parts, called respectively the vibrational energy and the rotational energy. This permits a simpler solution. These spectroscopic data suggest that it is possible to treat the vibration and rotation of the molecule quite separately and then to combine the results of the two calculations to represent the behaviour of the three atoms in the CO_2-molecule. The wave function of the molecule will then be the product of ψ_r, depending only on the rotational coördinates, and ψ_v which depends on the normal coördinates of the molecule.

This is equivalent to saying that we can neglect all interaction between rotational motion and vibrational motion of the molecule and that we may consider the rotational motion as that of a rigid rotator. The validity of this approximation requires two assumptions. Firstly we assume that the amplitudes of the vibrations of the atoms are, for the lower energy states, small compared with the equilibrium distance between the atoms. Secondly we assume that the force K_r between the atoms and which is induced by the rotation is small compared with the interatomic force K_v associated with the vibrations.

These two assumptions can be justified by means of the following calculations. Classically, we find the amplitude a of the ground state for the valence vibration to be given by

$$a = \left(\frac{h}{4\pi^2 \nu_1 \mu_1)}\right)^{\frac{1}{2}} = 5.8 \times 10^{-2}\ \text{Å},$$

which is very small compared with the distance of $L/2 = 1.13$ Å between the carbon and the oxygen atom. Further, we obtain from the classical values of $K_r = 2kT/L$ and $K_v = 4\pi^2 \nu_1^2\ \mu_1 a$ that

$$K_r/K_v = 8 \times 10^{-3}.$$

2.2. The normal modes of vibration

As we have mentioned, we shall employ the method of normal coördinates for treating the vibrational motion of the molecule. The linear CO_2-molecule has only two degrees of rotational freedom and hence we have $n = 3 \times 3 - 5$

or 4 vibrational degrees of freedom. The corresponding vibrational modes may be represented by the following model

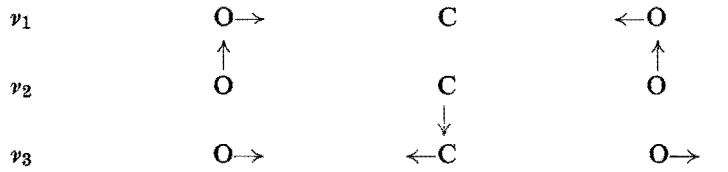

where vibration ν_1 with normal coördinates s_1 is longitudinal and symmetric (valence mode); the twofold degenerated vibration ν_2 with normal coördinates s_{21} and s_{22} describes the motion of the C-atom in a plane perpendicular to the axis of the figure; vibration ν_3 with normal coördinate s_3 is longitudinal and asymmetric. The vibrations ν_2 and ν_3 have the property in common that during the motion the distance between the O-atoms remains unchanged. In the vibration ν_1 the C-atom remains stationary.

The four vibrations are associated with three different wave numbers, which can be obtained from spectroscopic data. The corresponding frequencies are $\nu_1 = 4053 \times 10^{10}$ sec^{-1}; $\nu_2 = 2016 \times 10^{10}$ sec^{-1}; and $\nu_3 = 7189 \times 10^{10}$ sec^{-1}.

We may describe the positions of the atoms of a CO_2-molecule with a perpendicular set of Cartesian coördinates, the molecular axis being along the z-axis as indicated in fig. 1.

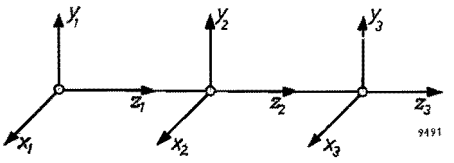

Fig. 1. Coördinates of atoms of a carbon dioxide molecule.

Let the O-atoms each have mass m and coördinates $x_1y_1z_1$ and $x_3y_3z_3$, while the C-atoms with mass M has the coördinates $x_2y_2z_2$. The kinetic energy is then given by

$$\mathbf{T} = \frac{m}{2}(\dot{x}_1^2 + \dot{y}_1^2 + \dot{z}_1^2 + \dot{x}_3^2 + \dot{y}_3^2 + \dot{z}_3^2) + \frac{M}{2}(\dot{x}_2^2 + \dot{y}_2^2 + \dot{z}_2^2). \quad (2.1a)$$

Next, we wish to express the kinetic energy of the vibrations in terms of the normal coördinates.

We find for the Cartesian coördinates

$$\dot{x}_1 = x_3 = \frac{M}{2m + M}\dot{s}_{21},$$

$$\dot{y}_1 = \dot{y}_3 = \frac{M}{2m + M}\,\dot{s}_{22},$$

$$\dot{z}_1 = \tfrac{1}{2}\,\dot{s}_1 + \frac{M}{2m + M}\,\dot{s}_3,$$

$$\dot{z}_3 = -\tfrac{1}{2}\,\dot{s}_1 + \frac{M}{2m + M}\,\dot{s}_3,$$

$$\dot{x}_2 = -\frac{2m}{2m + M}\,\dot{s}_{21},$$

$$\dot{y}_2 = -\frac{2m}{2m + M}\,\dot{s}_{22},$$

$$\dot{z}_2 = -\frac{2m}{2m + M}\,\dot{s}_3.$$

Substituting these values in the expression for **T** we find

$$T_v = \frac{\mu_1}{2}\,\dot{s}_1^2 + \frac{\mu_2}{2}\,(\dot{s}_{21}^2 + \dot{s}_{22}^2 + \dot{s}_3^2), \tag{2.1b}$$

where

$$\mu_1 = \frac{m}{2}, \quad \text{and} \quad \mu_2 = \frac{2mM}{2m + M}.$$

Having found the kinetic energy of the vibrations we may proceed to express the potential energy in terms of these four normal coördinates. The expressions for the potential energy will, to the first approximation, be of a homogeneous, quadratic form. The geometric symmetry of the molecule requires the potential to be an even function of the variables s_1, s_{21}, s_{22} and s_3. Consequently the coefficients of the cross terms vanish and we find

$$V_v = 2\pi^2\mu_1\nu_1^2 s_1^2 + 2\pi^2\mu_2\nu_2^2(s_{21}^2 + s_{22}^2) + 2\pi^2\mu_2\nu_3^2 s_3^2. \tag{2.2}$$

2.3. Wave equation

It is clear from the foregoing discussion that the approximate wave equation for the rotation and vibration of the CO_2-molecule has the form

$$(T_r + T_v + V_v)\psi_{\text{mol}} = E_{rv}\psi_{\text{mol}}, \tag{2.3}$$

where

E_{rv} is the sum total of the rotational and vibrational energies,
ψ_{mol} is the wave function describing rotation and vibration

$$T_r = -\frac{\hbar^2}{2I}\left\{\frac{1}{\sin\vartheta}\frac{\partial}{\partial\vartheta}\left(\sin\vartheta\,\frac{\partial}{\partial\vartheta}\right) + \frac{1}{\sin^2\vartheta}\,\frac{\partial^2}{\partial\varphi^2}\right\}$$

and

$$T_v = -\frac{\hbar^2}{2\mu_1}\frac{\partial^2}{\partial s_1{}^2} - \frac{\hbar^2}{2\mu_2}\left(\frac{\partial^2}{\partial s_{21}{}^2} + \frac{\partial^2}{\partial s_{22}{}^2} + \frac{\partial^2}{\partial s_3{}^2}\right).$$

I being the moment of inertia of the molecule.

We can separate this equation into two parts by expressing ψ_{mol} as the product of ψ_r, a function of φ and ϑ, and ψ_v, a function of s_1, s_{21}, s_{22} and s_3.

$$\psi_{\text{mol}} = \psi_r \psi_v \tag{2.4}$$

By substituting this in eq. (2.3) and dividing through $\psi_v\psi_r$, we find that the left-hand side of the equation consists of the sum of two parts, one depending only on the rotational coördinates and the other only on the vibrational coördinates. Each part must be equal to a constant. These two equations are

$$T_r\psi_r = E_r\psi_r \tag{2.3a}$$

and

$$(T_v + V_v)\psi_v = E_v\psi_v, \tag{2.3b}$$

where $E_{rv} = E_r + E_v$.

The rotational wave equation (2.3a) can be further separated into the coördinates φ and ϑ and then one finds the solution to be a spherical harmonic (see Schiff [16]), section 14, page 71):

$$\psi_r = \frac{1}{\sqrt{2\pi}}\, e^{im\varphi}\, N^{\frac{1}{2}}\, P_j{}^{m}(\cos\vartheta), \tag{2.5}$$

where m is a positive or negative integer or zero, j a positive integer or zero and N is given by

$$N = \frac{2j+1}{2}\frac{(j-|m|)!}{(j+|m|)!}.$$

The function $P_j{}^{m}$ is called the associated Legendre function and, for a particular value, it is $(2j+1)$—fold degenerated. The energy values of the rotation, which are determined by the eigenvalues of the equation, form a discrete set and are given by

$$E_r = \frac{\hbar^2 j(j+1)}{2I}.$$

The multiplying constants in eq. (2.5) will provide the normalization to unity over the range of the variables.

In a similar way we can further treat the vibrational wave equation by substituting in eq. (2.3b) the product of four wave functions

$$\psi_v = \psi_n(s_1)\psi_{m_1}(s_{21})\psi_{m_2}(s_{22})\psi_p(s_3), \tag{2.6}$$

where each of the factors depends only on one normal coördinate.

We then obtain four equations of the type

$$-\frac{\hbar^2}{2\mu}\frac{d^2\psi_n(s)}{ds^2} + 2\mu\pi^2\nu^2 s^2\psi_n(s) = Es\psi_n(s) \tag{2.7}$$

with the condition that

$$E_{S_1} + E_{S_{21}} + E_{S_{22}} + E_{S_3} = E_v.$$

The solution of this equation is given by Schiff [16]) (section 13, page 60). It turns out that E_S forms also a set of discrete values and is given by

$$E_S = h\nu(n + \tfrac{1}{2})$$

where n is an arbitrary positive integer or zero.

Finally we find as a result that quantum-mechanically the free motion of a CO_2-molecule (apart from the translational motion) may be described by a discrete set of eigenfunctions and energy values, so that the motion for particular energy values of rotation and vibration is given by

$$\left.\begin{aligned} \psi_{\text{mol}} &= \frac{1}{\sqrt{2\pi}} e^{im\varphi} N^{\frac{1}{2}} p_j^{\,m}(\cos\vartheta)\, \psi_n(s_1)\, \psi_{m_1}(s_{21})\, \psi_{m_2}(s_{22})\, \psi_p(s_3) \\ \text{and the energy is given by} & \\ E_{rv} &= \frac{\hbar^2 j(j+1)}{2I} + h\nu_1(n + \tfrac{1}{2}) + h\nu_2(m_1 + \tfrac{1}{2}) + h\nu_2(m_2 + \tfrac{1}{2}) \\ &\quad + h\nu_3(p + \tfrac{1}{2})\,. \end{aligned}\right\} \tag{2.8}$$

CHAPTER 3

THEORETICAL TREATMENT OF VIBRATIONAL EXCITATIONS IN CARBON DIOXIDE

3.1. Introduction

The vibrational excitations of a gas may be described by a kinetic process, which will, according to thermodynamics, finally result in thermal equilibrium between all degrees of freedom. This excitation process takes place during molecular collisions and it is basically described by each pair of colliding molecules. A more fundamental study of such a process will therefore start with a consideration in detail of the thermal collision between two molecules.

These collisions may be accompanied by rotational and vibrational transitions. As we have already seen in chapter I, the rotational excitation takes place very easily compared with vibrational excitation, so that rotational equilibrium will have been attained long before vibrational equilibrium. In this chapter we shall therefore begin with translational-rotational equilibrium and consider only those collisions in which the translational energy excites the vibrations with or without simultaneous rotational transitions. However, since rotational transition probabilities are very large compared with vibrational transition probabilities we may as well neglect the simultaneous rotational transitions and study all collisions as if there were no rotational transitions. Further, one might ask what chance there is of an energy exchange purely between rotation and vibration during collision. Because the time of a rotational cycle of the molecule is much larger than that of a vibrational period, this type of transition need not be expected from the point of view of the adiabatic principle. Thus we shall treat the vibrational excitation by considering the exchange of energy between translational and vibrational degrees of freedom.

The energy transitions can be treated in principle by solving the Schrödinger wave equation for the whole system. However, in doing this it is found convenient to describe the motion of the two colliding molecules in terms of the motion of the molecules relative to each other or to their centre of mass, of the free motion of the centre of mass of the complete system, and of the motion of the individual atoms of each molecule relative to its centre of mass. Quantum-mechanically this means that the wave equation may contain the product of the three corresponding wave functions. Now, the wave function describing the motion of the centre of mass of the complete system can be taken out; it is of no importance to our further considerations, because transitions can only be effected by the relative motion of the two molecules. The wave function for the atoms in a molecule has been derived in chapter 2. The appropriate solution of the wave function describing the relative motion of the colliding molecules will be our first aim in this treatment.

We shall start with the Schrödinger wave equation describing the relative motion of the two molecules. Then we must determine the intermolecular forces giving rise to the energy transitions. The straightforward solution of this equation is extremely laborious and almost impossible. Accordingly we have to introduce some approximations in these calculations and to find such simplifications as will preserve the essentials of the physical situation. The solution of this equation consists of three parts: the incident wave, the elastically scattered wave and the inelastically scattered wave. It turns out that the collision cross-section that can be derived from the solution of the wave equation is remarkably influenced by the overlapping between the initial and scattered wave functions. Therefore the Born approximation of taking the incoming and outgoing waves as simple plane waves is not adequate for molecular collisions. We shall employ the method of the distorted waves [17]), taking into account the distortion of the incident and outgoing waves produced by the interaction potential.

3.2. Fundamental equations

The problem is to find the probable states of the harmonic vibrations of the molecule, initially in specified states, after it has been perturbed by a time-dependent force which is initially zero and which returns to zero by the end of the collision. As we must study the result of all collisions of a molecule we prefer to use a time-independent approach in which the statistics of a succession of individual collisions are represented by a stationary wave function. This will be done by always considering the motion of the whole system of two colliding CO_2 molecules relative to its centre of mass. The configuration of the system is described with respect to a set of space-fixed axes as indicated in fig. 2. The corresponding wave function is described by, respectively, the coördinates r, θ and ϕ of the relative motion and the coördinates s_1, s_{21}, s_{22}, s_3, ϑ_1, φ_1 of the "considered" molecule, and s_1', s_{21}', s_{22}', s_3', ϑ_2, φ_2 of the colliding molecules. The wave function satisfies the wave equation

$$H\Psi = E_t\Psi, \tag{3.1}$$

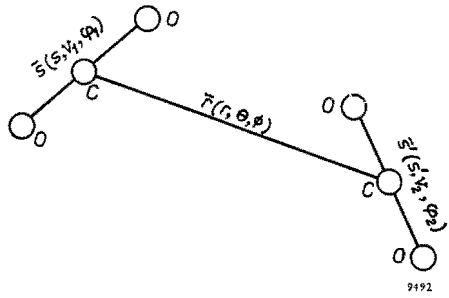

Fig. 2. Coördinates describing the relative position of two colliding molecules.

in which the Hamiltonian H is given by

$$H = -\frac{\hbar^2}{2\mu_r} \Delta_r^2 + V + T_{r1} + T_{v1} + V_{v1} + T_{r2} + T_{v2} + V_{v2}, \quad (3.1a)$$

where subscript 1 refers to the considered molecule,
subscript 2 refers to the colliding molecule, and
V is the interaction potential.

The energy E_t is the stationary total energy and equal to the sum of $\frac{\hbar^2 k^2}{2\mu_r}$ (the kinetic energy of the relative motion at infinity, where there is no interaction) and the energies $E_{r1} + E_{v1}$ and $E_{r2} + E_{v2}$ of the internal motion of the two colliding molecules:

$$E_t = \frac{\hbar^2 k^2}{2\mu_r} + E_{r1} + E_{v1} + E_{r2} + E_{v2}. \quad (3.1b)$$

Since the dependence of the internal motion of the molecules on the interaction potential is very small we shall expand the total wave function Ψ in terms of the unperturbed functions describing the internal motion and of the functions of the relative motion only, the latter being in the form of incident and reflected waves:

$$\Psi = \Sigma R_k \psi_{\text{mol}\,1} \psi_{\text{mol}\,2}, \quad (3.2)$$

where the summation is taken over all possible vibrational states of the two molecules. The asymptotic form of Ψ is given by

$$\Psi_r \underset{r\to\infty}{\rightarrow} \{e^{ik_o z} + \frac{1}{r} g_o(\theta)\, e^{ik_o r}\} \psi_{\text{mol}\,1o} \psi_{\text{mol}\,2o} + \Sigma \frac{1}{r} g_k(\theta)\, e^{ikr} \psi_{\text{mol}\,1} \psi_{\text{mol}\,2}. \quad (3.2a)$$

The subscript zero indicates the initial state of the two molecules. The first term represents the incoming particle moving along the polar axis $\theta = 0$. The second represents the elastically scattered particle that is moving radially outward. Further the summation is taken over all possible inelastically scattered waves that are moving radially outward. The factor $1/r$ provides the well-known decrease of amplitude with distance. Each term in this series contains for the two molecules the same quantum numbers j_1, m_1 and respectively j_2, m_2, because there are no rotational quantum jumps. R_k depends only on the relative motion of the centres of mass of the two molecules. The kinetic energy for this motion at infinity is obtained by using eq. (3.1b) as the difference of the total energy and the sum of vibrational and rotational energies.

Substitution of eq. (3.2) in eq. (3.1) and making use of eq. (2.3) we obtain

$$\Sigma \psi_{\text{mol}\,1} \psi_{\text{mol}\,2} \left\{\frac{\hbar^2}{2\mu_r} \Delta_r^2 + \frac{\hbar^2 k^2}{2\mu_r}\right\} R_k = \Sigma V \psi_{\text{mol}\,1} \psi_{\text{mol}\,2} R_k. \quad (3.3)$$

Before we continue solving this equation it is necessary to make some re-

marks concerning the interaction potential. It is well known that in thermal collisions the distance of closest approach is much larger than the interatomic distances inside the molecule. Moreover, the dependence of the intermolecular potential on the internal coördinates of the two molecules is assumed to be small. Therefore, the motion of the centre of mass of each molecule can be considered as subjected to the average potential field caused by each atom. This means that we can introduce for the function R_k an expansion in partial waves with spherical harmonics

$$R_k(r,\theta) = \sum_l P_l(\cos\theta)\frac{1}{r} f_{lk}(r), \tag{3.4}$$

where P_l is a Legendre polynomial of order l and which describes the angular dependence of the relative motion of the two centres of mass. Further, as we shall see in the next section, the potential function V will be the product of $V(r)$, which depends on the distance r between the two molecules, and U, which depends on the relative spherical orientation and internal coördinates of the two molecules:

$$V = V(r)U(\theta, \phi, \boldsymbol{s}, \boldsymbol{s}', \vartheta_1, \vartheta_2, \varphi_1, \varphi_2). \tag{3.5}$$

Substitution of eq. (3.4) in eq. (3.3) gives for a partial wave

$$\sum \psi_{\text{mol}\,1}\,\psi_{\text{mol}\,2}\left\{\frac{\mathrm{d}^2}{\mathrm{d}r^2} + k^2 - \frac{l(l+1)}{r^2}\right\} f_{lk} = \frac{2\mu_r}{\hbar^2} V(r)\, U \sum \psi_{\text{mol}\,1}\,\psi_{\text{mol}\,2} f_{lk}.$$

Again, the summation is taken over all possible vibrational states of two colliding molecules.

We study the excitation or de-excitation to other molecular states by multiplying both sides of this equation with the complex conjugated wave functions $\psi^*_{\text{mol}\,1n}$ and $\psi^*_{\text{mol}\,2n}$ associated with particular vibrational states of two free molecules, and then integrating over all vibrational spaces $\boldsymbol{s}$ and $\boldsymbol{s}'$ of these two free molecules. We make use of the orthogonality of the functions and obtain

$$\left\{\frac{\mathrm{d}^2}{\mathrm{d}r^2} + k^2 - \frac{l(l+1)}{r^2}\right\} f_{lk} = \frac{2\mu_r}{\hbar^2} V(r) \sum f_{lk} \int U\, \psi_{\text{mol}\,1}\,\psi_{\text{mol}\,2}\,\psi^*_{\text{mol}\,1n}\,\psi^*_{\text{mol}\,2n}\,\mathrm{d}\boldsymbol{s}\,\mathrm{d}\boldsymbol{s}'. \tag{3.6}$$

We shall find a solution of eq. (3.6) by applying the method of successive approximations. However, before we do this, it is necessary to make some remarks about the functions and the matrix elements of the right-hand side of eq. (3.6).

Let us first indicate the asymptotic form of f_{lk}. Since the conditions of the problem require one molecule to collide with the other, let us define function R_{k_0} as representing the incident and elastically scattered waves. This function

has the asymptotic form

$$R_{k_o} \underset{r\to\infty}{\rightarrow} e^{ik_o z} + \frac{1}{r} g_o(\theta)\, e^{ik_o r}$$

(see eq. (3.2a)). If we expand R_{k_o} into a series of partial waves f_{lk_o} we find their asymptotic values to be

$$f_{lk_o} \underset{r\to\infty}{\rightarrow} \frac{1}{k_o}(2l+1)\, i^l\, e^{i\delta_{lk_o}} \sin(k_o r - \tfrac{1}{2} l\pi + \delta_{lk_o}) \tag{3.4a}$$

(cf. appendix I).

Further, an inelastically scattered wave has the asymptotic form

$$R_k = \frac{1}{r} e^{ikr}\, g_k(\theta)\,. \tag{3.4b}$$

Consequently the partial waves f_{lk} of R_k have the same radial dependence.

Since the vibrational transition probabilities are very small, it is clear that the absolute value of the partial wave f_{lk} is also very small compared with that of f_{lk_o}. This means that by using the zero and first order approximations, we can put

$$f_{lk}^{(0)} = f_{lk_o}$$

and

$$f_{lk}^{(1)} = f_{lk}\,.$$

Next, it can be confirmed that the off-diagonal matrix elements in eq. (3.6) are small compared with the diagonal ones. The result is that we find the zero order approximation by neglecting the off-diagonal matrix elements, and we obtain for the elastic partial wave the equation

$$\left\{\frac{\mathrm{d}^2}{\mathrm{d}r^2} + k^2 - \frac{l(l+1)}{r^2}\right\} f_{lk_o} = \frac{2\mu_r}{\hbar^2} V(r) f_{lk_o} \int U\, \psi_{\mathrm{mol}\,1o}\, \psi_{\mathrm{mol}\,2o}\, \psi^*_{\mathrm{mol}\,1o}\, \psi^*_{\mathrm{mol}\,2o}\, \mathrm{d}s\, \mathrm{d}s'\,, \tag{3.6a}$$

where the subscript zero indicates the initial state of the vibrations of the molecules. The first approximation to f_{lk} is obtained by putting the zero approximation for f_{lk_o} in the right-hand side and neglecting other off-diagonal terms. Then we find for a particular inelastic wave

$$\left\{\frac{\mathrm{d}^2}{\mathrm{d}r^2} + k^2 - \frac{l(l+1)}{r^2}\right\} f_{lk} = \frac{2\mu_r}{\hbar^2} V(r) f_{lk_o} \int U\, \psi_{\mathrm{mol}\,1o}\, \psi_{\mathrm{mol}\,2o}\, \psi^*_{\mathrm{mol}\,1n}\, \psi^*_{\mathrm{mol}\,2n}\, \mathrm{d}s\mathrm{d}s' + \frac{2\mu_r}{\hbar^2} V(r) f_{lk} \int U\, \psi_{\mathrm{mol}\,1n}\, \psi_{\mathrm{mol}\,2n}\, \psi^*_{\mathrm{mol}\,1n}\, \psi^*_{\mathrm{mol}\,2n}\, \mathrm{d}s\mathrm{d}s'. \tag{3.6b}$$

The calculations of the symmetrical matrix elements on the right-hand side of eqs. (3.6a) and (3.6b) are straightforward. We substitute for ψ_{mol} the expression (2.8) and integrate over all spaces of the vibrational modes. As we shall see later, this integration gives for all modes unity, (except for the constant factor in the potential U). Furthermore, since the corresponding spherical harmonics in the diagonal matrix elements of eqs. (3.6a) and (3.6b) are identical, the result will for both elements be equal to M_σ. Going back to eqs. (3.6a) and (3.6b) we find as a result the following two fundamental equations

$$\left\{\frac{\mathrm{d}^2}{\mathrm{d}r^2} + k_o^2 - \frac{l(l+1)}{r^2} - \frac{2\mu_r}{\hbar^2} M_\sigma V(r)\right\} f_{lk_o} = 0 \tag{3.7a}$$

and

$$\left\{\frac{\mathrm{d}^2}{\mathrm{d}r^2} + k^2 - \frac{l(l+1)}{r^2} - \frac{2\mu_r}{\hbar^2} M_\sigma V(r)\right\} f_{lk} = \frac{2\mu_r}{\hbar^2} M_\alpha V(r) f_{lk_\delta}, \tag{3.7b}$$

where

$$M_\sigma = \int U \psi_{\mathrm{mol}\,1o} \psi_{\mathrm{mol}\,2o} \psi^*_{\mathrm{mol}\,1o} \psi^*_{\mathrm{mol}\,2o} \,\mathrm{d}s\,\mathrm{d}s' \tag{3.8a}$$

and

$$M_\alpha = \int U \psi_{\mathrm{mol}\,1o} \psi_{\mathrm{mol}\,2o} \psi^*_{\mathrm{mol}\,1n} \psi^*_{\mathrm{mol}\,2n} \,\mathrm{d}s\,\mathrm{d}s'. \tag{3.8b}$$

3.3. The interaction potential

So far we did not consider in detail the interaction potential which is the origin of the collisions and of the energy transfer. The calculation of the interaction forces and potential is a difficult problem, since we know very little of the complex molecular structure. It has not been possible to make a theoretical determination of these forces. Therefore one has tried to overcome, with success, these difficulties by deriving a semi-empirical formula such as the Lennard-Jones expression

$$V = 4\,\varepsilon_0 \left\{\left(\frac{r_0}{r}\right)^{12} - \left(\frac{r_0}{r}\right)^{6}\right\} = V' + V'', \tag{3.9a}$$

which describes the average potential between two molecules. It contains a repulsive part V' and a attractive part V''.

As a starting point one assumes spherical symmetry of the molecules. The sixth-power term represents the attraction of the molecules at larger distances. It is the so-called Van der Waals force, which has a long-range action. The twelfth-power term represents the short-range repulsive potential. The corresponding strong repulsive force at very small distances arises from the overlapping of the electron clouds of the two molecules. By using this expression one finds from the observed transport phenomena, such as viscosity data at various temperatures the unknown parameters. According to Hirschfelder and others [18]) these parameters, in the case of CO_2, are:

$$\frac{\varepsilon_0}{k} = 200\ ^\circ\mathrm{K} \quad \text{and} \quad r_0 = 3.95 \times 10^{-8}\ \mathrm{cm}\,.$$

Since the behaviour of the repulsive part of the Lennard-Jones potential is close to an exponential function and since the twelfth power has been chosen arbitrarily, it might just as well be possible to represent the repulsion by an exponential function such as

$$V' = V_0 \exp(-\alpha r), \tag{3.10a}$$

where V_0 and α are constants.

The advantage of this exponential potential is that it facilitates considerably the further mathematical treatment of the collision problem.

The attractive part of the potential is less important and just increases the relative speed of the incoming particle.

Fortunately it is not necessary to know the value V_0 of the potential since, as we shall see later, the transitions are independent of this quantity. Physically this can be indicated by the following argument. A strongly repulsive interaction field prevents the molecules from approaching closely; the absolute value of the wave function is therefore small in the region where the interaction is appreciable, so that the transition probability will decrease. On the other hand a strong interaction field produces a strongly repulsive force, which in turn will increase the transition probability.

According to Herzfeld [19]) the repulsive part of the Lennard-Jones potential can be treated as follows: We derive from eq. (3.9a)

$$\left(\frac{r_0}{r}\right)^6 = \tfrac{1}{2}\left[1 + \sqrt{\frac{V+\varepsilon_0}{\varepsilon_0}}\right]$$

and

$$-\frac{\mathrm{d}V}{\mathrm{d}r} = \frac{4\varepsilon_0}{r}\left\{12\left(\frac{r_0}{r}\right)^{12} - 6\left(\frac{r_0}{r}\right)^6\right\}.$$

From this

$$-\frac{r}{12}\left[1 + \sqrt{\frac{\varepsilon_0}{V+\varepsilon_0}}\right]^{-1}\frac{\mathrm{d}V}{\mathrm{d}r} = V + \varepsilon_0\,.$$

The factor $\frac{r}{12}\left[1 + \sqrt{\frac{\varepsilon_0}{V+\varepsilon_0}}\right]^{-1}$ changes but little with V in the region where collisions are effective, so that by taking this factor to be constant we have for $V+\varepsilon_0$ the differential equation for an exponential. In other words we have to use the potential

$$V = V_0\, e^{-\alpha r} - \varepsilon_0\,. \tag{3.9b}$$

The last term on the right-hand side represents the attractive part

$$V'' = -\varepsilon_0 . \tag{3.10b}$$

In order to find the unknown factor α, this potential is compared to the Lennard-Jones expression.

De Wette and Slawsky [20]) have required that the two potentials have two points in common. These points are r_o and r_c, respectively the zero point of the potential and the classical turning point for the most effective collisions. At the latter point the colliding molecule's kinetic energy at temperature T is such that the product of the area of cross-section of a collision and the Maxwell-Boltzmann factor reaches a maximum (see also eq. (3.23) below). We have

$$\varepsilon_0 = V_0 \, e^{-\alpha r_o} \tag{3.11a}$$

and

$$T_t = V_0 \, e^{-\alpha r_c} - \varepsilon_0 . \tag{3.11b}$$

Division of eq. (3.11a) by eq. (3.11b) yields

$$\frac{T_t + \varepsilon_0}{\varepsilon_0} = e^{\alpha(r_o - r_c)}$$

or

$$\alpha = \frac{1}{r_o - r_c} \log\left(\frac{T_t + \varepsilon_0}{\varepsilon_0}\right). \tag{3.12a}$$

From the Lennard-Jones expression for the potential we find the following relationship for r_c

$$\frac{r_o}{r_c} = \left\{ \tfrac{1}{2}\left(1 + \sqrt{\frac{T_t + \varepsilon_0}{\varepsilon_0}}\right) \right\}^{1/6}.$$

Substitution of this result in eq. (3.12a) yields

$$\alpha = \frac{1}{r_o}\left[\log\left(\frac{T_t + \varepsilon_0}{\varepsilon_0}\right)\right]\left[1 - \left\{ \tfrac{1}{2}\left(1 + \sqrt{\frac{T_t + \varepsilon_0}{\varepsilon_0}}\right) \right\}^{-1/6}\right]^{-1}. \tag{3.12b}$$

The values of α as a function of temperature are given in tabel I.

From this table we see that the factor α depends only slightly on the kinetic energy of the colliding particles and approaches a constant value at large energies and also at $\Delta E = 0$, the case of exact resonance. This affords the possibility of using below (section 3.6) one exponential repulsive potential with constant α in a consideration of all the kinetic energies of a Maxwell-Boltzmann distribution.

It is clear that such a semi-empirical formula, derived from a consideration of average orientations, can never be used in this form for the calculation of vibrational transitions, because vibrational excitations only arise when individual atoms are subjected to different fields of force. For this reason we want to

TABLE I

T	$\Delta E_2/k = 975°$		$\Delta E = 0$, or $k = k_o$	
	r_c [10^{-8} cm]	α [10^8 cm^{-1}]	r_c [10^{-8} cm]	α [10^8 cm^{-1}]
300	3.47	5.10	3.80	5.54
400	3.38	4.95	3.77	5.46
500	3.35	4.90	3.73	5.40
600	3.32	4.84	3.69	5.36
700	3.27	4.79	3.68	5.34
800	3.24	4.78	3.66	5.33
900	3.21	4.77	3.65	5.33
1000	3.19	4.77	3.64	5.33

obtain an expression for the potential, and without averaging over all orientations, so that the small dependence of the repulsive potential on the interatomic distances is included in this expression. In order to find this dependence in the potential function we may assume with Jackson and Howarth [21]), and with Herzfeld and Litovitz [5]) that the repulsive potential can be approximated by the sum of all interatomic repulsive potentials between the atoms of two colliding molecules. This includes the sum of the potential energy of one atom of a molecule and all atoms of the other molecule:

$$V' = \sum_{ij} V_{ij}(r_{ij}), \tag{3.13}$$

where i refers to any of the three atoms of one molecule and j to any of the atoms of the other molecule of carbon dioxide, and r_{ij} is the distance between atoms i and j. In this way the potential energy is considered to be built up of 9 terms. The next step is, in analogy with eq. (3.10a), to assume an exponential repulsive potential between such pairs of atoms, multiplied by a constant factor.

Since in thermal collisions the distance of closest approach is much larger than the interatomic distances, the atomic distance r_{ij} can be obtained quite simply by adding to r the projections of the atomic displacements in the direction of r.

The potential between two C-atoms is then

$$V_{cc} = V_{cc}^0 \exp -\alpha \{r + A_1 s_{21} \cos\beta_1 \sin\Gamma_1 + A_1 s_{22} \sin\beta_1 \sin\Gamma_1 + A_1 s_3 \cos\Gamma_1 + A_1 s_{21}' \cos\beta_2 \sin\Gamma_2 + A_1 s_{22}' \sin\beta_2 \sin\Gamma_2 + A_1 s_3' \cos\Gamma_2\}, \tag{3.13a}$$

where Γ and β describe the spherical orientation of the particle relative to the normal coördinates. Γ is the angle between the molecular axis and the vector r

of the relative motion. The potential between the C-atom of one molecule and the two O-atoms of the other molecule is

$$V_{co} = V_{co}^0 \exp -\alpha \{r + A_1 s_{21} \cos\beta_1 \sin\Gamma_1 + A_1 s_{22} \sin\beta_1 \sin\Gamma_1 + A_1 s_3 \cos\Gamma_1 \pm \frac{L}{2} \cos\Gamma_2 \pm A_2 s_1' \cos\Gamma_2 - A_3 s_{21}' \cos\beta_2 \sin\Gamma_2 - A_3 s_{22}' \sin\beta_2 \sin\Gamma_2 - A_3 s_3' \cos\Gamma_2\},$$

where L is the equilibrium distance between these two O-atoms. Since $\alpha A_2 s_1'$ is very small compared to unity it is convenient to substitute for the exponential function the first two terms of a series expansion

$$\exp(\alpha A_2 s_1' \cos\Gamma_2) = 1 + \alpha A_2 s_1' \cos\Gamma_2.$$

We then obtain

$$V_{co} = V_{co}^0 \left\{ 2\cosh\left(\frac{\alpha L \cos\Gamma_2}{2}\right) + 2\alpha A_2 s_1' \cos\Gamma_2 \sinh\left(\frac{\alpha L \cos\Gamma_2}{2}\right) \right\} \exp -\alpha \{r - A_3 s_{21}' \cos\beta_2 \sin\Gamma_2 - A_3 s_{22}' \sin\beta_2 \sin\Gamma_2 - A_3 s_3' \cos\Gamma_2 + A_1 s_{21} \cos\beta_1 \sin\Gamma_1 + A_1 s_{22} \sin\beta_1 \sin\Gamma_1 + A_1 s_3 \cos\Gamma_1\}. \quad (3.13b)$$

Similarly we can sum the four potentials between the four pairs of O-atoms in two different molecules as

$$V_{oo} = V_{oo}^0 \left\{ 2\cosh\left(\frac{\alpha L \cos\Gamma_1}{2}\right) + 2\alpha A_2 s_1 \cos\Gamma_1 \sinh\left(\frac{\alpha L \cos\Gamma_1}{2}\right) \right\} \left\{ 2\cosh\left(\frac{\alpha L \cos\Gamma_2}{2}\right) + 2\alpha A_2 s_1' \cos\Gamma_2 \sinh\left(\frac{\alpha L \cos\Gamma_2}{2}\right) \right\} \exp -\alpha \{r - A_3 s_{21} \cos\beta_1 \sin\Gamma_1 - A_3 s_{22} \sin\beta_1 \sin\Gamma_1 - A_3 s_3 \cos\Gamma_1 - A_3 s_{21}' \cos\beta_2 \sin\Gamma_2 - A_3 s_{22}' \sin\beta_2 \sin\Gamma_2 - A_3 s_3' \cos\Gamma_2\}. \quad (3.13c)$$

Finally, in analogy with eq. (3.13b), we find the potential between the two O-atoms of one molecule and the C-atom of the other one as

$$V_{co} = V_{co}^0 \left\{ 2\cosh\left(\frac{\alpha L \cos\Gamma_1}{2}\right) + 2\alpha A_2 s_1 \cos\Gamma_1 \sinh\left(\frac{\alpha L \cos\Gamma_1}{2}\right) \right\} \exp -\alpha \{r - A_3 s_{21} \cos\beta_1 \sin\Gamma_1 - A_3 s_{22} \sin\beta_1 \sin\Gamma_1 - A_3 s_3 \cos\Gamma_1 + A_1 s_{21}' \cos\beta_2 \sin\Gamma_2 + A_1 s_{22}' \sin\beta_2 \sin\Gamma_2 + A_1 s_3' \cos\Gamma_2\}. \quad (3.13d)$$

The internal-motion coefficients A_1, A_2 and A_3 are given by ratios, each of which is the ratio of the atomic vibrational amplitude to the normal coördinate of the corresponding vibration. These coefficients can be easily obtained by considering the conservation of momentum for the internal motion of the molecules. We find

$$A_1 = \frac{2m}{2m+M} = \frac{8}{11}, \qquad A_2 = \frac{m}{2m} = \frac{1}{2} \quad \text{and} \quad A_3 = \frac{M}{2m+M} = \frac{3}{11}.$$

It is clear that in our case we have to compare the sum of these nine potential terms with the Lennard-Jones potential in order to find α. This can be done as follows. The amplitudes of the vibrations for the lower energy states are very small compared with the distance of closest approach, so that the potential depends very little on these amplitudes. Therefore in our comparison with the spherically symmetric expression we neglect this dependence on the vibrational amplitudes and then find

$$V_0 = V_{cc}^0 + V_{co}^0 \left\{2\cosh\left(\frac{\alpha L\cos\Gamma_1}{2}\right) + 2\cosh\left(\frac{\alpha L\cos\Gamma_2}{2}\right)\right\} + V_{oo}^0 \left\{2\cosh\left(\frac{\alpha L\cos\Gamma_1}{2}\right)\right\}\left\{2\cosh\left(\frac{\alpha L\cos\Gamma_2}{2}\right)\right\}. \quad (3.14)$$

We may therefore conclude that the interaction potential can be suitably represented by the difference between an exponential function $V_0\exp(-\alpha r)$ and a constant ε_0. However, when substituting such a potential in the eqs. (3.7a) and (3.7b) we may as well add the constant to the kinetic energy and consider the interaction potential as a purely exponential function.

3.4. General expression for the cross-section

The following section is concerned with the mathematical treatment of equations (3.7a) and (3.7b), which we may use to obtain a solution for f_{lk}. This will be done analogously to the one-dimensional problem as treated by Jackson and Mott [8]). Let us first consider the auxiliary function F_{lk} satisfying the equation

$$\left\{\frac{\mathrm{d}^2}{\mathrm{d}r^2} + k^2 - \frac{l(l+1)}{r^2} - \frac{2\mu_r}{\hbar^2} M_\sigma\, e^{-\alpha r}\right\} F_{lk} = 0 \quad (3.15)$$

with boundary conditions $F_{lk} = 0$ for $r = 0$ and asymptotic value

$$F_{lk} \underset{r\to\infty}{\longrightarrow} \sin(kr - \tfrac{1}{2}l\pi + \delta_{lk}).$$

By comparing the asymptotic value of F_{lk_o} with that of f_{lk_δ} in eq. (3.4a) we obtain

$$f_{lk_o} = \frac{1}{k_o}(2l+1)\, i^l\, e^{i\delta_{lk_\delta}} F_{lk_\delta}.$$

Next, we substitute $f_{lk} = YF_{lk}$ in eq. (3.7b) and obtain

$$2\frac{\mathrm{d}F_{lk}}{\mathrm{d}r}\frac{\mathrm{d}Y}{\mathrm{d}r} + F_{lk}\frac{\mathrm{d}^2Y}{\mathrm{d}r^2} = \frac{2\mu_r}{\hbar^2}\exp(-\alpha r)\frac{2l+1}{k_o} i^l\, e^{i\delta_{lk_\delta}} F_{lk_o} M_\alpha.$$

Multiplying both sides by F_{lk} and integrating with respect to r between the limits 0 and r we obtain

$$F_{lk}{}^2 \frac{\mathrm{d}Y}{\mathrm{d}r} = \frac{2\mu_r}{\hbar^2} \frac{2l+1}{k_o} i^l e^{i\delta_{lk_o}} M_a \int_0^r F_{lk} F_{lk_o} \exp(-\alpha r)\, \mathrm{d}r.$$

Since we know the asymptotic value of F_{lk} we can integrate the last equation for large values of r. We then find

$$Y = \frac{1}{k}\left\{ - \cot(kr - \tfrac{1}{2} l\pi + \delta_{lk}) + \text{Const}\right\} \frac{2l+1}{k_o} i^l e^{i\delta_{lk_o}} A_{lk} M_a,$$

where we have introduced the abbreviation

$$A_{lk} = \frac{2\mu_r}{\hbar^2} \int_0^\infty F_{lk_o} F_{lk} \exp(-\alpha r)\, \mathrm{d}r. \tag{3.16}$$

With this result we find for $r \to \infty$

$$f_{lk} = \frac{1}{k}\{-\cos(kr - \tfrac{1}{2} l\pi + \delta_{lk}) + \text{Const.} \sin(kr - \tfrac{1}{2} l\pi + \delta_{lk})\} \frac{2l+1}{k_0} i^l e^{i\delta_{lk_o}} A_{lk} M_a.$$

When comparing this with the asymptotic expression (3.4b) we can find the integration constant before the sine term:

$$f_{lk} = -\exp\{i(kr - \tfrac{1}{2} l\pi + \delta_{lk})\} \frac{2l+1}{k_o k} i^l e^{i\delta_{lk_o}} A_{lk} M_a. \tag{3.17}$$

From expression (3.4b) we deduce that $\frac{1}{r^2} |g_k(\theta)|^2$ is the number of molecules per unit volume at distance r which have undergone a transition in their vibrational states during the collision. Of these, the number crossing unit area per unit time is proportional to $\frac{k}{r^2} |g_k(\theta)|^2$, whereas in the incident beam the number crossing unit area per unit time is proportional to k_o. Hence we have for the particle flux per unit angle and per unit incident flux

$$\sigma(\theta) = \frac{k}{k_o} |g_k(\theta)|^2,$$

which is called the differential cross-section.

By substituting for $g_k(\theta)$ the expression in partial waves and using the asymptotic expression of eq. (3.17) we find for the differential cross-section

$$\sigma(\theta) = \frac{1}{k_o{}^3 k} \left| M_a \sum_{l=0}^{\infty} \exp\{i(\delta_{lk} + \delta_{lk_o})\} (2l+1) P_l A_{lk} \right|^2. \tag{3.18}$$

The total inelastic cross-section σ_i is the total particle flux per unit incident

flux and therefore the integral of eq. (3.18) over the sphere with unit radius. As we shall see later, the product of the quantities M_a and A_{lk} is independent of the coördinates θ and ϕ of the relative motion. Consequently, the evaluation of the total cross-section is straightforward. Because of the orthogonality of the Legendre polynomials it contains no products of factors involving different values of l. We find

$$\sigma_i = \frac{4\pi}{k_o{}^3 k} M_a{}^2 \sum_{l=0}^{\infty} (2l+1)\, A_{lk}{}^2 . \tag{3.19}$$

3.5. Calculation of the values of A_{lk}

The exact solution of A_{lk} as defined by eq. (3.16) cannot be obtained except for the case of $l = 0$. On account of the relatively slow variation in the quasi-potential energy of the centrifugal force compared with the exponential form, this potential will not produce any transition. The centrifugal potential will only slow down the relative motion, so that according to Schwartz et al. [7]) we can calculate A_{lk} by substituting in eq. (3.15)

$$k_e{}^2 = k^2 - \frac{l(l+1)}{r_c{}^2} . \tag{3.20}$$

Here we take the centrifugal potential to be a constant, its largest value being at the classical turning point $r = r_c$. This means that it is sufficient to consider A_{ok} and then find A_{lk} for any value of l by substituting in the result for $l = 0$ the effective collision velocity k_e, in analogy with eq. (3.20).

The calculation of A_{ok} is similar to the one-dimensional problem and has been carried out by Jackson and Mott [8]). If we substitute

$$z = \frac{2}{\alpha} \left\{ \frac{2\mu_r}{\hbar^2} M_\sigma \right\}^{1/2} \exp\left(-\tfrac{1}{2}\alpha r\right)$$

in eq. (3.15) and take $l = 0$, we obtain the equation

$$\frac{\mathrm{d}^2 F}{\mathrm{d}z^2} + \frac{1}{z}\frac{\mathrm{d}F}{\mathrm{d}z} + \left(\frac{q^2}{z^2} - 1\right) F = 0 ,$$

where $q = \dfrac{2k}{\alpha}$. F is a Bessel function of order iq and argument iz. The solution of this equation turns out to be a modified Bessel function of the second kind

$$K_{iq}(z) = \int_0^\infty e^{-z\cosh u} \cos q\, u \, \mathrm{d}u . \tag{3.21}$$

We now have to show that this solution satisfies the boundary conditions.

For $r = 0$ we have $z = \frac{2}{\alpha}\left\{\frac{2\mu_r}{\hbar^2} M_\sigma\right\}^{1/2}$. We may suppose that V_0 is very large, because the interaction potential goes to infinity as r approaches zero, i.e. $z \to \infty$ as $r \to 0$. But $K_{iq}(\infty)$ is zero, and this accords with the boundary condition for $r = 0$.

For $r \to \infty$, we have $z = 0$. The value of $K_{iq}(0)$ can be obtained as follows. If we substitute $v = z \cosh u$ in eq. (3.21) when $z \to 0$, we find for small values of z

$$K_{iq}(z) = \int_0^\infty e^{-v} \tfrac{1}{2}\left[\left(\frac{2v}{z}\right)^{iq} + \left(\frac{2v}{z}\right)^{-iq}\right] \frac{\mathrm{d}v}{v}.$$

From this it follows that

$$K_{iq}(z) = \tfrac{1}{2}\left(\frac{z}{2}\right)^{-iq} \Gamma(iq) + \tfrac{1}{2}\left(\frac{z}{2}\right)^{iq} \Gamma(-iq)$$

or

$$K_{iq}(z) = \tfrac{1}{2}\left[\frac{1}{\alpha}\left\{\frac{2\mu_r}{\hbar^2} M_\sigma\right\}^{1/2}\right]^{-iq} e^{ikr}\, \Gamma(iq) + \tfrac{1}{2}\left[\frac{1}{\alpha}\left\{\frac{2\mu_r}{\hbar^2} M_\sigma\right\}^{1/2}\right]^{iq} e^{-ikr}\, \Gamma(-iq).$$

Hence

$$K_{iq}(0) = \left(\frac{\pi}{q \sinh \pi q}\right)^{1/2} \cos(kr + \eta_0),$$

where η_0 is a phase shift. So we obtain

$$F_{lk} = \left(\frac{q \sinh \pi q}{\pi}\right)^{1/2} K_{iq}(z)$$

and with this

$$A_{ok} = \frac{\alpha}{2\pi} (q_o\, q \sinh \pi q_o \sinh \pi q)^{1/2} \frac{1}{M_\sigma} \int_0^\infty K_{iq_o} K_{iq}\, z\, \mathrm{d}z\,.$$

By using eq. (3.21) the integral in the equation above becomes

$$\int_0^\infty \int_0^\infty \int_0^\infty z\, e^{-z(\cosh t + \cosh u)} \cos q_o u \cos qt\, \mathrm{d}u\, \mathrm{d}t\, \mathrm{d}z\,.$$

Jackson and Mott first integrated with respect to z, substituted in the result $t + u = 2\mathrm{T}$ and $t - u = 2\mathrm{U}$, and obtained

$$\frac{1}{2} \int_0^\infty \frac{\cos(q + q_o)\mathrm{T}}{\cosh^2 \mathrm{T}}\, \mathrm{dT} \int_0^\infty \frac{\cos(q_o - q)\mathrm{U}}{\cosh^2 \mathrm{U}}\, \mathrm{dU}$$

for this triple integral.

If we integrate $e^{ipz}/\cosh^2 z$ round a closed rectangular contour $-\infty, +\infty, +\infty + \pi i, -\infty + \pi i$, which encloses $z = \frac{1}{2}\pi i$, we find

$$\int_0^\infty \frac{\cos px}{\cosh^2 x}\,\mathrm{d}x = \tfrac{1}{2}\pi p/\sinh \tfrac{1}{2}\pi p\,.$$

This result was used by Jackson and Mott in their solution for the triple integral. Thus the result is

$$A_{lk} = \frac{\pi a}{8}\frac{1}{M_\sigma}(q_e^2 - q_{oe}^2)\frac{(q_{oe}q_e \sinh \pi q_{oe} \sinh \pi q_e)^{1/2}}{\cosh \pi q_e - \cosh \pi q_{oe}}, \tag{3.22}$$

where

$$q_e = \frac{2k}{a}\left\{1 - \frac{l(l+1)}{k^2 r_c^2}\right\}^{1/2}$$

and

$$q_{oe} = \frac{2k_o}{a}\left\{1 - \frac{l(l+1)}{k_o^2 r_c^2}\right\}^{1/2}.$$

3.6. Total effective collisions per unit time

We notice that translation for our purpose can be considered as an external degree of freedom and we therefore assume that the velocities of the molecules are distributed according to the Maxwell-Boltzmann distribution law. The number of molecules per unit volume with velocities in the given ranges $\mathrm{d}v_x$, $\mathrm{d}v_y$, $\mathrm{d}v_z$ is then given by

$$\mathrm{d}N_v = N_o\left(\frac{m}{2\pi kT}\right)^{3/2} e^{-\overline{m}(v_x^2+v_y^2+v_z^2)/2kT}\,\mathrm{d}v_x\,\mathrm{d}v_y\,\mathrm{d}v_z\,,$$

where N_0 is the total number of molecules per unit volume and $\overline{m}$ is the mass of one molecule. We are interested in the collisions of the molecules with each other. Therefore instead of dealing with all the molecules separately we consider each time the relative motion of all molecules to one given molecule. The energy of the relative motion of the two colliding molecules is equal to $\frac{1}{2}\mu_r v_r^2$ where $\mu_r = \frac{1}{2}\overline{m}$ is their reduced mass and v_r their relative velocity. Hence the distribution of the gas molecules over the relative velocities can be obtained quite simply by replacing $\overline{m}$ by μ_r.

We can express this with spherical coördinates and then obtain, for the number of molecules per unit volume whose velocities relative to the given molecule lie between v_r and $v_r + \mathrm{d}v_r$, the expression

$$\mathrm{d}N_{v_r} = \frac{\pi}{2}N_o\left(\frac{2\mu_r}{\pi kT}\right)^{3/2}\int_0^\infty e^{-\mu_r v_r^2/2kT}\,v_r^2\,\mathrm{d}v_r\,.$$

The total number of effective collisions, i.e. collisions bringing about a certain vibrational transition, which are suffered by one molecule per unit time is then equal to

$$Q = \frac{\pi}{2} N_o \left(\frac{2\mu_r}{\pi kT}\right)^{3/2} \int_0^\infty e^{-\mu_r v_r^2/2kT} \sigma_i v_r^3 \, dv_r , \tag{3.23}$$

where σ_i is the cross-section of the molecules producing an effective collision for a certain excitation process.

Let us first consider the collisions which activate the vibration. We can substitute $v_r = \frac{\hbar k_o}{\mu_r}$ and integrate with respect to k between the limits zero and infinity, using the condition

$$k_o^2 - k^2 = \frac{2\mu_r}{\hbar^2} \Delta E , \tag{3.24}$$

where ΔE is the energy exchanged with the vibrations. We obtain by using eqs. (3.19) and (3.22)

$$Q_a = \pi N_o \left(\frac{2\mu_r}{\pi kT}\right)^{3/2} \left(\frac{\hbar}{\mu_r}\right)^4 \frac{\pi^3}{a^3} \left(\frac{2\mu_r \Delta E}{\hbar^2}\right) \frac{M_a^2}{M_o^2} e^{-\Delta E/kT} \int_0^\infty e^{-\hbar^2 k^2/2\mu kT} \sum_{l=0}^{\infty} (2l+1) \frac{q_e \sinh \pi q_{oe} \sinh \pi q_e}{(\cosh \pi q_e - \cosh \pi q_{oe})^2} \, dk , \tag{3.25}$$

where we have put

$$\frac{q_{oe}}{k_o} = \frac{2}{a} \left\{ 1 - \frac{l(l+1)}{k_o^2 r_e^2} \right\}^{1/2} \approx \frac{2}{a} ,$$

because $\frac{l(l+1)}{k_o^2 r_e^2}$ is negligible.

The preceding integral cannot be evaluated in closed form. However, the following considerations will lead to a suitable solution. First of all we shall only consider the integration for $l = 0$ and, in accordance with Schwartz et al. [7]), we find the integral for higher values of l by assuming that the only effect of the long-range centrifugal force consists of a shift of the collision velocity.

Next, according to section 3, the kinetic energy in the expression for the cross-section contains a shift ε_0. Therefore it is convenient to shift also the exponent of the Maxwell-Boltzmann factor by the same amount, and for this we multiply the integral by exp (ε_0/kT).

The integral has a sharp maximum, since the cross-section increases with increasing k_o while the Maxwell distribution decreases with increasing k_o. The value of k_o for which the integrand reaches its maximum depends only slightly on the temperature, viz. on $T^{-1/6}$. At room temperature its maximum is

about e^{-20}. This means that in a broad temperature range we can simplify the integrand by using the first two terms of the expansion of eq. (3.24):

$$k_o \approx k + \frac{\mu_r}{k\hbar^2} \Delta E, \tag{3.24a}$$

so that we may write

$$\frac{\sinh \pi q_o \sinh \pi q}{(\cosh \pi q_o - \cosh \pi q)^2} \approx e^{-2\pi/a\,(k_o - k)}. \tag{3.26}$$

Then we obtain in the integrand the expression

$$\exp\left\{-\frac{\hbar^2 k^2}{2\mu_r kT} - \frac{2\pi}{a}(k_o - k)\right\}. \tag{3.27}$$

Thus far the integral is still too complicated. However, only molecules with velocities near the maximum will play an important role. Then it is justifiable to use the approximation of developing the exponential factor into a power series around its maximum, as was done by Landau and Teller [1]). Accordingly we find for (3.27)

$$\exp\left\{-\frac{\hbar^2 k^2}{2\mu_r kT} - \frac{2\pi}{a}(k_o - k)\right\} = \exp\{-3b^2 - 3(x-b)^2\}, \tag{3.27a}$$

where

$$b = \left\{\frac{\pi\,\mu_r\,\Delta E}{a\hbar(2\mu_r\,kT)^{1/2}}\right\}^{1/3}$$

and

$$x^2 = \frac{\hbar^2\,k^2}{2\mu kT}.$$

The dependence of the integrand on the remaining factor, namely q_e, is negligible in comparison with the dependence on the exponential function; therefore we may conveniently replace q by its value at the maximum of the integrand. The integral for $l = 0$ then becomes

$$\frac{4\mu_r kT}{a\hbar^2}\, b\, e^{-3b^2 + \epsilon_0/kT} \int_0^\infty e^{-3(x-b)^2}\, dx. \tag{3.28}$$

Further, we make the substitution $y = x - b$ in (3.28) and then use the limits $-\infty$ to $+\infty$ in the integral instead of $-b$ to $+\infty$; we thus obtain for the integral

$$\frac{4\mu_r kT}{a\hbar^2}\, b\, e^{-3b^2 + \epsilon_0/kT} \sqrt{\frac{\pi}{3}}. \tag{3.28a}$$

So far we have found the integral for $l = 0$. Now, by considering the other values of l, we notice that according to eq. (3.20) the effective collision velocity becomes smaller as l increases. This means that if we replace the exponential

Maxwell-Boltzmann factor by

$$\exp\left\{-\frac{\hbar^2}{2\mu_r kT}\left(k^2-\frac{l(l+1)}{r_c^2}\right)\right\}$$

we find also for those integrals the result given in (3.28a). Consequently, we may write the integral over all terms as

$$\frac{4\mu_r kT}{a\hbar^2} b\, e^{-3b^2+\epsilon_0/kT}\sqrt{\frac{\pi}{3}}\sum_{l=0}^{\infty}(2l+1)\, e^{-\hbar^2/2\mu_r kT\{l(l+1)/r_c^2\}}. \qquad (3.29)$$

Since the product in the exponent changes by 10^{-4} for unit change of l we can replace the summation by integration and then find for expression (3.29)

$$8\sqrt{\frac{\pi}{3}}\frac{(\mu_r kTr_c)^2}{a\hbar^4} b\, e^{-3b^2+\epsilon_0/kT}. \qquad (3.29a)$$

Finally, we find

$$Q_a = \frac{64}{3}\sqrt{6}\,\pi^3 N_o \frac{\mu_r^{3/2}(kT)^{1/2}(\Delta E)^2 r_c^2 b\, e^{-\Delta E/kT-3b^2+\epsilon_0/kT}}{\hbar^4 a^4}\frac{M_a^2}{M_o^2}. \qquad (3.25a)$$

Next, we consider the collisions which de-activate the vibrations. During these collisions there will be some energy transferred from the vibration to the relative translational motion. It will be found that the evaluation of the de-activation process is similar to that of the activation process. Since k_o is smaller than k, the integration is now with respect to k_o between the limits zero and infinity. We use the condition $k^2-k_o^2=\frac{2\mu_r}{\hbar^2}\Delta E$ and obtain analogously

$$Q_d = \frac{64}{3}\sqrt{6}\,\pi^3 N_0 \frac{\mu_r^{3/2}(kT)^{1/2}(\Delta E)^2 r_c^2 b\, e^{-3b^2+\epsilon_0/kT}}{\hbar^4 a^4}\frac{M_a^2}{M_o^2}. \qquad (3.25b)$$

If ΔE is large compared with the mean kinetic energy kT, Q_a is much smaller than Q_d; the physical explanation is that collisions which activate the vibration need more energy than those which de-activate the vibration, and are consequently rarer.

So far we have derived an expression for the effective collisions per unit time in the event of energy transfer between vibration and translation. However, the method of approximation includes the following conditions. Firstly, we have in expression (3.26) made the denominator equal to one. This is only acceptable if

$$\left\{\frac{2\pi^2\mu_r(\Delta E)^2}{\hbar^2 a^2 kT}\right\}^{1/3} > 1 \qquad \text{(1st condition)}.$$

Secondly, in order to apply the expansion in eq. (3.24a) ΔE may not be too

large, i.e.

$$\left\{\frac{2a\hbar\,(\Delta E)^{1/2}}{\pi(2\mu_r)^{1/2}\,kT}\right\}^{2/3} < 1 \qquad \text{(2nd condition).}$$

In table II the numerical values of these two conditions for the direct transfer of one energy quantum at room temperature are given.

TABLE II

	1st condition	2nd condition
bending vibration	13.3	0.49
symmetrical valence vibration	21.1	0.62
asymmetrical valence vibration	30.6	0.74

We notice that the second condition is always fulfilled at temperatures above room temperature.

Next, let us consider the case that the first condition is not satisfied. This happens in exact resonance, where we have no translational energy transfer but only transfer between the vibrational modes. The propagation vectors of incoming and outgoing particle are equal. This also applies to large translational energies, where we can neglect the difference in propagation vectors. We simplify eq. (3.25) by substituting

$$\lim_{k \to k_o} \left(\frac{2\mu_r\,\Delta E}{\hbar^2}\right)^2 \frac{\sinh \pi q_o \sinh \pi q}{(\cosh \pi q_o - \cosh \pi q)^2} = \frac{k_o^2 a^2}{\pi^2}$$

and so obtain for the effective collisions in the limit $k \to k_o$

$$Q_e = \frac{\pi^2}{2} N_o \left(\frac{2}{\alpha}\right)^2 \left(\frac{\hbar}{\mu_r}\right)^4 \left(\frac{2\mu_r}{\pi kT}\right)^{3/2} \frac{M_a^2}{M_\sigma^2} \int_0^\infty e^{-\hbar^2 k^2/2\mu_r kT} \sum_{l=0}^{\infty} (2l+1) k^3\, dk\,.$$

The integration is straightforward and the evaluation of the sum will be similar to the derivation of eq. (3.25a). We finally find

$$Q_e = 16\sqrt{2\pi}\, N_o \frac{\mu_r^{1/2}\,(kT)^{3/2}\, r_c^2\, e^{\epsilon_0/kT}}{\hbar^2\,\alpha^2} \frac{M_a^2}{M_\sigma^2}. \tag{3.30}$$

We may write for convenience

$$Q_{a,d,e} = N_o\, P_{a,d,e^2} \frac{M_a^2}{M_\sigma^2}, \tag{3.31}$$

where

$$P_a^2(\Delta E) = \frac{64}{3}\sqrt{6}\,\pi^3 \frac{\mu_r^{3/2}\,(kT)^{1/2}\,(\Delta E)^2\,r_c^2\,b}{\hbar^4\,\alpha^4}\,e^{-\Delta E/kT-\,3b^2\,+\,\epsilon_0/kT}, \qquad (3.31a)$$

$$P_d^2(\Delta E) = \frac{64}{3}\sqrt{6}\,\pi^3 \frac{\mu_r^{3/2}\,(kT)^{1/2}\,(\Delta E)^2\,r_c^2\,b}{\hbar^4\,\alpha^4}\,e^{-3b^2\,+\,\epsilon_0/kT}, \qquad (3.31b)$$

$$P_e^2\,(\Delta E = 0) = 16\,\sqrt{2\pi}\,\frac{\mu_r^{1/2}\,(kT)^{3/2}\,r_c^2}{\hbar^2\,\alpha^2}\,e^{\epsilon_0/kT}. \qquad (3.31c)$$

We can consider P^2 as the translational transition probability for the excitation of one molecule per unit time. Its values have been calculated and are given in table III as a function of temperature.

TABLE III

Translational Transition Probabilities

	$\Delta E_2/k = 975$ °K		$\Delta E_3/k = 530$ °K		$\Delta E = 0$
T	P_a^2	P_d^2	P_a^2	P_d^2	P_e^2
300	7.7×10^{-15}	2.0×10^{-13}	7.4×10^{-12}	4.3×10^{-11}	1.7×10^{-8}
400	3.3×10^{-13}	3.8×10^{-12}	7.4×10^{-11}	2.8×10^{-10}	2.2×10^{-8}
500	3.4×10^{-12}	2.4×10^{-11}	3.3×10^{-10}	9.3×10^{-10}	2.8×10^{-8}
600	1.8×10^{-11}	9.2×10^{-11}	1.1×10^{-9}	2.5×10^{-9}	3.4×10^{-8}
700	6.5×10^{-11}	2.6×10^{-10}	2.4×10^{-9}	5.1×10^{-9}	4.1×10^{-8}
800	1.9×10^{-10}	6.6×10^{-10}	4.5×10^{-9}	8.7×10^{-9}	4.9×10^{-8}
900	4.6×10^{-10}	1.4×10^{-9}	8.1×10^{-8}	1.5×10^{-8}	5.7×10^{-8}
1000	9.2×10^{-10}	2.5×10^{-9}	1.3×10^{-8}	2.2×10^{-8}	6.4×10^{-8}

In this table ΔE_2 represents the energy exchange between translational motion and bending vibration. ΔE_3 represents the energy obtained from the translational motion when there is excitation of an asymmetric vibration at the expense of a bending and a symmetric valence vibration.

The transition probabilities of the inelastic collisions are influenced remarkably by the dependence of the translational transition probabilities on ΔE, the energy exchanged with translation. It is easy to understand that the inelastic collision can hardly occur in the low-energy region. In endothermic reactions, transitions cannot take place when the initial energy is less than the quantum jump. On the other hand, from the expression obtained for the de-activation probability we see that also for the exothermic reactions the transition probabi-

lity increases with temperature. However, the result is that on balance we find the excitation rate to become higher at higher temperatures. But when the initial energy is extremely large, so that there is no appreciable difference between the wave numbers of initial and final wave, we find that the excitation process does not depend so strongly on the temperature. Physically, this can be described by the following argument: if the initial velocity is extremely large, there will be no time for the transition to take place during the collision and consequently the probability will be small. On the other hand the total number of collisions increases with temperature, so that the effective collisions may still increase with temperature.

3.7. Transition probabilities of harmonic oscillators

The transition probability for vibrational excitation depends strongly on the relative motion and the magnitude of the energy exchanged. It also depends, but much less strongly, on transitions of the vibrational states. In this section we shall only consider the transition probability as far as it depends on the vibrational states. The dependence is described by the matrix element M_a, as defined by eq. (3.8b). This expression can be evaluated for any quantum jump by using the harmonic-oscillator wave functions. The wave functions are given by Schiff [16]:

$$\psi_x(s) = \left(\frac{\xi}{\pi^{1/2}\, 2^x\, x!}\right)^{1/2} H_x(\xi s) \exp(-\tfrac{1}{2}\,\xi^2 s^2),$$

where H_x is the Hermite polynomial of order x, and

$$\xi = \left(\frac{2\pi\mu\nu}{\hbar}\right)^{1/2}.$$

The wave functions belonging to different states are orthogonal to each other. Further the Hermite polynomials have the following recurrence relations:

$$\xi s H_x = \tfrac{1}{2} H_{x+1} + x H_{x-1} \tag{3.32a}$$

and

$$(\xi s)^2 H_x = \tfrac{1}{4} H_{x+2} + \frac{2x+1}{2} H_x + x(x-1) H_{x-2}. \tag{3.32b}$$

In working out M_a it is convenient to express the exponential functions of the potential as power series in normal coördinates. Each exponential function is of the form $\exp(-a\chi s)$, where s is one of the normal coördinates and χ a function of the spherical orientation of the molecule. If we integrate over the coördinate s we obtain an expression depending on χ:

$$T_{x,x'} = \int_{-\infty}^{\infty} \psi_x \{1 - a\chi s + \frac{1}{2!}(a\chi s)^2 \ldots\} \psi_{x'}\, \mathrm{d}s\ .$$

For $x = x'$ (i.e. if no energy has been transferred to this mode) the integral turns out to be practically unity, i.e.

$$T_{x,x} = 1. \tag{3.33}$$

When there is an activation or de-activation by one quantum we can easily evaluate the integral by using the recurrence relation (3.32a) and the orthogonal property of the wave functions. We find, by neglecting higher-order terms,

$$T_{x,x+1} = -\alpha\chi \left[\frac{\hbar(x+1)}{4\pi\mu\nu}\right]^{1/2} \quad \text{(activation)} \tag{3.34a}$$

and

$$T_{x,x-1} = -\alpha\chi \left[\frac{\hbar x}{4\pi\mu\nu}\right]^{1/2} \quad \text{(de-activation).} \tag{3.34b}$$

When two quantum jumps are involved we similarly find, by using relation (3.32b) and neglecting higher-order terms,

$$T_{x,x+2} = \tfrac{1}{2}(\alpha\chi)^2 \left[\frac{\hbar^2(x+2)\,(x+1)}{16\pi^2\mu^2\nu^2}\right]^{1/2} \quad \text{(activation)} \tag{3.35a}$$

and

$$T_{x,x-2} = \tfrac{1}{2}(\alpha\chi)^2 \left[\frac{\hbar^2 x(x-1)}{16\pi^2\mu^2\nu^2}\right]^{1/2} \quad \text{(de-activation).} \tag{3.35b}$$

Although there is no restriction that only one or two jumps be possible, we can calculate that a change by more quanta in any mode during a collision is so improbably as to be negligible.

If we work out the symmetrical matrix element M_σ, eq. (3.8a), we find by using eq. (3.33) that

$$M_\sigma = V_0\, \psi_{r1}\, \psi_{r2}, \tag{3.36}$$

where V_0 is given by eq. (3.14).

3.8. Effective collisions causing the excitation of bending vibrations

The general expression for the effective collisions of the vibrational excitation has been derived in section 6 of this chapter and is given by eq. (3.31). It is clear that these effective collisions describe the role of the complex collisions in which vibrational quanta plus or minus the necessary increment of translational energy are exchanged between the colliding pair of molecules. This exchange among or with the vibrational modes is described by the asymmetrical matrix element $M\alpha$, defined by eq. (3.8b). However, before we can carry out the integration of $M\alpha$ we have to specify which type of collisions at a particular time are of importance. We always consider the case that the vibrational energy is not in equilibrium with the rotational and translational energy and that we shall reach the final equilibrium by energy transfer between translational and vibrational degrees of freedom.

Depending on the transfer process we can distinguish two possibilities. Part of the collisions produce a direct energy transfer between translation and vibration. Other collisions give rise to an energy exchange among the various modes and thus produce indirect excitation.

The energy quanta of the ν_1 and ν_3 vibrations are respectively twice and about four times as large as those of the ν_2 vibration. As was mentioned above, the translational transition probability of the cross-section for direct excitation is very sensitive to the magnitude of the energy exchange, so that by calculating the cross-sections for direct excitation of the vibrations we find that as far as they depend on translational motion the cross-sections of the ν_1 and ν_3 vibrations are many orders of magnitude smaller than the value found for the ν_2 vibration. This means that a direct excitation of the ν_1 and ν_3 vibrations is much less probable than that of the ν_2 vibration. Further, as we have seen in section 7 of this chapter, the part of the transition probabilities that depends on the vibrational state is for one quantum jump inversely proportional to the energy quantum, and inversely proportional to the square of the quantum for two quantum jumps. It is therefore found that for the ν_1 and ν_3 vibrations a direct excitation process is much less probable than an indirect excitation process.

Since there has to be an energy exchange between translation and vibration we may conclude that most of the vibrational energy by far is first fed into the bending modes. Then, when the bending vibration has been excited, there may be exchange among the vibrational modes.

In this section we shall calculate the effective collisions for the direct excitation of the bending modes. It is sufficient to consider only one of the twofold degenerated modes and to multiply the result with two in order to obtain the total energy transferred into the bending modes. Furthermore we can, of course, neglect multiple quantum jumps. During these collisions no energy is fed into the ν_1, ν_3 and degenerated ν_2 vibrations. Their quantum numbers do not change and according eq. (3.33) we substitute

$$B_{n_o,n} = 1, \qquad C_{m_{2o},m_2} = 1, \qquad D_{p_o,p} = 1,$$

where B, C and D refer to the transition probabilities of respectively the ν_1, degenerated ν_2 and ν_3 vibrations.

By using the four potential functions given in eqs. (3.13a), (3.13b), (3.13c) and (3.13d) and also eq. (3.34a), we find for activation

$$M_a(\nu_2) = -\left[A_1 V_{cc^0} + A_1 V_{co^0}\left\{2\cosh\left(\frac{\alpha L\cos\Gamma_2}{2}\right)\right\}\right.$$
$$- A_3 V_{oo^0}\left\{2\cosh\left(\frac{\alpha L\cos\Gamma_1}{2}\right)\right\}\left\{2\cosh\left(\frac{\alpha L\cos\Gamma_2}{2}\right)\right\}$$
$$\left. - A_3 V_{co^0}\left\{2\cosh\left(\frac{\alpha L\cos\Gamma_1}{2}\right)\right\}\right]\alpha\cos\beta_1\sin\Gamma_1\left[\frac{\hbar(m_{1o}+1)}{4\pi\mu_2\nu_2}\right]^{1/2}\psi_{r1}\,\psi_{r2},$$

where $M_a(v_2)$ is the asymmetric matrix element of activation for the bending mode. By using eq. (3.14) we obtain

$$M_a(v_2) = -a \cos \beta_1 \sin \Gamma_1 \, A \left[\frac{h(m_{1o}+1)}{4\pi\mu_2 v_2}\right]^{1/2} V_0 \, \psi_{r1} \, \psi_{r2}\,, \tag{3.37}$$

where A is some value between 0 and 8/11.

In the absence of any theoretical information concerning the constant potential factors we may assume that these factors, namely $V_{cc}{}^0$, $V_{co}{}^0$ and $V_{oo}{}^0$, are of the same order of magnitude. If this is true we may say that, on account of the large average argument of the hyperbolic functions, the factor A will be close to A_3. Therefore we substitute $A = {}^3/_{11}$.

So far we have found the matrix element for a particular orientation and a particular rotational state (j, m). Fortunately we do not have to consider all rotational states, since by calculating the effective collisions from eq. (3.31) we find that the rotational wave functions in eq. (3.37) for M_a and in eq. (3.36) for M_σ cancel. Therefore, we only have to consider all possible orientations (ϑ, φ) according to the Maxwell-Boltzmann distribution law. This dependence of the effective collisions will then be found in the following integral

$$\frac{1}{4\pi}\int_0^{2\pi}\int_0^{\pi} \sin^2 \Gamma_1 \sin \vartheta_1 \, \mathrm{d}\vartheta_1 \, \mathrm{d}\varphi_1\,, \tag{3.38}$$

where Γ_1 is the angle between the molecular axis and the vector r. Γ_1 can be expressed in terms of θ, ϑ_1 and φ_1 by the following equation:

$$\sin^2 \Gamma_1 = 1 - \cos^2 \theta \cos^2 \vartheta_1 - \sin^2 \theta \sin^2 \vartheta_1 \cos^2 \varphi_1 - 2 \cos \theta \cos \vartheta_1 \sin \theta \sin \vartheta_1 \cos \varphi_1\,.$$

These terms are substituted in (3.38) for the integration. The last term will then have a value of 1. The other terms give, after integration,

$$-\tfrac{1}{3}\cos^2 \theta - \sin^2 \theta \,(1-\tfrac{1}{3})\,\tfrac{1}{2} = -\tfrac{1}{3}.$$

Thus the integral describing the spherical orientation of the molecule has the value $\frac{2}{3}$.

Further, since we consider only one bending mode, $\cos \beta_1$, may have any value, so that we have to substitute for $\cos^2 \beta_1$ its average value, which is equal to $\frac{1}{2}$.

The total number of effective collisions for the excitation of the bending vibration can readily be found by substituting in the general expression for the effective collisions, eq. (3.31), the matrix element for the bending vibration as given by eq. (3.37) and the symmetrical matrix element as given by eq. (3.36). We find

$$Q_a(v_2) = \tfrac{1}{3} N_o \, C_{m_{1o},m_{1o}+1}{}^2 \, P_a{}^2 \, (\Delta E_2)\,, \tag{3.39a}$$

where

$$C_{m_{1o},m_{1o}+1}{}^2 = \alpha^2 A_3{}^2 \left[\frac{\hbar(m_{1o}+1)}{4\pi\mu_2\nu_2}\right]. \tag{3.40a}$$

Similarly, one derives the effective collisions for de-excitation of one bending mode and finds

$$Q_d(\nu_2) = \tfrac{1}{3} N_0 C_{m_{1o},m_{1o}-1}{}^2 P_d{}^2(\Delta E_2), \tag{3.39b}$$

where

$$C_{m_{1o},m_{1o}-1}{}^2 = \alpha^2 A_3{}^2 \left[\frac{\hbar m_{1o}}{4\pi\mu_2\nu_2}\right] \tag{3.40b}$$

and $\Delta E_2 = h\nu_2$ is the vibrational energy quantum of the bending mode.

3.9. Relaxation equation for the bending vibrations

The amount of energy supplied per unit time to the bending mode can be obtained by multiplying $Q_a(\nu_2) - Q_d(\nu_2)$ with the energy quantum associated with this mode. By considering all molecules in a volume we notice that there are many initial states of vibration and each state has an occupation density q. We define q_{m_1} as the number of molecules (per unit volume) in the vibrational state m_1. Further, it is sufficient to consider only one degenerated bending mode and to multiply the result with two in order to obtain the total energy transferred into the bending vibration. By applying eqs. (3.39a) and (3.39b) for all molecules per unit volume we get the following series for the rate of energy transfer E_2 of the bending vibration.

$$\frac{dE_2}{dt} = \tfrac{2}{3} h\nu_2 \{q_0 C_{0,1}{}^2 + q_1 C_{1,2}{}^2 + \ldots q_{m_1} C_{m_1,m_1+1}{}^2 + \ldots\} N_o P_a{}^2$$

$$-\tfrac{2}{3} h\nu_2 \{q_1 C_{1,0}{}^2 + q_2 C_{2,1}{}^2 + \ldots q_{m_1} C_{m_1,m_1-1}{}^2 + \ldots\} N_o P_d{}^2 - \frac{dE}{dt}, \tag{3.41a}$$

where we have neglected double or other multiple quantum jumps because their probabilities are many orders of magnitude smaller. The first part expresses activation and the second part de-activation. The last term on the right-hand side represents the exchange between ν_2 and other vibrations. This series can be simplified by using the following relationships, which are obtained from eqs. (3.40a) and (3.40b):

$$C_{m_1,m_1+1}{}^2 = (m_1 + 1) C_{0,1}{}^2 \tag{3.42a}$$

and

$$C_{m_1,m_1-1}{}^2 = m_1 C_{0,1}{}^2 . \tag{3.42b}$$

By using eqs. (3.31a) and (3.31b) we also obtain the relationship

$$P_d{}^2(\Delta E_2) = P_a{}^2(\Delta E_2)\, e^{\Delta E_2/kT}.$$

Eq. (3.41a) becomes

$$\frac{dE_2}{dt} = \tfrac{2}{3}\, h\nu_2\, N_o\, P_a{}^2\, C_{0,1}{}^2 \left\{ \sum_{m_1=0}^{\infty} (m_1+1) q_{m_1} - e^{h\nu_2/kT} \sum_{m_1=0}^{\infty} m_1\, q_{m_1} \right\} - \frac{dE}{dt}\,. \tag{3.41b}$$

Next we use the equations

$$E_2 = 2 \sum_{m_1=0}^{\infty} m_1\, h\nu_2\, q_{m_1} \quad \text{and} \quad \sum_{m_1=0}^{\infty} q_{m_1} = N_o\,.$$

We then find

$$\frac{dE_2}{dt} = \tfrac{1}{3}\, N_o\, C_{0,1}{}^2\, P_a{}^2\, (e^{h\nu_2/kT} - 1)\, \{E_2(T) - E_2\} - \frac{dE}{dt}\,, \tag{3.41c}$$

where $E_2(T) = \dfrac{2\, N_o\, h\nu_2}{\exp(h\nu_2/kT) - 1}$, in other words $E_2(T)$ is the equilibrium energy of the bending vibration for the translational temperature T, and E_2 is its actual value.

If we neglect the last term in eq. (3.41c), so that we do not consider the exchange between bending and other vibrations, it can be shown by Montroll and Schuler's [22]) theory that, if the bending vibrations are initially distributed in their energy levels according to the Maxwell-Boltzmann distribution, this distribution will persist during the excitation process, but that the effective temperature will vary monotonically until the translational temperature is achieved (see also appendix II). Although in our case there is at the same time transfer of energy from bending vibrations to valence vibrations, we notice that at low temperatures relatively little energy will be transferred in this way, so that any possible disturbance of the Maxwell-Boltzmann distribution will be so small as to be negligible. Thus at any time the bending modes have a definite vibrational temperature.

3.10. Effective collisions causing the excitation of the symmetrical valence vibration

In this section we shall consider a more complicated excitation process, namely that of the valence mode, in which we shall again neglect the very small probabilities of double or other multiple quantum jumps. We shall see that energy can be supplied in various ways to the valence vibration and each process is described by its own cross-section [23]). Whe shall find ten different probabilities for each collision in the excitation of the valence mode. In principle we can distinguish four different transfer processes. Firstly we have the possibility that a quantum is transferred by direct excitation. We obtain for this part of the energy transfer an expression for the cross-section similar to that of the bending vibration. However, it turns out that this cross-section is negligibly small. Secondly there is a possibility that the transferred quantum $h\nu_1$ is ob-

tained partly from one quantum $h\nu_2$ of one of the bending modes and the rest from the translation during a collision. But also in this combination of direct and indirect excitation processes the calculated transition probabilities are very small compared with the third and fourth types of process.

Thirdly we consider the case that the energy is only exchanged between ν_1 and ν_2 vibrations during elastic collisions. Since two bending quanta are practically equal to one valence quantum, this transfer may occur without any additional energy of translation. Then the ν_1 vibration is activated by the gaining of one quantum, while the ν_2 vibrations are de-activated by the losing of two quanta. There are of course different ways in which this exchange can take place. Therefore it is a convenient arrangement to consider now only those collisions for which the quantum number of one of the four bending modes in a colliding pair of molecules changes by two. In other words we consider the four cross-sections for the energy transfer between one valence mode and one bending mode.

The general expression for the effective collisions is given by eq. (3.31). The first step in the evaluation of this expression is to study the asymmetrical matrix element M_a, given by eq. (3.8b). During these binary collisions only the quantum numbers of the ν_1 vibration will change by one and one ν_2 vibration by two. The remaining six vibrational modes will remain unchanged and consequently the integration over the corresponding coördinates, according to eq. (3.33) yields practically unity.

Let us consider the case in which the energy is exchanged within the molecule. By using the four potential functions, eqs. (3.13a), (3.13b), (3.13c) and (3.13d), as well as eqs. (3.34a) and (3.35b) we find for M_a in the case of activation

$$M_a{}^I(\nu_1) = \left[V_{oo}{}^0 \left\{ 2 \sinh \left(\frac{aL \cos \Gamma_1}{2} \right) \right\} \left\{ 2 \cosh \left(\frac{aL \cos \Gamma_2}{2} \right) \right\} + V_{co}{}^0 \left\{ 2 \sinh \left(\frac{aL \cos \Gamma_1}{2} \right) \right\} \right] aA_2 \cos \Gamma_1 \tfrac{1}{2} (aA_3 \cos \beta_1 \sin \Gamma_1)^2 \left[\frac{\hbar(n_o+1)}{4\pi\mu_1\nu_1} \right]^{1/2} \left[\frac{h^2 m_{1o}(m_{1o}-1)}{16\pi^2 \mu_2{}^2 \nu_2{}^2} \right]^{1/2} \psi_{r1} \psi_{r2} , \tag{3.43a}$$

where $M_a{}^I(\nu_1)$ is the asymmetric matrix element of activation for the first type of process. On account of the large average argument of the hyperbolic functions we may replace $\sinh \left(\frac{aL \cos \Gamma}{2} \right)$ by $\cosh \left(\frac{aL \cos \Gamma}{2} \right)$, and assuming again that the constant potential factors are of the same order of magnitude we find

$$M_a{}^I(\nu_1) = \tfrac{1}{2} aA_2 \cos \Gamma_1 (aA_3 \cos \beta_1 \sin \Gamma_1)^2 \left[\frac{\hbar(n_o+1)}{4\pi_1\mu_1\nu_1} \right]^{1/2} \left[\frac{\hbar^2 m_{1o}(m_{1o}-1)}{16\pi^2 \mu_2{}^2 \nu_2{}^2} \right]^{1/2} V_0 \psi_{r1} \psi_{r2} . \tag{3.43b}$$

This is the matrix element for a particular orientation (Γ_1, β_1) of the considered molecule. The result will be substituted in eq. (3.31). The value for M_σ is given by eq. (3.36). Again we see that V_0 and the rotational wave functions cancel. Next, we consider the Maxwell-Boltzmann distribution for the rotational degrees of freedom. We do not have to consider the summation over the energy states, but only the integration over the rotational coördinates. This integration gives

$$\frac{1}{4\pi}\int_0^{2\pi}\int_0^{\pi} \sin^4 \Gamma_1 \cos^2 \Gamma_1 \sin \vartheta_1 \, \mathrm{d}\vartheta_1 \, \mathrm{d}\varphi_1 .$$

$\mathrm{Sin}^4 \Gamma_1 \cos^2 \Gamma_1$ can be expressed in terms of θ, ϑ_1 and φ_1. However, it is easier to transform the integration variables ϑ_1 and φ_1 by taking the direction of r as the polar axis. This gives for the integral

$$\frac{1}{4\pi}\int_0^{2\pi}\int_0^{\pi} \sin^4 \Gamma_1 \cos^2 \Gamma_1 \sin \Gamma_1 \, \mathrm{d}\Gamma_1 \, \mathrm{d}\varphi_1 = \frac{8}{105}.$$

Since $\cos \beta_1$ can have all possible values between -1 and $+1$, and as expression (3.43b) appears in the form of its square after it has been substituted in eq. (3.31), we must use the average value of $\cos^4 \beta_1$, which is $\frac{1}{5}$.

The total number of effective collisions, according to the first process, suffered by one molecule per unit time during the activation of the valence mode by one of its bending modes can be readily found by substituting in eq. (3.31) the matrix element for the valence vibration, as given by eq. (3.43b), and the symmetrical matrix element, as given by eq. (3.36). We find

$$Q_a{}^I(\nu_1) = \frac{1}{35} N_o \, B_{n_o, n_o+1}{}^2 \, C_{m_{1o}, m_{1o}-2}{}^2 \, P_e{}^2, \tag{3.44a}$$

where

$$B_{n_o, n_o+1}{}^2 = \alpha^2 \, A_2{}^2 \left[\frac{\hbar(n_o+1)}{4\pi\mu_1\nu_1}\right] \tag{3.45a}$$

and

$$C_{m_{1o}, m_{1o}-2}{}^2 = \tfrac{1}{4} \alpha^4 A_3{}^4 \left[\frac{\hbar^2 \, m_{1o}(m_{1o}-1)}{16\,\pi^2 \, \mu_2{}^2 \, \nu_2{}^2}\right]. \tag{3.46a}$$

In a similar way we can calculate the de-activation of the valence mode by one of its bending modes. We find

$$Q_d{}^I(\nu_1) = \frac{1}{35} N_o \, B_{n_o, n_o-1}{}^2 \, C_{m_{1o}, m_{1o}+2}{}^2, \tag{3.44b}$$

where

$$B_{n_o, n_o-1}{}^2 = \alpha^2 A_2{}^2 \left[\frac{\hbar n_o}{4\pi \, \mu_1 \, \nu_1}\right] \tag{3.45b}$$

and

$$C_{m_{1o},m_{1o}+2}{}^2 = \tfrac{1}{4}\,\alpha^4 A_3{}^4 \left[\frac{\hbar^2(m_{1o}+2)\,(m_{1o}+1)}{16\pi^2\,\mu_2{}^2\,\nu_2{}^2}\right]. \tag{3.46b}$$

So far we have considered the exchange with one of its bending modes of the molecule under consideration. The calculation for the other mode is of course similar, the only difference being that we now have to average over $\sin^4\beta_1$ instead of $\cos^4\beta_1$. Then we find for this type of transfer process

$$Q_a{}^{II}(v_1) = \frac{1}{35}\,N_o\,B_{n_o,n_o+1}{}^2\,C_{m_{2o},m_{2o}-2}{}^2\,P_e{}^2 \tag{3.47a}$$

and

$$Q_d{}^{II}(v_1) = \frac{1}{35}\,N_o\,B_{n_o,n_o-1}{}^2\,C_{m_{2o},m_{2o}+2}{}^2\,P_e{}^2. \tag{3.47b}$$

The following possibility in this treatment is that the two bending quanta are supplied by one bending mode of the incident molecule. Again, by using the potential functions represented by eqs. (3.13a), (3.13b), (3.13c) and (3.13d), we find for the asymmetric matrix element the following form:

$$M_a{}^{III}(v_1) = \left[V_{oo}{}^0\left\{2\sinh\left(\frac{\alpha L\cos\Gamma_1}{2}\right)\right\}\left\{2\cosh\left(\frac{\alpha L\cos\Gamma_2}{2}\right)\right\}\right.$$
$$\left. + \left(\frac{A_1}{A_3}\right)^2 V_{co}{}^0\left\{2\sinh\left(\frac{\alpha L\cos\Gamma_1}{2}\right)\right\}\right]\alpha A_2\cos\Gamma_1\,\tfrac{1}{2}\,(\alpha A_3\cos\beta_2\sin\Gamma_2)^2$$
$$\left[\frac{\hbar(n_o+1)}{4\pi\mu_1\nu_1}\right]^{1/2}\left[\frac{\hbar^2 m_1(m_1-1)}{16\,\pi^2\,\mu_2{}^2\,\nu_2{}^2}\right]^{1/2}\psi_{r1}\,\psi_{r2}\,.$$

By using the foregoing discussion this can be simplified to

$$M_a{}^{III}(v_1) = \tfrac{1}{2}\,\alpha A_2\cos\Gamma_1\,(\alpha A_3\cos\beta_2\sin\Gamma_2)^2\left[\frac{\hbar(n_o+1)}{4\pi\mu_1\nu_1}\right]^{1/2}$$
$$\left[\frac{\hbar^2 m_1(m_1-1)}{16\pi^2\mu_2{}^2\nu_2{}^2}\right]^{1/2} V_0\,\psi_{r1}\,\psi_{r2}\,.$$

We notice that the matrix element is now a function of the rotational coördinates of both molecules. Each orientation is described by its rotational degrees of freedom and distributed according the Maxwell-Boltzmann distribution law. By considering all orientations of the two colliding molecules, we have to evaluate the following two integrals.

(i) $$\frac{1}{4\pi}\int_0^{2\pi}\int_0^{\pi}\sin^4\Gamma_2\sin\vartheta_2\,\mathrm{d}\vartheta_2\,\mathrm{d}\varphi_2\,,$$

where Γ_2 is the angle between the molecular axis of the incident molecule and the vector r of the relative action. By transforming the integration variables so that we take the direction of r as the polar axis we find for the integral $\frac{8}{15}$.

(ii)
$$\frac{1}{4\pi}\int_0^{2\pi}\int_0^{\pi} \cos^2 \Gamma_1 \sin\vartheta_1 \, \mathrm{d}\vartheta_1 \, \mathrm{d}\varphi_1 = \tfrac{1}{3}\,.$$

If we substitute these values in the equation for $M_a^{III}(v_1)$ we find for the cross-section of process III

$$\sigma_a^{III}(v_1) = \frac{1}{15} B_{n_o,n_o+1}{}^2 \, C_{m_1,m_1-2}{}^2 \frac{4\pi}{k_o{}^3 k} \sum_{l=0}^{\infty} (2l+1) \frac{k_e{}^4}{a^2}\,. \qquad (3.48)$$

Since in eq. (3.48) the cross-section does not only depend on the relative motion of the incident molecule we cannot simply integrate the cross-section over all translational energies in order to find the total number of effective collisions per unit time. After all, the incident molecule can be in any vibrational state. Therefore we shall describe each incident molecule by the sum of all possible vibrational energy states and replace the matrix element $C_{m_1,m_1-2}{}^2$ by

$$\frac{\sum_{m_1=0}^{\infty} C_{m_1,m_1-2}{}^2 \, q_{m_1}}{\sum_{m_1=0}^{\infty} q_{m_1}}\,.$$

Now we can integrate the cross-section in eq. (3.48), and find, similarly to the derivation of eqs. (3.44a) and (3.44b),

$$Q_a^{III}(v_1) = \frac{1}{15} N_o P_e{}^2 B_{n_o,n_o+1}{}^2 \frac{\sum_{m_1=0}^{\infty} C_{m_1,m_1-2}{}^2 \, q_{m_1}}{\sum_{m_1=0}^{\infty} q_{m_1}} \qquad (3.49a)$$

and

$$Q_d^{III}(v_1) = \frac{1}{15} N_o P_e{}^2 B_{n_o,n_o-1}{}^2 \frac{\sum_{m_1=0}^{\infty} C_{m_1,m_1+2}{}^2 \, q_{m_1}}{\sum_{m_1=0}^{\infty} q_{m_1}}\,. \qquad (3.49b)$$

The effective collisions with the other bending mode result in

$$Q_a^{IV}(v_1) = \frac{1}{15} N_o P_e{}^2 B_{n_o,n_o+1}{}^2 \frac{\sum_{m_2=0}^{\infty} C_{m_2,m_2-2}{}^2 \, q_{m_2}}{\sum_{m_2=0}^{\infty} q_{m_2}} \qquad (3.50a)$$

and

$$Q_a{}^{IV}(v_1) = \frac{1}{15} N_o P_e{}^2 B_{n_o,n_o-1}{}^2 \frac{\sum_{m_2=0}^{\infty} C_{m_2,m_2+2}{}^2 q_{m_2}}{\sum_{m_2=0}^{\infty} q_{m_2}} . \qquad (3.50b)$$

Fourthly we have to consider the excitation process in which the valence quantum is obtained from two of the four available bending modes, each giving one quantum. This process is then described by six cross-sections. It is clear that the mutual orientation of the respective normal coördinates given by the rotational coördinates is not the same in each combination. Let us begin with the exchange within the considered molecule. Here the quantum numbers of the valence mode and the two bending modes each change by one. The remaining five modes do not change so that the integration of these modes gives unity. We find then for the asymmetric matrix element the following expression:

$$M_a{}^V(v_1) = \left[V_{oo}{}^0 \left\{ 2 \sinh\left(\frac{\alpha L \cos \Gamma_1}{2}\right) \right\} \left\{ 2 \cosh\left(\frac{\alpha L \cos \Gamma_2}{2}\right) \right\} + V_{co}{}^0 \left\{ 2 \sinh\left(\frac{\alpha L \cos \Gamma_1}{2}\right) \right\} \right] \alpha A_2 \cos \Gamma_1 (\alpha A_3 \sin \Gamma_1)^2 \cos \beta_1 \sin \beta_1 \left[\frac{\hbar(n_o+1)}{4\pi\mu_1 \nu_1}\right]^{1/2} \left[\frac{\hbar m_{1o}}{4\pi\mu_2 \nu_2}\right]^{1/2} \left[\frac{\hbar m_{2o}}{4\pi\mu_2 \nu_2}\right]^{1/2} \psi_{r1}\, \psi_{r2} .$$

Again the rotational wave functions cancel when we calculate the effective collisions, so that the further mathematical treatment of the effective collisions runs parallel to eqs. (3.44a) and (3.44b). But now in the Maxwell-Boltzmann distribution of the rotational coördinates we only have the following integral:

$$\frac{1}{4\pi} \int_0^{2\pi} \int_0^{\pi} \sin^4 \Gamma_1 \cos^2 \Gamma_1 \sin \vartheta_1 \, d\vartheta_1 \, d\varphi_1 = \frac{8}{105} .$$

We must average over $\sin^2 \beta_1 \cos^2 \beta_1$, which gives $\frac{1}{8}$ and then we find for the effective collisions

$$Q_a{}^V(v_1) = \frac{1}{105} N_o B_{n_o,n_o+1}{}^2 C_{m_{1o},m_{1o}-1}{}^2 C_{m_{2o},m_{2o}-1}{}^2 P_e{}^2 \qquad (3.51a)$$

and

$$Q_a{}^V(v_1) = \frac{1}{105} N_o B_{n_o,n_o-1}{}^2 C_{m_{1o},m_{1o}+1}{}^2 C_{m_{2o},m_{2o}+1}{}^2 P_e{}^2. \qquad (3.51b)$$

Next, we consider the possibility that the valence quantum is supplied by one bending mode of the considered molecule and by one bending mode of an incident molecule, each giving one quantum. We find for the asymmetric matrix element

$$M_a^{VI}(v_1) = \left[V_{oo}^0 \left\{ 2 \sinh\left(\frac{aL \cos \Gamma_1}{2}\right)\right\}\left\{ 2 \cosh\left(\frac{aL \cos \Gamma_2}{2}\right)\right\} \right.$$

$$\left.\left(\frac{A_1}{A_3}\right) V_{co}^0 \left\{2 \sinh\left(\frac{aL \cos \Gamma_1}{2}\right)\right\}\right] a^3 A_2 \cos \Gamma_1 A_3^2 \sin \Gamma_1 \cos \beta_1 \sin \Gamma_2 \cos \beta_2$$

$$\left[\frac{\hbar(n_o+1)}{4\pi\mu_1\nu_1}\right]^{1/2}\left[\frac{\hbar m_{1o}}{4\pi\,\mu_2\nu_2}\right]^{1/2}\left[\frac{\hbar m_1}{4\pi\,\mu_2\nu_2}\right]^{1/2} \psi_{r1}\,\psi_{r2}\,.$$

By studying all orientations in the effective collisions we find with the Maxwell-Boltzmann distributions the following two integrals for the two colliding molcules:

(i)
$$\frac{1}{4\pi}\int_0^{2\pi}\int_0^{\pi} \cos^2 \Gamma_1 \sin^2 \Gamma_1 \sin \vartheta_1 \,\mathrm{d}\vartheta_1 \,\mathrm{d}\varphi_1 = \frac{2}{15}$$

and

(ii)
$$\frac{1}{4\pi}\int_0^{2\pi}\int_0^{\pi} \sin^2 \Gamma_2 \sin \vartheta_2 \,\mathrm{d}\vartheta_2 \,\mathrm{d}\varphi_2 = \frac{2}{3}\,.$$

In the calculation of the effective collisions there are many vibrational states m_1 for the incident molecules. Therefore it is convenient to describe each incident molecule by the average state m_1 of all colliding molecules and replace $C_{m_1 m_1-1^2}$ by

$$\frac{\sum_{m_1=0}^{\infty} C_{m_1,m_1-1^2}\, q_{m_1}}{\sum_{m_1=0}^{\infty} q_{m_1}}\,.$$

In this way we then find for the effective collisions

$$Q_a^{VI}(v_1) = \frac{1}{45}\, N_o\, P_e\, B_{n_o,n_o+1^2}\, C_{m_{1o},m_{1o}-1^2}\, \frac{\sum_{m_1=0}^{\infty} C_{m_1,m_1-1^2}\, q_{m_1}}{\sum_{m_1=0}^{\infty} q_{m_1}} \qquad (3.52a)$$

and

$$Q_d^{VI}(v_1) = \frac{1}{45}\, N_o\, P_e\, B_{n_o,n_o-1^2}\, C_{m_{1o},m_{1o}+1^2}\, \frac{\sum_{m_1=0}^{\infty} C_{m_1,m_1+1^2}\, q_{m_1}}{\sum_{m_1=0}^{\infty} q_{m_1}}\,. \qquad (3.52b)$$

With these results it is now easy to write down the effective collisions for the other three combinations in which each of the two colliding molecules gives one quantum. They are

$$Q_a^{VII}(\nu_1) = \frac{1}{45} N_o P_e^2 B_{n_o,n_o+1^2} C_{m_{1\delta},m_{1\delta}-1^2} \frac{\sum_{m_2=0}^{\infty} C_{m_2,m_2-1^2} q_{m_2}}{\sum_{m_2=0}^{\infty} q_{m_2}} \quad (3.53a)$$

and

$$Q_d^{VII}(\nu_1) = \frac{1}{45} N_o P_e^2 B_{n_o,n_o-1^2} C_{m_{1\delta},m_{1\delta}+1^2} \frac{\sum_{m_2=0}^{\infty} C_{m_2,m_2+1^2} q_{m_2}}{\sum_{m_2=0}^{\infty} q_{m_2}}, \quad (3.53b)$$

$$Q_a^{VIII}(\nu_1) = \frac{1}{45} N_o P_e{}^2 B_{n_o,n_o+1^2} C_{m_{2\delta},m_{2\delta}-1^2} \frac{\sum_{m_1=0}^{\infty} C_{m_1,m_1-1^2} q_{m_1}}{\sum_{m_1=0}^{\infty} q_{m_1}} \quad (3.54a)$$

and

$$Q_d^{VIII}(\nu_1) = \frac{1}{45} N_o P_e^2 B_{n_o,n_o-1^2} C_{m_{2\delta},m_{2\delta}+1^2} \frac{\sum_{m_1=0}^{\infty} C_{m_1,m_1+1^2} q_{m_1}}{\sum_{m_1=0}^{\infty} q_{m_1}}, \quad (3.54b)$$

$$Q_a^{IX}(\nu_1) = \frac{1}{45} N_o P_e^2 B_{n_o,n_o+1^2} C_{m_{2\delta},m_{2\delta}-1^2} \frac{\sum_{m_2=0}^{\infty} C_{m_2,m_2-1^2} q_{m_2}}{\sum_{m_2=0}^{\infty} q_{m_2}} \quad (3.55a)$$

and

$$Q_d^{IX}(\nu_1) = \frac{1}{45} N_o P_e^2 B_{n_o,n_o-1^2} C_{m_{2\delta},m_{2\delta}+1^2} \frac{\sum_{m_2=0}^{\infty} C_{m_2,m_2+1^2} q_{m_2}}{\sum_{m_2=0}^{\infty} q_{m_2}}. \quad (3.55b)$$

Finally, we have the probability that the valence quantum is obtained from the two bending modes of the incident molecule, each giving one quantum. For this case the asymmetric matrix element turns out to be

$$M_a^X(\nu_1) = \left[V_{oo}{}^0 \left\{ 2 \sinh\left(\frac{\alpha L \cos \Gamma_1}{2}\right)\right\}\left\{ 2 \cosh\left(\frac{\alpha L \cos \Gamma_2}{2}\right)\right\} + \left(\frac{A_1}{A_3}\right)^2 V_{co}{}^0 \left\{ 2 \sinh\left(\frac{\alpha L \cos \Gamma_1}{2}\right)\right\}\right] \alpha A_2 \cos \Gamma_1 (\alpha A_3 \sin \Gamma_2)^2 \cos \beta_2 \sin \beta_2 \left[\frac{\hbar(n_o+1)}{4\pi\mu_1\nu_1}\right]^{1/2} \left[\frac{\hbar m_1}{4\pi\mu_2\nu_2}\right]^{1/2} \left[\frac{\hbar m_2}{4\pi\mu_2\nu_2}\right]^{1/2} \psi_{r1}\, \psi_{r2}.$$

We find for all orientations of these two colliding molecules the following two

integrals:

(i) $$\frac{1}{4\pi}\int_0^{2\pi}\int_0^{\pi}\cos^2\Gamma_1\sin\vartheta_1\,\mathrm{d}\vartheta_1\,\mathrm{d}\varphi_1=\frac{1}{3}$$

(ii) $$\frac{1}{4\pi}\int_0^{2\pi}\int_0^{\pi}\sin^4\Gamma_2\sin\vartheta_2\,\mathrm{d}\vartheta_2\,\mathrm{d}\varphi_2=\frac{8}{15}.$$

The average value of $\sin^2\beta_2\cos^2\beta_2$ is $\frac{1}{8}$. The evaluation of the effective collisions runs parallel to eqs. (3.52a) and (3.52b). We find

$$Q_a{}^X(\nu_1)=\frac{1}{45}N_o P_e{}^2 B_{n_o,n_o+1}{}^2\,\frac{\sum_{m_1=0}^{\infty}C_{m_1,m_1-1}{}^2 q_{m_1}}{\sum_{m_1=0}^{\infty}q_{m_1}}\,\frac{\sum_{m_2=0}^{\infty}C_{m_2,m_2-1}{}^2 q_{m_2}}{\sum_{m_2=0}^{\infty}q_{m_2}}$$

and (3.56a)

$$Q_d{}^X(\nu_1)=\frac{1}{45}N_o P_e{}^2 B_{n_o,n_o-1}{}^2\,\frac{\sum_{m_1=0}^{\infty}C_{m_1,m_1+1}{}^2 q_{m_1}}{\sum_{m_1=0}^{\infty}q_{m_1}}\,\frac{\sum_{m_2=0}^{\infty}C_{m_2,m_2+1}{}^2 q_{m_2}}{\sum_{m_2=0}^{\infty}q_{m_2}}.$$

(3.56b)

3.11. Relaxation equation for the symmetrical valence vibration

In the preceding section we have studied the various ways in which the valence mode of a considered molecule can be activated or de-activated. As we have seen it turns out that there are ten different probabilities. The probability of an effective collision is very small, so that we can take the sum of these ten probabilities for calculating the effectiveness of a collision. From these probabilities we find the corresponding effective collisions per unit time. If we now multiply the difference between the activating and de-activating collisions by the energy quantum we find the amount of excitation energy supplied per unit time to the valence mode of one molecule. By considering the sum of all molecules we shall find the relaxation equation for this excitation process.

However, mathematically it is found more convenient to treat the different excitation processes separately, so that we find each time the amount of energy supplied per unit time to the valence mode of all molecules. Then, by taking the sum of these results, we shall finally have the total rate of energy transferred into the valence modes of all molecules. Let us start with the sum of all molecules excited in accordance with process I of section 10 of this chapter. We get

$$\frac{\mathrm{d}E_1{}^I}{\mathrm{d}t}=\frac{1}{35}N_o P_e{}^2 h\nu_1\Big\{B_{0,1}{}^2 C_{2,0}{}^2 q_{02}+B_{0,1}{}^2 C_{3,1}{}^2 q_{03}+\ldots B_{0,1}{}^2 C_{m_1,m_1-2}{}^2 q_{0m_1}$$

$$+B_{1,2}{}^2\sum_{m_1=2}^{\infty}C_{m_1,m_1-2}{}^2 q_{1m_1}+\ldots-\sum_{n=1}^{\infty}\sum_{m_1=0}^{\infty}B_{n,n-1}{}^2 C_{m_1,m_1+2}{}^2 q_{nm_1}\Big\}. \quad (3.57a)$$

where q_{nm_1} is the number of molecules per unit volume with the vibration v_1 in state n and the vibration v_2 in state m_1.

This series can be simplified by using the following relationships, obtained from eqs. (3.45a). (3.45b), (3.46a) and (3.46b):

$$B_{n,n+1}{}^2 = (n+1)B_{0,1}{}^2 \ , \tag{3.58a}$$

$$B_{n,n-1}{}^2 = nB_{0,1}{}^2 \ , \tag{3.58b}$$

$$C_{m_1,m_1+2}{}^2 = \tfrac{1}{2}(m_1+2)\,(m_1+1)C_{0,2}{}^2 \ , \tag{3.59a}$$

$$C_{m_1,m_1-2}{}^2 = \tfrac{1}{2}\,m_1(m_1-1)\,C_{0,2}{}^2 \ . \tag{3.59b}$$

We obtain

$$\frac{\mathrm{d}E_1{}^I}{\mathrm{d}t} = \frac{1}{35}\,N_o\,P_e{}^2\,B_{0,1}{}^2\,C_{0,2}{}^2\,h\nu_1 \left\{ \sum_{n=0}^{\infty}\sum_{m_1=0}^{\infty} \tfrac{1}{2}\,(m_1{}^2 - 4nm_1 - 2n - m_1)\,q_{nm_1} \right\}. \tag{3.57b}$$

Since the molecules are at any time distributed according to the Maxwell-Boltzmann distribution law (cf. appendix II), we write

$$q_{nm_1m_2p} = \frac{N_o \exp\{-(n+\tfrac{1}{2})h\nu_1/\mathrm{k}T_1 - (m_1+\tfrac{1}{2})h\nu_2/\mathrm{k}T_2 - (m_2+\tfrac{1}{2})h\nu_2/\mathrm{k}T_2 - (p+\tfrac{1}{2})h\nu_3/\mathrm{k}T_3\}}{\sum_{n=0}^{\infty}\sum_{m_1=0}^{\infty}\sum_{m_2=0}^{\infty}\sum_{p=0}^{\infty} \exp\{-(n+1)h\nu_1/\mathrm{k}T_1 - (m_1+\tfrac{1}{2})h\nu_2/\mathrm{k}T_2 - (m_2+\tfrac{1}{2})h\nu_2/\mathrm{k}T_2 - (p+\tfrac{1}{2})h\nu_3/\mathrm{k}T_3\}}. \tag{3.60}$$

This is the number of molecules per unit volume with the vibration v_1 in state n, the vibration v_2 in states m_1 and m_2, and the vibration v_3 in state p. With the aid of this expression we derive

$$\sum_{n=0}^{\infty}\sum_{m_1=0}^{\infty} m_1{}^2\,q_{nm_1} = N_o \frac{\sum_{m_1=0}^{\infty} m_1{}^2 \exp\left(-\dfrac{m_1h\nu_2}{\mathrm{k}T_2}\right)}{\sum_{m_1=0}^{\infty} \exp\left(-\dfrac{m_1h\nu_2}{\mathrm{k}T_2}\right)} \ . \tag{3.61}$$

If we use the following abbreviation:

$$S = \sum_{m_1=0}^{\infty} \exp\left(-\frac{m_1h\nu_2}{\mathrm{k}T_2}\right) = \frac{1}{1-\exp\,(-h\nu_2/\mathrm{k}T_2)},$$

eq. (3.61) becomes

$$\sum_{n=0}^{\infty}\sum_{m_1=0}^{\infty} m_1{}^2\,q_{nm_1} = N_o \left(\frac{\mathrm{k}T_2}{h}\right)^2 \frac{\mathrm{d}^2S/\mathrm{d}\nu_2{}^2}{S} = \frac{1+\exp\,(h\nu_2/\mathrm{k}T_2)}{\{\exp\,(h\nu_2/\mathrm{k}T_2)-1\}^2}\,N_o. \tag{3.62a}$$

We derive similarly

$$\sum_{n=0}^{\infty}\sum_{m_1=0}^{\infty} -4nm_1 q_{nm_1} = \frac{-4N_o}{\{\exp(h\nu_2/kT_2)-1\}\{\exp(h\nu_1/kT_1)-1\}}, \quad (3.62b)$$

$$\sum_{n=0}^{\infty}\sum_{m_1=0}^{\infty} -2n\, q_{nm_1} = \frac{-2N_o}{\{\exp(h\nu_1/kT_1)-1\}}, \quad (3.62c)$$

$$\sum_{n=0}^{\infty}\sum_{m_1=0}^{\infty} -m_1\, q_{nm_1} = \frac{-N_o}{\{\exp(h\nu_2/kT_2)-1\}}. \quad (3.62d)$$

Eq. (3.57b) becomes with these expressions

$$\frac{dE_1^I}{dt} = \frac{1}{35} N_o^2 P_e^2 B_{0,1}^2 C_{0,2}^2 h\nu_1 \left[\frac{1}{\{\exp(h\nu_2/kT_2)-1\}^2} - \frac{1+\exp(h\nu_2/kT_2)}{\{\exp(h\nu_2/kT_2)-1\}\{\exp(h\nu_1/kT_1)-1\}}\right]. \quad (3.57c)$$

By multiplying the first term on the right-hand side by

$$\frac{1+\exp(h\nu_2/kT_2)}{1+\exp(h\nu_2/kT_2)}$$

and by using the relationship $2\nu_2 = \nu_1$ we derive from eqs. (3.40a) and (3.46b) $C_{0,2}^2 = \frac{1}{2} C_{0,1}^4$ and find

$$\frac{dE_1^I}{dt} = \frac{1}{70} N_o P_e^2 B_{0,1}^2 C_{0,1}^4 \left\{\frac{\exp(h\nu_2/kT_2)+1}{\exp(h\nu_2/kT_2)-1}\right\} \{E_1(T_2) - E_1\}, \quad (3.57d)$$

where $$E_1(T_2) = \frac{h\nu_1 N_o}{\exp(h\nu_1/kT_2)-1}$$

and $$E_1(T_1) = \frac{h\nu_1 N_o}{\exp(h\nu_1/kT_1)-1}$$

represent the respective equilibrium energies of the valence vibration for the temperatures T_1 and T_2.

The same expression for the rate of energy transfer will be found by considering the second excitation process, eqs. (3.47a) and (3.47b), in which we consider the other bending mode.

Next we take the sum of all molecules which are activated or de-activated according the third probability, described for each molecule by eqs. (3.49a) and (3.49b). By substituting eqs. (3.58a) - (3.59b) into the eqs. (3.49a) and (3.49b) we find

$$Q_a^{III}(\nu_1) - Q_{\bar{a}}^{III}(\nu_1) = \frac{1}{15} N_o P_e^2 C_{0,2}^2 B_{0,1}^2 \left\{ \frac{\sum_{m_1=0}^{\infty} \frac{1}{2}(m_1^2 - 4m_1 n - 2n - m_1)\, q_{m_1}}{\sum_{m_1=0}^{\infty} q_{m_1}} \right\}. \tag{3.63a}$$

If we use the Maxwell-Boltzmann distribution for all q_{m_1} we can evaluate the series and find

$$Q_a^{III}(\nu_1) - Q_{\bar{a}}^{III}(\nu_1) = \frac{1}{15} N_o P_e^2 C_{0,2}^2 B_{0,1}^2 \left\{ \frac{1}{\{\exp(h\nu_2/kT_2) - 1\}^2} - n \frac{\{\exp(h\nu_2/kT_2) + 1\}}{\{\exp(h\nu_2/kT_2) - 1\}} \right\}. \tag{3.63b}$$

The rate of energy transferred to all molecules is

$$\frac{dE_1^{III}}{dt} = \sum_{n=0}^{\infty} q_n \{Q_a^{III}(\nu_1) - Q_{\bar{a}}^{III}(\nu_1)\} h\nu_1 . \tag{3.64a}$$

We finally find

$$\frac{dE_1^{III}}{dt} = \frac{1}{15} N_o^2 P_e^2 B_{0,1}^2 C_{0,2}^2 h\nu_1 \left[\frac{1}{\{\exp(h\nu_2/kT_2) - 1\}^2} - \frac{1 + \exp(h\nu_2/kT_2)}{\{\exp(h\nu_2/kT_2) - 1\}\{\exp(h\nu_1/kT_1) - 1\}} \right]. \tag{3.64b}$$

By comparing this result with eq. (3.57c) we find at once

$$\frac{dE_1^{III}}{dt} = \frac{1}{30} N_o P_e^2 B_{0,1}^2 C_{0,1}^4 \left\{ \frac{\exp(h\nu_2/kT_2) + 1}{\exp(h\nu_2/kT_2) - 1} \right\} \{E_1(T_2) - E_1\} \tag{3.64c}$$

The same result will be obtained by considering eqs. (3.50a) and (3.50b) over all molecules.

Next, we shall continue to evaluate the energy rates associated with the last six excitation probabilities, numbered with the indices V to X in the preceding section.

The evaluation of eqs. (3.51a) and (3.51b) over all molecules is straightforward. We then find

$$\frac{dE_1^{V}}{dt} = \frac{1}{105} N_o P_e^2 h\nu_1 \left\{ \sum_{n=0}^{\infty} \sum_{m_1=0}^{\infty} \sum_{m_2=0}^{\infty} (B_{n,n+1}^2 C_{m_1,m_1-1}^2 C_{m_2,m_2-1}^2 - B_{n,n-1}^2 C_{m_1,m_1+1}^2 C_{m_2,m_2+1}^2) q_{nm_1m_2} \right\}, \tag{3.65a}$$

which reduces to

$$\frac{dE_1^{V}}{dt} = \frac{1}{105} N_o P_e^2 h\nu_1 B_{0,1}^2 C_{0,1}^4 \left\{ \sum_{n=0}^{\infty} \sum_{m_1=0}^{\infty} \sum_{m_2=0}^{\infty} (m_1 m_2 - n m_1 - n m_2 - n) q_{nm_1m_2} \right\}. \tag{3.65b}$$

By using the Maxwell-Boltzmann distribution of eq. (3.60) we find for the series

$$\sum_{n=0}^{\infty}\sum_{m_1=0}^{\infty}\sum_{m_2=0}^{\infty} m_1 m_2\, q_{n m_1 m_2} = \frac{N_o}{\{\exp(h\nu_2/kT_2)-1\}^2}, \tag{3.66a}$$

$$\sum_{n=0}^{\infty}\sum_{m_1=0}^{\infty}\sum_{m_2=0}^{\infty} -2nm_1\, q_{n m_1 m_2} = \frac{-2N_o}{\{\exp(h\nu_1/kT_1)-1\}\{\exp(h\nu_2/kT_2)-1\}}, \tag{3.66b}$$

$$\sum_{n=0}^{\infty}\sum_{m_1=0}^{\infty}\sum_{m_2=0}^{\infty} -n\, q_{n m_1 m_2} = \frac{-N_o}{\{\exp(h\nu_1/kT_1)-1\}}. \tag{3.66c}$$

With these expressions eq. (3.65b) becomes

$$\frac{dE_1^V}{dt} = \frac{1}{105} N_o^2 P_e^2 B_{0,1}^2 C_{0,1}^4 h\nu_1 \left[\frac{1}{\{\exp(h\nu_2/kT_2)-1\}^2} - \frac{1+\exp(h\nu_2/kT_2)}{\{\exp(h\nu_1/kT_1)-1\}\{\exp(h\nu_2/kT_2)-1\}}\right]. \tag{3.65c}$$

Again, comparing this result with eq. (3.57c) we find

$$\frac{dE_1^V}{dt} = \frac{1}{105} N_o P_e^2 B_{0,1}^2 C_{0,1}^4 \left\{\frac{\exp(h\nu_2/kT_2)+1}{\exp(h\nu_2/kT_2)-1}\right\} \{E_1(T_2)-E_1\}.$$

From eqs. (3.52a) and (3.52b) we find the rate of energy transfer for one molecule to be

$$h\nu_1 \{Q_a^{VI}(\nu_1) - Q_d^{VI}(\nu_1)\} = \frac{1}{45} N_o P_e^2 B_{0,1}^2 C_{0,1}^4 h\nu_1 \left\{\frac{\sum_{m_1=0}^{\infty}(m_{1o}m_1 - nm_{1o} - nm_1 - n)\, q_{m_1}}{\sum_{m_1=0}^{\infty} q_{m_1}}\right\}. \tag{3.67a}$$

Substituting for q_{m_1} the Maxwell-Boltzmann distribution we find

$$h\nu_1 \{Q_a^{VI}(\nu_1) - Q_d^{VI}(\nu_1)\} = \frac{1}{45} N_o P_e^2 B_{0,1}^2 C_{0,1}^4 h\nu_1 \left[\frac{m_{1o}-n}{\{\exp(h\nu_2/kT_2)-1\}} - nm_{1o} - n\right]. \tag{3.67b}$$

By taking all molecules we obtain

$$\frac{dE_1^{VI}}{dt} = \frac{1}{45} N_o P_e^2 B_{0,1}^2 C_{0,1}^4 h\nu_1 \sum_{n=0}^{\infty}\sum_{m_1=0}^{\infty} q_{n m_1}\left[\frac{m_{1o}-n}{\{\exp(h\nu_2/kT_2)-1\}} - nm_{1o} - n\right]. \tag{3.68a}$$

The further evaluation runs parallel to E_1^V and so we find

$$\frac{dE_1^{VI}}{dt} = \frac{1}{45} N_o P_e^2 B_{0,1}^2 C_{0,1}^4 \left\{\frac{\exp(h\nu_2/kT_2)+1}{\exp(h\nu_2/kT_2)-1}\right\} \{E_1(T_2)-E_1\}. \tag{3.68b}$$

It is clear that combinations of eqs. (3.53a) with (3.53b), (3.54a) with (3.54b), and (3.55a) with (3.55b) will lead to the same result as the combination of eqs. (3.52a) with (3.52b).

Finally, we shall evaluate $Q_a{}^X(\nu_1)$ and $Q_a{}^X(\nu_1)$ for all molecules. The rate of energy transfer for one molecule is obtained from the eqs. (3.56a) and (3.56b)

$$h\nu_1 \{Q_a{}^X(\nu_1) - Q_a{}^X(\nu_1)\} =$$

$$\frac{1}{45} N_o P_e{}^2 B_{0,1}{}^2 C_{0,1}{}^4 h\nu_1 \left\{ \frac{\sum_{m_1=0}^{\infty} \sum_{m_2=0}^{\infty} (m_1 m_2 - n m_1 - n m_2 - n)\, q_{m_1 m_2}}{\sum_{m_1=0}^{\infty} q_{m_1} \sum_{m_2=0}^{\infty} q_{m_2}} \right\} \quad (3.69a)$$

$$= \frac{1}{45} N_o P_e{}^2 B_{0,1}{}^2 C_{0,1}{}^4 h\nu_1 \left[\frac{1}{\{\exp(h\nu_2/kT_2) - 1\}^2} - \frac{2n}{\{\exp(h\nu_2/kT_2) - 1\}} - n \right]. \quad (3.69b)$$

We obtain for all molecules

$$\frac{dE_1{}^X}{dt} = \frac{1}{45} N_o P_e{}^2 B_{0,1}{}^2 C_{0,1}{}^4 h\nu_1 \sum_{n=0}^{\infty} q_n \left[\frac{1}{\{\exp(h\nu_2/kT_2) - 1\}^2} - \frac{2n}{\{\exp(h\nu_2/kT_2) - 1\}} - n \right], \quad (3.70a)$$

which results in

$$\frac{dE_1{}^X}{dt} = \frac{1}{45} N_o P_e{}^2 B_{0,1}{}^2 C_{0,1}{}^4 \left\{ \frac{\exp(h\nu_2/kT_2) + 1}{\exp(h\nu_2/kT_2) - 1} \right\} \{E_1(T_2) - E_1.\}. \quad (3.70b)$$

The total energy transferred per unit time to the valence mode of all molecules as the result of the ten excitation probabilities in each collision is simply obtained by taking the sum of the ten terms E_1, i.e. $E_1{}^{I-X}$. However, as we shall see in the next section, the symmetric valence mode will also transfer some of its energy into the asymmetric valence mode. Therefore we have to substract this energy exchange from the calculated excitation energy.

$$\frac{dE_1}{dt} = 0.216\, N_o P_e{}^2 B_{0,1}{}^2 C_{0,1}{}^4 \left\{ \frac{\exp(h\nu_2/kT_2) + 1}{\exp(h\nu_2/kT_2) - 1} \right\} \{E_1(T_2) - E_1\} - \frac{dE_3'}{dt}. \quad (3.71)$$

3.12. Effective collisions causing the excitation of the asymmetric valence vibration

Since the energy quanta of the ν_3 vibration are much larger than those of the other vibrations, direct excitation will have negligible probability. We find also for this vibration an indirect excitation process. This mode will obtain most of its energy from the other vibrational modes. During a collision each of the six available modes can transfer a part of its energy into the ν_3 mode. How-

ever, the largest excitation probability will be found when one quantum of the ν_3 vibration is exchanged with one quantum of the ν_1 and one quantum of the ν_2 vibration, while the excess energy is exchanged with the translational motion. The other probabilities are negligibly small. In other words, we find that the energy of the asymmetric vibration is supplied by the energy of the symmetric valence vibration and of the bending vibrations. The energy of the valence vibration is in turn obtained from the bending vibrations. The bending vibrations, as we know, are directly excited by the translation.

It turns out that we have to consider eight excitation probabilities which describe the whole excitation process. These probabilities are very small compared with those for the excitation of the bending and the symmetric valence vibrations, so that this excitation process still has to start when the other vibrations have already reached the translational temperature.

Let us for our first process consider the case that the energy exchange is confined to the considered molecule. Again we start from the general expression for the effective collisions, as given by eq. (3.31), and evaluate the asymmetric matrix element given by eq. (3.8b). The quantum numbers of the ν_1, ν_2 and ν_3 vibrations change by one. The remaining five vibrational modes are unchanged, so that the integration of eq. (3.8b) over their normal coördinates gives unity. By using the four potential functions of eqs. (3.13a), (3.13b), (3.13c) and (3.13d), we find for activation

$$M_a{}^I(\nu_3) = \left[V_{oo}{}^0 \left\{ 2 \sinh\left(\frac{aL\cos\Gamma_1}{2}\right)\right\}\left\{ 2\cosh\left(\frac{aL\cos\Gamma_2}{2}\right)\right\} + V_{co}{}^0 \left\{ 2\sinh\left(\frac{aL\cos\Gamma_1}{2}\right)\right\}\right] a^3 A_2 \cos^2\Gamma_1 A_3{}^2 \sin\Gamma_1 \cos\beta_1 \left[\frac{\hbar(p_o+1)}{4\pi\mu_2\nu_3}\right]^{1/2}\left[\frac{\hbar n_o}{4\pi\mu_1\nu_1}\right]^{1/2}\left[\frac{\hbar m_{1o}}{4\pi\mu_2\nu_2}\right]^{1/2} \psi_{r1}\,\psi_{r2}\,,$$

where $M_a{}^I(\nu_3)$ is the asymmetric matrix element of activation of the ν_3 vibration for the first type of process. On account of the large average argument of the hyperbolic functions we may replace $\sinh\left(\frac{aL\cos\Gamma_1}{2}\right)$ by $\cosh\left(\frac{aL\cos\Gamma_1}{2}\right)$, and assuming again that the constant potential factors are of the same order of magnitude, we find

$$M_a{}^I(\nu_3) = a^3 A_2 A_3{}^2 \sin\Gamma_1 \cos^2\Gamma_1 \cos\beta_1 \left[\frac{\hbar(p_o+1)}{4\pi\mu_2\nu_3}\right]^{1/2}\left[\frac{\hbar n_o}{4\pi\mu_1\nu_1}\right]^{1/2}\left[\frac{\hbar m_{1o}}{4\pi\mu_2\nu_2}\right]^{1/2} V_0\,\psi_{r1}\,\psi_{r2}\,. \quad (3.72)$$

The integration over all rotational orientations gives

$$\frac{1}{4\pi}\int_0^{2\pi}\int_0^{\pi} \sin^2 \Gamma_1 \cos^4 \Gamma_1 \sin \vartheta_1 \, d\vartheta_1 \, d\varphi_1 = \frac{2}{35}.$$

Further, we substitute for $\cos^2 \beta_1$ its average value, which is equal to $\frac{1}{2}$. Again we see that V_o and the rotational wave functions cancel. The calculation of the cross-section is straightforward. We notice, however, that the energy of one quantum jump of the asymmetric valence vibration is larger than the sum of one quantum of the ν_1 vibration, and one quantum of the ν_2 vibration, so that we do not have the case of exact resonance encountered in section 10. The excess energy has to be exchanged with the translation.

We find for the effective collisions

$$Q_a^I(\nu_3) = \frac{1}{35} N_o P_a^2 D_{p_o,p_o+1}^2 B_{n_o,n_o-1}^2 C_{m_{1\delta},m_{1\delta}-1}^2 \tag{3.72a}$$

and

$$Q_d^I(\nu_3) = \frac{1}{35} N_o P_d^2 D_{p_o,p_o-1}^2 B_{n_o,n_o+1}^2 C_{m_{1\delta},m_{1\delta}+1}^2, \tag{3.72b}$$

where

$$D_{p_o,p_o+1}^2 = \alpha^2 A_3^2 \left[\frac{\hbar(p_o+1)}{4\pi\mu_2\nu_3}\right] \tag{3.73a}$$

and

$$D_{p_o,p_o-1}^2 = \alpha^2 A_3^2 \left[\frac{\hbar p_o}{4\pi\mu_2\nu_3}\right]. \tag{3.73b}$$

In the solving of eqs. (3.72a) and (3.72b), P_a and P_d are calculated in accordance with eq. (3.31) by substituting $\Delta E = \Delta E_3$, $\Delta E_3 = h\nu_3 - h\nu_1 - h\nu_2$ being the excess energy transferred by the translational energy.

Since the bending mode is degenerated, we can for our second process take the other bending mode. This will, of course, give the same value as that found for process I, or expressed mathematically

$$Q_a^{II}(\nu_3) = \frac{1}{35} N_o P_a^2 D_{p_o,p_o+1}^2 B_{n_o,n_o-1}^2 C_{m_{2\delta},m_{2\delta}-1}^2 \tag{3.74a}$$

and

$$Q_d^{II}(\nu_3) = \frac{1}{35} N_o P_d^2 D_{p_o,p_o-1}^2 B_{n_o,n_o+1}^2 C_{m_{2\delta},m_{2\delta}+1}^2. \tag{3.74b}$$

For our third process let us consider that the energy quantum $h\nu_3$ is supplied by one of the bending modes of the incident molecule. The evaluation of the effective collisions runs parallel to the foregoing processes. We find for the integration over the rotational coördinates of the colliding molecules

(i) $$\frac{1}{4\pi}\int_0^{2\pi}\int_0^{\pi}\cos^4\Gamma_1\sin\vartheta_1\,\mathrm{d}\vartheta_1\,\mathrm{d}\varphi_1=\frac{1}{5}$$

and

(ii) $$\frac{1}{4\pi}\int_0^{2\pi}\int_0^{\pi}\sin^2\Gamma_2\sin\vartheta_2\,\mathrm{d}\vartheta_2\,\mathrm{d}\varphi_2=\frac{2}{3}.$$

Furthermore, just as in the substitution of eq. (3.72) in eq. (3.31), we have to average $\cos^2\beta_2$, which gives $\frac{1}{2}$. When we work out the effective collisions according to this process we notice that each of the incident molecules can be in any state m_1. Therefore we have to replace $C_{m_1,m_1-1}{}^2$ by the average value of all matrix elements. Thus we find

$$Q_a^{III}(v_3)=\frac{1}{15}N_o\,P_a{}^2\,D_{p_o,p_o+1}{}^2\,B_{n_o,n_o-1}{}^2\,\frac{\sum_{m_1=0}^{\infty}C_{m_1,m_1-1}{}^2\,q_{m_1}}{\sum_{m_1=0}^{\infty}q_{m_1}} \tag{3.75a}$$

and

$$Q_a^{III}(v_3)=\frac{1}{15}N_o\,P_a{}^2\,D_{p_o,p_o-1}{}^2\,B_{n_o,n_o+1}{}^2\,\frac{\sum_{m_1=0}^{\infty}C_{m_1,m_1+1}{}^2\,q_{m_1}}{\sum_{m_1=0}^{\infty}q_{m_1}}. \tag{3.75b}$$

If for our fourth process we consider that the bending mode of the incident molecule is degenerated, we find analogously

$$Q_a^{IV}(v_3)=\frac{1}{15}N_o\,P_a{}^2\,D_{p_o,p_o+1}{}^2\,B_{n_o,n_o-1}{}^2\,\frac{\sum_{m_2=0}^{\infty}C_{m_2,m_2-1}{}^2\,q_{m_2}}{\sum_{m_2=0}^{\infty}q_{m_2}} \tag{3.76a}$$

and

$$Q_a^{IV}(v_3)=\frac{1}{15}N_o\,P_a{}^2\,D_{p_o,p_o-1}{}^2\,B_{n_o,n_o+1}{}^2\,\frac{\sum_{m_2=0}^{\infty}C_{m_2,m_2+1}{}^2\,q_{m_2}}{\sum_{m_2=0}^{\infty}q_{m_2}}. \tag{3.76b}$$

A fifth possibility is the supply of the valence quantum by the incident molecule, and of the bending quantum by the considered molecule. The matrix element according to this probability becomes, by using the potential functions in eqs. (3.13a), (3.13b), (3.13c) and (3.13d)

$$M_a{}^V(\nu_3) = \left[V_{oo}{}^0 \left\{ 2\cosh\left(\frac{aL\cos\Gamma_1}{2}\right)\right\}\left\{ 2\sinh\left(\frac{aL\cos\Gamma_2}{2}\right)\right\}+ \left(\frac{A_1}{A_3}\right)^2 V_{co}{}^0 \left\{ 2\sinh\left(\frac{aL\cos\Gamma_2}{2}\right)\right\}\right] a^3 A_2 \cos\Gamma_2 A_3{}^2 \cos\Gamma_1 \sin\Gamma_1 \cos\beta_1 \left[\frac{\hbar(p_o+1)}{4\pi\mu_2\nu_3}\right]^{1/2}\left[\frac{\hbar n_o}{4\pi\mu_1\nu_1}\right]^{1/2}\left[\frac{\hbar m_{1o}}{4\pi\mu_2\nu_2}\right]^{1/2} \psi_{r1}\,\psi_{r2}\,. \tag{3.77}$$

As usually we substitute this in eq. (3.31) and integrate over all rotational coördinates. This integration yields the product of the following two integrals:

(i) $$\frac{1}{4\pi}\int_0^{2\pi}\int_0^{\pi} \cos^2\Gamma_1 \sin^2\Gamma_1 \sin\vartheta_1\, d\vartheta_1\, d\varphi_1 = \frac{2}{15}$$

and

(ii) $$\frac{1}{4\pi}\int_0^{2\pi}\int_0^{\pi} \cos^2\Gamma_2 \sin\vartheta_2\, d\vartheta_2\, d\varphi_2 = \frac{1}{3}\,.$$

Furthermore in eq. (3.77) we must substitute the average value of $\cos^2\beta$, which is equal to $\frac{1}{2}$.

The evaluation of the effective collisions according to this process gives

$$Q_a{}^V(\nu_3) = \frac{1}{45} N_o P_a{}^2 D_{p_o,p_o+1}{}^2 C_{m_{1o},m_{1o}-1}{}^2 \frac{\sum_{n=0}^{\infty} B_{n,n-1}{}^2 q_n}{\sum_{n=0}^{\infty} q_n} \tag{3.78a}$$

and

$$Q_d{}^V(\nu_3) = \frac{1}{45} N_o P_d{}^2 D_{p_o,p_o-1}{}^2 C_{m_{1o},m_{1o}+1}{}^2 \frac{\sum_{n=0}^{\infty} B_{n,n+1}{}^2 q_n}{\sum_{n=0}^{\infty} q_n}\,. \tag{3.78b}$$

If we now consider the other bending mode for our sixth process we find that the effective collisions are given by

$$Q_a{}^{VI}(\nu_3) = \frac{1}{45} N_o P_a{}^2 D_{p_o,p_o+1}{}^2 C_{m_{2o},m_{2o}-1}{}^2 \frac{\sum_{n=0}^{\infty} B_{n,n-1}{}^2 q_n}{\sum_{n=0}^{\infty} q_n} \tag{3.79a}$$

and

$$Q_d{}^{VI}(\nu_3) = \frac{1}{45} N_o P_d{}^2 D_{p_o,p_o-1}{}^2 C_{m_{2o},m_{2o}+1}{}^2 \frac{\sum_{n=0}^{\infty} B_{n,n+1}{}^2 q_n}{\sum_{n=0}^{\infty} q_n}\,. \tag{3.79b}$$

For our seventh and eighth possibilities let us consider that the two quanta are both supplied by the incident molecule. The matrix element becomes

$$M_a^{VII}(\nu_3) = \left[V_{oo}^0 \left\{ 2\cosh\left(\frac{\alpha L \cos \Gamma_1}{2}\right)\right\}\left\{ 2\sinh\left(\frac{\alpha L \cos \Gamma_2}{2}\right)\right\} + \right.$$
$$\left. - \frac{A_1}{A_3} V_{co}^0 \left\{ 2\sinh\left(\frac{\alpha L \cos \Gamma_2}{2}\right)\right\}\right] \alpha^3 A_2 \cos \Gamma_2 A_3^2 \cos \Gamma_1 \sin \Gamma_2 \cos \beta_2$$
$$\left[\frac{\hbar(p_o+1)}{4\pi\mu_2\nu_3}\right]^{1/2} \left[\frac{\hbar n}{4\pi\mu_1\nu_1}\right]^{1/2} \left[\frac{\hbar m_{1o}}{4\pi\mu_2\tau_2}\right]^{1/2} \psi_{r1}\,\psi_{r2}.$$

(The matrix element of the eighth possibility can be found analogously).

In working out the effective collisions we have to evaluate the product of the following two integrals for the rotational coördinates:

(i) $$\frac{1}{4\pi}\int_0^{2\pi}\int_0^{\pi} \cos^2 \Gamma_1 \sin \vartheta_1 \, d\vartheta_1 \, d\varphi_1 = \frac{1}{3}$$

and

(ii) $$\frac{1}{4\pi}\int_0^{2\pi}\int_0^{\pi} \sin^2 \Gamma_2 \cos^2 \Gamma_2 \sin \vartheta_2 \, d\vartheta_2 \, d\varphi_2 = \frac{2}{15}.$$

We then find for the effective collisions of the seventh process

$$Q_a^{VII}(\nu_3) = \frac{1}{45} N_o P_a^2 D_{p_o,p_o+1^2} \frac{\sum_{n=0}^{\infty} B_{n,n-1^2} q_n}{\sum_{n=0}^{\infty} q_n} \frac{\sum_{m_1=0}^{\infty} C_{m_1,m_1-1^2} q_{m_1}}{\sum_{m_1=0}^{\infty} q_{m_1}} \tag{3.80a}$$

and

$$Q_d^{VII}(\nu_3) = \frac{1}{45} N_o P_d^2 D_{p_o,p_o-1^2} \frac{\sum_{n=0}^{\infty} B_{n,n+1^2} q_n}{\sum_{n=0}^{\infty} q_n} \frac{\sum_{m_1=0}^{\infty} C_{m_1,m_1+1^2} q_{m_1}}{\sum_{m_1=0}^{\infty} q_{m_1}}. \tag{3.80b}$$

If we now consider the other bending mode of the incident molecule, the eighth process will yield

$$Q_a^{VIII}(\nu_3) = \frac{1}{45} N_o P_a^2 D_{p_o,p_o+1^2} \frac{\sum_{n=0}^{\infty} B_{n,n-1^2} q_n}{\sum_{n=0}^{\infty} q_n} \frac{\sum_{m_2=0}^{\infty} C_{m_2,m_2-1^2} q_{m_2}}{\sum_{m_2=0}^{\infty} q_{m_2}} \tag{3.81a}$$

and

$$Q_d^{VIII}(\nu_3) = \frac{1}{45} N_o P_d^2 D_{p_o,p_o-1^2} \frac{\sum_{n=0}^{\infty} B_{n,n+1^2} q_n}{\sum_{n=0}^{\infty} q_n} \frac{\sum_{m_2=0}^{\infty} C_{m_2,m_2+1^2} q_{m_2}}{\sum_{m_2=0}^{\infty} q_{m_2}}. \tag{3.81b}$$

3.13. Relaxation equation for the asymmetric valence vibration

The relaxation equation for the excitation of the ν_3 vibration can be found by considering the effective collisions of the preceding section for all molecules. This procedure runs for a great deal parallel to the evaluation of the relaxation equation for the symmetric valence vibration. The principal difference is that now we have at the same time also an energy exchange with the translation, so that $P_a{}^2$ is smaller than $P_d{}^2$.

Let us work out in detail process I for the excitation of the asymmetric valence vibration. The rate at which energy is transferred to all molecules will be

$$\frac{\mathrm{d}E_3{}^I}{\mathrm{d}t} = \sum_{n=0}^{\infty}\sum_{m_1=0}^{\infty}\sum_{p=0}^{\infty} q_{nm_1p}\,\{Q_a{}^I(\nu_3) - Q_d{}^I(\nu_3)\}\,h\nu_3\,. \tag{3.82a}$$

By using eqs. (3.72a) and (3.72b) this becomes

$$\frac{\mathrm{d}E_3{}^I}{\mathrm{d}t} = \frac{1}{35} N_o\, h\nu_3 \sum_{n=0}^{\infty}\sum_{m_1=0}^{\infty}\sum_{p=0}^{\infty} q_{nm_1p}\,\{P_a{}^2\, D_{p,p+1}{}^2\, B_{n,n-1}{}^2\, C_{m_1,m_1-1}{}^2 - P_d{}^2\, D_{p,p-1}{}^2\, B_{n,n+1}{}^2\, C_{m_1,m_1+1}{}^2\}\,. \tag{3.82b}$$

This series can be simplified by using eqs. (3.40a), (3.40b) and (3.58a), (3.58b). Furthermore we use the following relationships obtained from eqs. (3.73a) and (3.73b):

$$D_{p,p+1}{}^2 = (p+1)\,D_{0,1}{}^2 \tag{3.83a}$$

and

$$D_{p,p-1}{}^2 = pD_{0,1}{}^2\,. \tag{3.83b}$$

We shall then find

$$\frac{\mathrm{d}E_3{}^I}{\mathrm{d}t} = \frac{1}{35} N_o\, P_a{}^2\, B_{0,1}{}^2\, C_{0,1}{}^2\, D_{0,1}{}^2\, h\nu_3 \left[\sum_{n=0}^{\infty}\sum_{m_1=0}^{\infty}\sum_{p=0}^{\infty} \{nm_1(p+1) - p(n+1)\,(m_1+1)\; e^{\Delta E_3/\mathrm{k}T}\}\; q_{nm_1p}\right], \tag{3.82c}$$

where we have used eq. (3.31).

Since the vibrations have a Maxwell-Boltzmann distribution we can easily evaluate the series in eq. (3.82c) by using eq. (3.60). Then we find

$$\sum_{n=0}^{\infty}\sum_{m_1=0}^{\infty}\sum_{p=0}^{\infty} nm_1p\, q_{nm_1p} = \frac{N_o}{\{\exp(h\nu_1/\mathrm{k}T_1)-1\}\{\exp(h\nu_2/\mathrm{k}T_2)-1\}\{\exp(h\nu_3/\mathrm{k}T_3)-1\}}, \tag{3.84a}$$

$$\sum_{n=0}^{\infty}\sum_{m_1=0}^{\infty}\sum_{p=0}^{\infty} nm_1\, q_{nm_1p} = \frac{N_o}{\{\exp(h\nu_1/\mathrm{k}T_1)-1\}\{\exp(h\nu_2/\mathrm{k}T_2)-1\}}, \tag{3.84b}$$

$$\sum_{n=0}^{\infty}\sum_{m_1=0}^{\infty}\sum_{p=0}^{\infty} np\, q_{nm_1p} = \frac{N_o}{\{\exp(h\nu_1/\mathrm{k}T_1)-1\}\{\exp(h\nu_3/\mathrm{k}T_3)-1\}}, \tag{3.84c}$$

$$\sum_{n=0}^{\infty}\sum_{m_1=0}^{\infty}\sum_{p=0}^{\infty} m_1\, p\, q_{nm_1p} = \frac{N_o}{\{\exp(h\nu_2/kT_2)-1\}\{\exp(h\nu_3/kT_3)-1\}}, \quad (3.84d)$$

$$\sum_{n=0}^{\infty}\sum_{m_1=0}^{\infty}\sum_{p=0}^{\infty} p\, q_{nm_1p} = \frac{N_o}{\{\exp(h\nu_3/kT_3)-1\}}. \quad (3.84e)$$

With these expressions eq. (3.82c) becomes

$$\frac{dE_3^I}{dt} = \frac{1}{35} N_o P_a^2 B_{0,1}^2 C_{0,1}^2 D_{0,1}^2 \frac{\{\exp(h\nu_1/kT_1 + h\nu_2/kT_2 + \Delta E_3/kT)-1\}}{\{\exp(h\nu_1/kT_1)-1\}\{\exp(h\nu_2/kT_2)-1\}} [E_3(T,T_1,T_2) - E_3], \quad (3.82d)$$

where E_3 = actual energy of the asymmetric valence vibration, and

$$E_3(T,T_1,T_2) = \frac{N_o h\nu_3}{\{\exp(h\nu_1/kT_1 + h\nu_2/kT_2 + \Delta E_3/kT)-1\}};$$

this being the energy for the asymmetric valence vibration at the temperature determined by the translation as well as by the bending and symmetric valence vibrations. This temperature can be represented by $\bar{T}$, such that

$$\bar{T} = \frac{h\nu_3/k}{h\nu_1/kT_1 + h\nu_2/kT_2 + \Delta E_3/kT}.$$

However, since this excitation process starts after the other vibrations have reached the translational temperature, we find $\bar{T}$ equal to the translational temperature T.

Just as we have evaluated the relaxation equation associated with process I, we can evaluate each of the other seven processes. We shall then find that, apart from a numerical factor, these equations are all of the same form as that of process I. These numerical factors are also found in the corresponding effective collisions.

By taking the sum of the results for the eight excitation processes of the ν_3 vibration, we finally find the energy transferred per unit time:

$$\frac{dE_3}{dt} = 0.28\, N_o P_a^2 B_{0,1}^2 C_{0,1}^2 D_{0,1}^2 \frac{\{\exp(h\nu_1/kT_1 + h\nu_2/kT_2 + \Delta E_3/kT)-1\}}{\{\exp(h\nu_1/kT_1)-1\}\{\exp(h\nu_2/kT_2)-1\}} [E_3(T) - E_3], \quad (3.85)$$

where $E_3(T)$ is the energy of the ν_3 vibration at the translational temperature.

3.14. Relaxation times

The theory presented in this chapter for the calculation of the transfer of vibrational energy provides also the relaxation time for the excitation of the three vibrations. From the energy transfer equations (3.41c), (3.71) and (3.85)

we see that the energy of molecules is connected with temperature hysteresis, the value of the temperature depending also on the past value of the energy.

If one supplies energy to a gas, this energy is first supplied to the translational and rotational degrees of freedom, so that the temperature will at first be relatively high. Then, during a much slower process, the vibrational degrees of the molecule absorb their share of the energy at the expense of the translational and rotational energies. Consequently, during the period of excitation of the vibrations the translational temperature will decrease toward an equilibrium, which is of course also the equilibrium value of the vibrational temperature. In other words the vibrational excitation has a time delay of which the characteristic value is called the relaxation time. For the three vibrations these values are as follows:

symmetric valence vibration

$$\tau_{12} = \left[0.216\, N_o\, P_e^2\, B_{0,1}^2\, C_{0,1}^4 \left\{ \frac{\exp\,(h\nu_2/\mathrm{k}T_2) + 1}{\exp\,(h\nu_2/\mathrm{k}T_2) - 1} \right\} \right]^{-1}, \tag{3.86}$$

bending vibration

$$\tau_2 = \left[0.33\, N_o P_a^2 (\Delta E_2)\, C_{0,1}^2 \left\{ \exp\,(h\nu_2/\mathrm{k}T_2) - 1 \right\} \right]^{-1}, \tag{3.87}$$

asymmetric valence vibration

$$\tau_3 = \left[0.28\, N_o\, P_a^2 (\Delta E_3)\, B_{0,1}^2\, C_{0,1}^2\, D_{0,1}^2 \frac{\{\exp\,(h\nu_1/\mathrm{k}T_1 + h\nu_2/\mathrm{k}T_2 + \Delta E_3/\mathrm{k}T) - 1\}}{\{\exp\,(h\nu_1/\mathrm{k}T_1) - 1\}\,\{\exp\,(h\nu_2/\mathrm{k}T_2) - 1\}} \right]^{-1}. \tag{3.88}$$

The numerical values of the relaxation times are given in table IV as functions of the translational temperature.

TABLE IV

Relaxation Times

T	τ_{12} [sec]	τ_2 [sec]	τ_3 [sec]
300	3.7×10^{-5}	1.2×10^{-4}	3.8×10^{-2}
400	3.5×10^{-5}	8.8×10^{-6}	7.5×10^{-3}
500	3.1×10^{-5}	1.9×10^{-6}	2.6×10^{-3}
600	2.7×10^{-5}	6.4×10^{-7}	1.1×10^{-3}
700	2.4×10^{-5}	2.7×10^{-7}	5.8×10^{-4}
800	2.1×10^{-5}	1.3×10^{-7}	3.8×10^{-4}
900	1.8×10^{-5}	7.9×10^{-8}	2.4×10^{-4}
1000	1.6×10^{-5}	5.1×10^{-8}	1.6×10^{-4}

Further, we have seen in this chapter that all energy is first supplied to the most easily excited vibration. The other two vibrations obtain their share of the energy from this vibration. Similar results are expected for other polyatomic molecules which may have many vibrational frequencies. The vibrations with higher frequencies will then be excited indirectly at the cost of the vibration with the lowest frequency and only the small difference of energy quanta will be exchanged with the translation. But, even in an exchange among the vibrational modes, one can find very small transition probabilities, as we have seen for the excitation of the asymmetric valence vibration.

CHAPTER 4

EXPERIMENTAL PROCEDURE FOR MEASURING THE DENSITY PROFILE BEHIND SHOCK WAVES

4.1. Shock waves

In the preceding chapter we have studied theoretically the energy transfer among the vibrational degrees of freedom of a suddenly heated gas. Such a process can be realized with shock waves produced in a shock tube. The construction of a shock tube [24–25]) is illustrated schematically in fig. 3a. Basically, it consists of a high-pressure and low-pressure chamber, separated by a thin diaphragm. The low-pressure chamber contains the test gas in the initial condition. Compressed helium from a high-pressure cylinder is forced

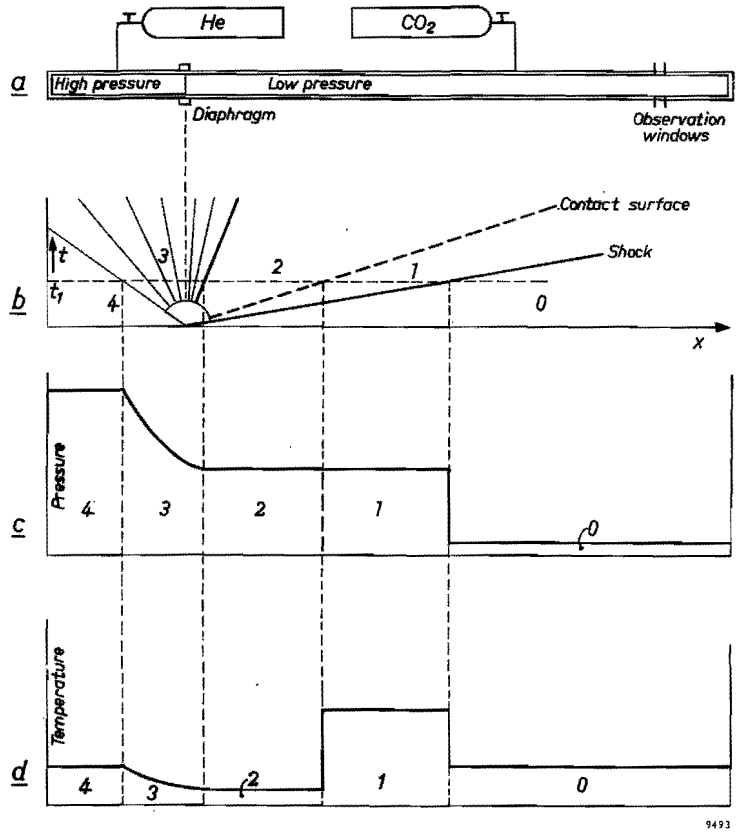

Fig. 3. a. Schematic representation of the shock tube, the length of which is set out along the x-axis of the three following graphs; b. gas flow along the shock tube as a function of time; c. pressure distribution along the shock tube at time t_1; d. temperature distribution along the shock tube at time t_1.

into the high-pressure chamber of the shock tube until the diaphragm bursts. As the material of the diaphragm is highly stressed prior to rupture, it rapidly flattens against the wall of the tube. After the diaphragm has burst, a compression wave moves into the test gas. The compression wave causes an abrupt, steep transition in the pressure of the test gas, i.e. it forms a shock wave. At the same time the expanding high-pressure gas moves also into the low-pressure chamber.

Usually the motion of the flow is represented by an x-t diagram, as shown in fig. 3b. Here x is the coördinate of a point in the long axis of the shock tube and t represents the time. The regions indicated by 0, 1, 2, 3 and 4 are respectively low-pressure gas, test gas behind the shock front, the expanded high-pressure gas, the expansion fan of the high-pressure gas, and finally the high-pressure gas still in its initial condition. The surface separating the two gasses is called the contact surface. Figs. 3c and 3d show the pressure and temperature distribution along the shock tube at a time t_1 after the diaphragm has burst.

The discontinuity conditions at the shock front can be derived from the principles governing the conservation of mass, momentum and energy [26]). If we consider these principles in a coördinate system that is moving with the shock front, so that the flow is reduced to a steady flow, we have the following equations:

$$\text{mass} \quad : \quad \rho_o u_o = \rho_s u_s \tag{4.1}$$

$$\text{momentum:} \quad p_o + \rho_o \mu_o^2 = p_s + \rho_s u_s^2 \tag{4.2}$$

$$\text{energy} \quad : \quad C_P T_o + \tfrac{1}{2} u_o^2 = C_P T_s + \tfrac{1}{2} u_s^2, \tag{4.3}$$

where ρ is the density, p is the pressure, u is the velocity, T is the absolute temperature and C_P is the specific heat at constant pressure. The suffix o indicates the initial state of the test gas, while the suffix s refers to the state of the test gas immediately behind the shock front.

For convenience, we restrict ourselves to an ideal gas with constant specific heat:

$$C_P T = \frac{\gamma}{\gamma - 1} RT = \frac{\gamma}{\gamma - 1} \frac{p}{\rho} = \frac{c^2}{\gamma - 1}, \tag{4.4}$$

where γ is the ratio of the specific heats at constant pressure and constant volume, i.e. C_P/C_V.

Next we shall introduce the shock-strength parameter ε, which is equal to half the relative velocities of the gas on both sides of the shock front [27]):

$$u_o = v_o (1 + \varepsilon)$$

and

$$u_s = v_o (1 - \varepsilon). \tag{4.5}$$

From eqs. (4.1)-(4.5) we can derive the following expressions:

$$\frac{\rho_o}{\rho_s} = \frac{1-\varepsilon}{1+\varepsilon}, \tag{4.6}$$

$$\frac{p_o}{p_s} = \frac{1-\gamma\varepsilon}{1+\gamma\varepsilon}, \tag{4.7}$$

$$\frac{T_o}{T_s} = \frac{(1-\gamma\varepsilon)(1+\varepsilon)}{(1+\gamma\varepsilon)(1-\varepsilon)}. \tag{4.8}$$

Further, the Mach numbers defined by u/c become

$$M_o^2 = \frac{1+\varepsilon}{1-\gamma\varepsilon} \tag{4.9}$$

and

$$M_s^2 = \frac{1-\varepsilon}{1+\gamma\varepsilon}. \tag{4.10}$$

Since all these physical quantities are positive, the shock-strength parameter is limited by the following restrictions:

$$0 < \varepsilon < 1/\gamma. \tag{4.11}$$

At the instant of bursting of the diaphragm, a centered rarefaction wave propagates into the high-pressure chamber. From the unsteady isentropic expansion the following relationship can be derived. By considering Newton's law of motion, $F\mathrm{d}t = m\mathrm{d}u$, for a one-dimensional fluid element of thickness $\mathrm{d}x$ during the passage of a sound wave, we get

$$\mathrm{d}p\mathrm{d}t = -\rho\mathrm{d}x\mathrm{d}u.$$

We substitute $\mathrm{d}t = \frac{1}{c}\mathrm{d}x$, where c is the velocity of sound in our gas, and find

$$\mathrm{d}p = -\rho c\mathrm{d}u. \tag{4.12}$$

Poisson's equation of state gives

$$\frac{\mathrm{d}p}{p} = \frac{\gamma}{\gamma-1}\frac{\mathrm{d}T}{T}. \tag{4.13}$$

By using eq. (4.4) one finds from eqs. (4.12) and (4.13)

$$\frac{2}{\gamma_4-1}\mathrm{d}c + \mathrm{d}u = 0,$$

where the suffix 4 refers to the high-pressure gas. This integrates to

$$\frac{2}{\gamma_4-1}c + u = \text{constant}. \tag{4.14}$$

The latter equation will be applied in region 3 in order to relate the pressure in region 4 to that in region 1.

From eq. (4.4) we find

$$\left(\frac{p_4}{p_2}\right) = \left(\frac{c_4}{c_2}\right)^{2\gamma_4/\gamma_4 - 1}.$$

Applying eq. (4.14) we get

$$\frac{2}{\gamma_4 - 1} c_4 = \frac{2}{\gamma_4 - 1} c_2 + u_2.$$

Further we know that the gas conditions across the contact surface are

$$p_2 = p_s$$

and

$$u_2 = u_i,$$

where u_i is the velocity of the test gas behind the shock front, but relative to the shock tube. Hence the equation relating the pressure in the high-pressure chamber to that behind the shock front is given by

$$\frac{p_4}{p_s} = \left(\frac{c_4}{c_4 - \frac{1}{2}(\gamma_4 - 1)\, u_i}\right)^{2\gamma_4/\gamma_4 - 1}. \tag{4.15}$$

The pressure behind the moving shock wave can be expressed in terms of the pressure before the shock front by eq. (4.7). The induced velocity $u_i = u_o - u_s$ imparted by the shock wave to the test gas can be obtained from eqs. (4.1)-(4.5):

$$u_i = \frac{2\, c_o\, \varepsilon}{\{(1 - \gamma\varepsilon)(1 + \varepsilon)\}^{1/2}}.$$

Finally we obtain the desired result relating the strength of the shock wave to the given initial conditions of the two gases in respectively the high-pressure and low-pressure chambers

$$\frac{p_4}{p_o} = \frac{1 + \gamma\varepsilon}{1 - \gamma\varepsilon}\left[\frac{\{(1 - \gamma\varepsilon)(1 + \varepsilon)\}^{1/2}}{\{(1 - \gamma\varepsilon)(1 + \varepsilon)\}^{1/2} - (\gamma_4 - 1)\varepsilon\ c_o/c_4}\right]^{2\gamma_4/\gamma_4 - 1}. \tag{4.16}$$

This equation relates the shock strength parameter ε to the pressure ratio and the velocity-of-sound ratio across the diaphragm. It is clear that, in order to produce strong shock waves, the ratio c_o/c_4 must be as small as possible. This can be ensured by using gases with low molecular weight, such as hydrogen and helium, at high temperatures. In fig. 4 the pressure ratio p_4/p_o and the temperature, density and pressure ratios across the shock front have been plotted as functions of the shock strength parameter, both gases being initially at room temperature. We have used $\gamma = 1.4$ and $\gamma_4 = 1.67$. It is seen that with shock waves very high pressures and temperatures can be produced.

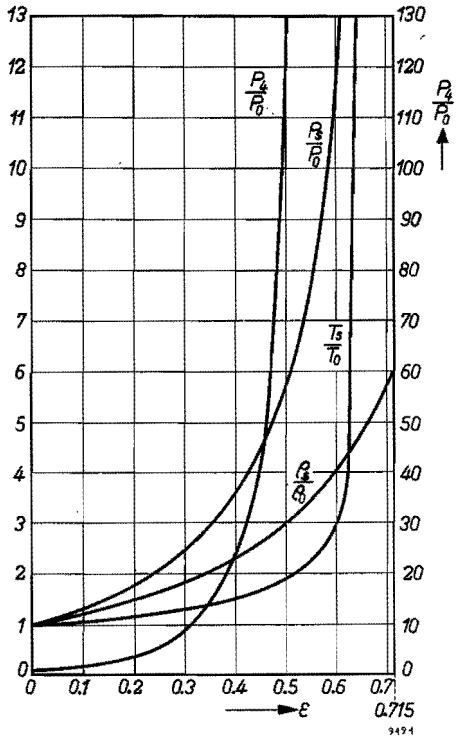

Fig. 4. The pressure ratio p_4/p_0 and the temperature, density and pressure ratios across the shock front plotted as functions of the shock-strength parameter ϵ.

Although in practice we also have to make allowances for heat conduction, frictional effects along the wall and variations of the specific heat with temperature, all of which we have neglected so far, the shock tube appears to approximate the theoretical performance reasonably well, at least for weak shocks.

The experiments were performed with a constant-area shock tube made of steel and having a rectangular cross-section of 30 mm by 18 mm. The lengths of the high-pressure and low-pressure chambers were about 1 m and 6 m respectively. The rather big length of the low-pressure chamber was chosen in order to improve the flatness of the shock wave and to decrease the effect of disturbances due to the contact surface.

4.2. Some physical aspects to be considered when working with shock tubes

Shock waves have been used extensively to study the properties of gases at high temperatures. The one-dimensional flow in a constant-area shock tube provides unique possibilities for studying rapid physical and chemical processes under controlled conditions of temperature and pressure.

In the preceding section we have seen that there is a sudden increase in enthalpy across the discontinuity surface of the shock wave. The energy of flow

is here converted into random thermal energy. The gas behind the shock front is, therefore, disturbed from its original equilibrium state. The effects most likely to be important as the gas is heated are, besides the translational and rotational excitation, firstly excitation of the vibrational degrees of freedom of the molecules, secondly dissociation of the molecules into atoms, thirdly electronic excitation of the atoms, and finally ionization. However, as in our case the enthalpy increase is not too large, we need only expect vibrational excitation.

In order to achieve a new equilibrium among all degrees of freedom of the molecules several molecular collisions are needed. This number of collisions is different for each degree of freedom. The translational degrees of freedom obtain their share very quickly and arrive again at a Maxwell-Boltzmann distribution with only a few collisions. It is also known that the rotational degrees of freedom approach equilibrium with the translational energy very rapidly by means of several molecular collisions. This does not hold for hydrogen because its moment of inertia is smaller than that of other molecules and consequently the spacing between the rotational energy levels is larger. For this reason the rotational relaxation time of hydrogen is larger than that of other molecules. The relaxation times τ_t and τ_r for translation and rotation are for most gases of the order of 10^{-9} sec. or less.

So far the vibrational states of the molecule have not yet reached their final equilibrium states. The time necessary for these vibrational modes to attain equilibrium is known to be of the order of thousands of times that required for translation and rotation. Since the vibrational relaxation times are some orders of magnitude larger, we shall for our purpose consider translation and rotation as external degrees of freedom having no relaxation time associated with them.

The vibrational degrees of freedom of the molecule absorb their share of energy at the expense of the translational and rotational energies. Generally, during the period of excitation of the vibrations, the translational temperature will decrease toward an equilibrium value, which is, of course, also the equilibrium value of the vibrational temperature. However, as will be calculated in the next chapter, the flow speed decreases in the period of excitation and consequently extra kinetic energy is converted into thermal energy. Therefore it might be possible for the overall effect of exciting the vibrations to increase the temperature. It has been pointed out by Broer [28]) that this happens with sufficiently weak shock waves.

During the excitation the density will increase. At the same time the gas moves over a certain distance, which we shall call the transition zone of the vibrations. This density increase is studied in the present work.

4.3. Description of the instrument

The general principle of the system [29–30]) is illustrated in fig. 5, which

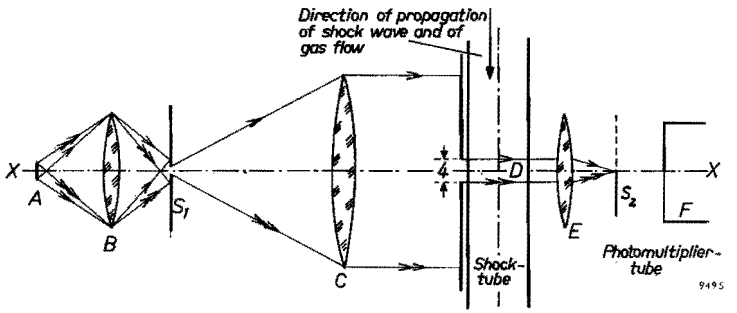

Fig. 5. Schematic representation of the experimental set-up for measuring density profiles by means of a uniform light beam parallel to the shock front. The explanation of the symbols used is given with fig. 6.

essentially reproduces the arrangement used by us. Light from a rectangular source A (we used a mercury arc lamp with its axis normal to the plane of the drawing) is focused on the slit S_1 by the lens B. The source slit S_1 has a length of about 20 mm and a width of about 0.2 mm. S_1 is in the focal plane of the lens C. The light passing through the region D of the shock tube is focused by the lens E on an inclined knife-edge S_2. If the inclined knife-edge S_2 is displaced so far that it just intercepts the rays forming the image of S_1, no light will reach the photomultiplier F. This holds when there are no gradients of the index of refraction in the gas traversed by the light beam. We neglect diffraction effects and assume that the lenses are of good optical quality (free from chromatic and spherical aberration and from astigmatism). On the other hand, if the gas is disturbed in the region D, for example by a shock wave, some of the light rays will be deflected, so that they may pass above the knife-edge S_2 and thus reach the photomultiplier F.

The windows in the shock tube consist of two plane-parallel plates, 2.5 cm thick and 1.8 cm in diameter. Since we require a rectangular beam of light to traverse the shock tube, there is a slit measuring 4 by 14 mm just outside the left-hand side window. The slit can be adjusted very accurately with a worm-wheel drive so as to make the long axis of the slit run parallel to the shock front.

The focal length of C is about 20 cm and its diameter 5 cm. The projection of the light rays through D in a plane normal to that of the drawing must be as parallel as possible. This can be achieved by reducing the width of S_1, the slit that represents our source. With such a set-up the maximum deviation is about 5×10^{-4} radians; we shall see that this will give us a negligible measuring error. The slit S_1 uses only a small part of the image of the light source and we can therefore work with light of a good uniform intensity across this virtual source.

Fig. 6 is a sketch of the set-up in the plane XX and perpendicular to the plane of fig. 5. PQ is the total length of slit S_1, our virtual source. It is seen that the

angle α subtended by half the length of the light source at the center of lens C is approximately 10/200 radians. Every point of the source slit gives a fan of rays which, after passage through the lens, form parallel beams making angles α' to the optical axis, where $0 < \alpha' < \alpha$. For a constant flux of light across the window it is necessary that every point of the window can be reached by all possible directions of light rays .Therefore the distance v between the shock tube and the lens C should not be too large, and its maximum value is given by $(25—7)/v = 10/200$, from which $v_{max} = 360$ mm.

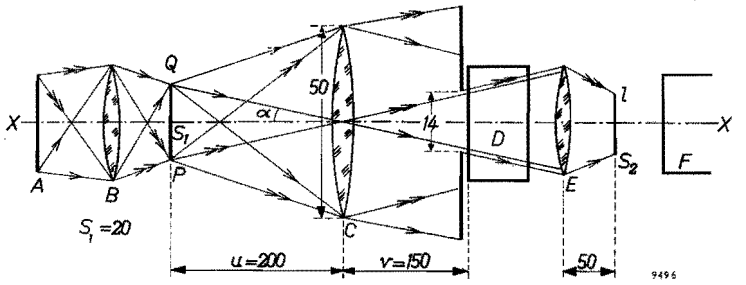

Fig. 6. A sketch of the set-up in the plane XX of fig. 5. Lens B produces a real image (S_1) of course A in the focal plane of lens C. D is the region of the shock tube traversed by the light beam. Lens E forms a real image (l) of S_1 at the inclined knife-edge S_2. F is the photomultiplier tube.

The diameter of lens E is large enough to catch all the light rays emerging from D. Its focal length is rather short, namely about 50 mm. This leads to a short image of the slit and makes it possible to use only a small part of the photomultiplier surface. We have found that not every point of the photomultiplier has the same sensitivity, and therefore we use only the central part, where the sensitivity is practically constant.

By moving a narrow slit of 1 mm width over the window of the shock tube and observing the voltage indicated by the photomultiplier, we have checked that the amount of light coming through the various points of the window is nearly constant, the maximum deviation being not more than 5 % of the average value.

We used a Du Mont photomultiplier, type 6292, which was adjusted so as to produce an output proportional to the amount of incident light. We used a Tektronix 545 oscilloscope which has high writing speeds and reproduces the incoming signals faithfully. If the photomultiplier tube is coupled to the oscilloscope by means of a cathode follower able to respond to pulses of 10^{-8} second, a time resolution of approximately 10^{-7} second is achieved.

The light source used was a General Electric BH-6 mercury arc, air cooled.

4.4. Analysis of the method

At the moment the shock wave is passing through the parallel light beam, the light is not only deflected by the density gradient just upstream from the shock front but also refracted by the discontinuity of density in the shock front. Refraction would not occur if we were dealing with a straight shock front, whose narrow thickness could not affect the light rays.

It is known that the interaction of the shock wave with the boundary layer on the wall of the shock tube (produced by the flow behind the shock) results in a small curvature of the otherwise straight shock front near the wall. This problem was studied theoretically by Hartunian [31]), who considered two-dimensional flow with a shock wave and a laminar boundary layer, and experimentally by Duff [32]). The former by using the linearized shock relations found for the shape of the shock wave

$$x_s = 2B_s \sqrt{y_s}, \tag{4.17}$$

where B_s is a complicated function of Mach number, Prantle number and viscosity, and x_s and y_s are the coördinates respectively along, and perpendicular to, the shock tube. For carbon dioxide we find from this equation $B_s = 0.024$.

Because of this curvature effect of the shock front, we have to deal with the oblique shock relations. However, we find the deviation of the average temperature of the gas behind the shock wave, compared with the calculated temperature obtained from the normal shock relations, to be so small as to be negligible. Therefore the properties of the gas behind the shock wave are described sufficiently well by the normal shock relations.

But, as we shall see in the next section, the results obtained with the integrated Schlieren method include the curvature effect. Fortunately, the length of this effect (maximum of x_s) is small compared with the transition zone. For carbon dioxide it is not more than 0.25 mm.

In this section we shall study the part of the optical signal that is only related to the density gradient of the gas as the result of vibrational excitation. We start our treatment with an exact determination of the path of a light ray in a medium in which the index of refraction varies in one dimension only (x-direction). The principle is illustrated in fig. 7. The light originally travels in the y-direction. Let us consider a small segment AB of the wave front of a deviated light wave which makes an angle of ϕ with the x-axis. If the refractive index at A is μ and at B is $\mu + \mathrm{d}\mu$, then after time Δt, the wave will have moved to the position $A'B'$, where

$$AA' = \Delta s = \frac{\Delta S}{\mu} \quad \text{and} \quad BB' = \frac{\Delta S}{\mu + \mathrm{d}\mu}.$$

Here $\Delta S = c\Delta t$ is the optical path of the wave front. Consequently

$$\Delta\phi = \frac{AQ}{AB} = \frac{\Delta S}{\mu}\,\frac{1}{\mu}\,\frac{\mathrm{d}\mu}{\mathrm{d}x}\cos\phi = \frac{1}{\mu}\,\frac{\mathrm{d}\mu}{\mathrm{d}x}\,\Delta y,$$

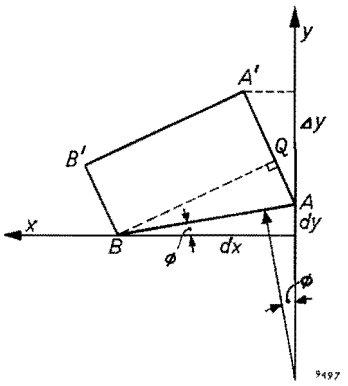

Fig. 7. The deflection of a light beam in a medium whose refractive index varies in the x-direction.

where $\Delta y = \Delta s \cos \phi$. It follows that the angle between the direction of the ray and the y coördinate is given by

$$\phi = \int_0^y \frac{1}{\mu} \frac{\mathrm{d}\mu}{\mathrm{d}x} \mathrm{d}y' . \tag{4.18}$$

The refractive index μ is related to gas density ρ by $\mu = 1 + \kappa\rho$, where κ is the Gladstone-Dale constant depending on the gas and on the wavelength. In most cases the value of $\kappa\rho$ is of the order of 10^{-4}. Therefore, we can take the factor $1/\mu$ in eq. (4.18) to be practically equal to unity.

Our purpose is to know how a density pattern will be recorded. Therefore it is sufficient, for the sake of simplicity, to assume an exponential density increase over the transition zone and see what happens to the recording. In fig. 8 the shock front DE is moving to the right. Downstream from the front (to the right

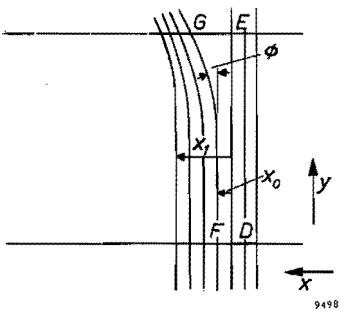

Fig. 8. The paths of light rays through the transition zone behind the shock front DE. The shock moves to the right and FG is an arbitrary ray at a distance x_0 behind the shock front.

in fig. 8) the gas still has its original density. The density behind the shock front DE (to the left in fig. 8) can then be represented by

$$\rho = \rho_s + \Delta\rho\,(1 - e^{-x/\lambda}), \tag{4.19}$$

where ρ_s, $\Delta\rho$ and λ are respectively the density just behind the shock front, the total density variation over the transition zone, and the relaxation distance. Along the light path FG of a ray coming into the transition zone at the point x_0, we have, by using eqs. (4.18) and (4.19),

$$\frac{\mathrm{d}\phi}{\mathrm{d}y} = \frac{\mathrm{d}\mu}{\mathrm{d}x} = \frac{\kappa\Delta\rho}{\lambda}\, e^{-x/\lambda}. \tag{4.20}$$

In practice ϕ is usually small and therefore equal to $\mathrm{d}x/\mathrm{d}y$ on GF. Hence eq. (4.20) becomes

$$\frac{\mathrm{d}^2x}{\mathrm{d}y^2} = \frac{\kappa\Delta\rho}{\lambda}\, e^{-x/\lambda}.$$

To solve this differential equation we multiply both sides by $2\,\mathrm{d}x/\mathrm{d}y$, integrate with respect to y and apply the boundary condition $\mathrm{d}x/\mathrm{d}y = 0$ at $y = 0$, for which $x = x_0$. We then obtain

$$\frac{\mathrm{d}x}{\mathrm{d}y} = (2\kappa\Delta\rho\, e^{-x_0/\lambda})^{1/2}\,(1 - e^{(x_0-x)/\lambda})^{1/2}.$$

This equation can be solved by making the substitution $w = \left\{1 - \exp\left(\frac{x_0 - x}{\lambda}\right)\right\}^{1/2}$ and applying the boundary condition $x = x_0$ for $y = 0$. We finally get the following expression

$$e^{-x/\lambda} = e^{-x_0/\lambda}\left[1 - \tanh^2\left\{\frac{y}{2\lambda}\,(2\kappa\Delta\rho\, e^{-x_0/\lambda})^{1/2}\right\}\right],$$

holding along FG. With the aid of this expression we can integrate eq. (4.20) in order to find the total deflection ϕ of a light ray passing through the disturbed region. We obtain

$$\phi = (2\kappa\Delta\rho\, e^{-x_0/\lambda})^{1/2} \tanh\left\{\frac{\mathrm{b}}{2\lambda}\,(2\kappa\Delta\rho\, e^{-x_0/\lambda})^{1/2}\right\}, \tag{4.21}$$

where b is the breadth of the shock tube.

Next, we consider the light coming in over the small region $\mathrm{d}x_0$. Part of this light will escape the inclined knife-edge and be caught by the photomultiplier, in an amount proportional to the angle ϕ. Consequently, if the disturbed region has advanced into the light beam to the point $x = x_1$, we get a signal on the oscilloscope screen equal to

$$\rho_{signal} = C \int_0^{x_1} \phi \, dx_o ,$$

where C is a proportionality constant determined by the properties of the instrument. By using eq. (4.21) we get

$$\rho_{signal} = \frac{4C\lambda^2}{b} \left[\log\cosh\left\{\frac{b}{2\lambda}(2\kappa\Delta\rho)^{1/2}\right\} - \log\cosh\left\{\frac{b}{2\lambda}(2\kappa\Delta\rho e^{-x_1/\lambda})^{1/2}\right\}\right]. \quad (4.22)$$

If we use the abbreviation $z = \frac{b}{2\lambda}(2\kappa\Delta\rho)^{1/2}$, the equation takes the form

$$\rho_{signal} = \frac{4C\lambda^2}{b} \left[\log\cosh(z) - \log\cosh(z\, e^{-x_1/2\lambda})\right].$$

The quantity z is usually small. In our experiments b = 18 mm; $\kappa = 2.31 \times 10^{-4}$ m³/kg; $\lambda \approx 0.5$ mm; $\Delta\rho \approx 0.48$ kg/m³ and consequently $z \approx 0.26$. It is therefore convenient to substitute an expansion of log cosh (z) in powers of z:

$$\log\cosh z = \frac{z^2}{2} - \frac{z^4}{12} + \frac{z^6}{45} - \quad . \quad (4.23)$$

By neglecting all terms but the first on the right-hand side of eq. (4.23) the relative uncertainty would be only 1 per cent for $z = 0.26$. By subsituting $\log\cosh(z) = z^2/2$ in eq. (4.22) the expression for the signals becomes

$$\rho_{signal} = C\, b\, \kappa\Delta\rho\,(1 - e^{-x_1/\lambda}). \quad (4.24)$$

On comparing eqs. (4.24) and (4.19) we notice that the signal received on the oscilloscope is proportional to the increase of the density distribution in the transition zone.

The relaxation length λ can be obtained from a picture of the signal. It is equal to the ratio of the final value of ρ_{signal}, which we call $\Delta\rho_{signal}$, to its derivative at the point $x = 0$. Using eq. (4.22) we derive

$$\frac{\Delta\rho_{signal}}{\left(\frac{d\rho_{signal}}{dx}\right)_{x=0}} = \lambda \frac{2\log\cosh z}{z\tanh z}. \quad (4.25)$$

The expression $\frac{2\log\cosh z}{z\tanh z} = \eta$ is plotted in fig. 9 and may be considered as a correction factor. In the range in which we made our observations the value of η was about 1.02.

Next we consider the effect of the inclination β of the knife-edge, which is shown in fig. 10. The optical system is arranged in such a way that we have

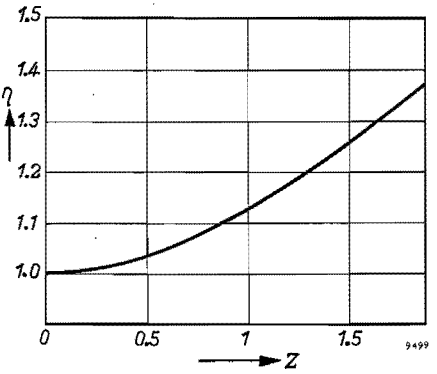

Fig. 9. Correction factor η as a function of $z = (b/2\lambda)(2\mu\Delta\rho)^{\frac{1}{2}}$.

the straight line l projected completely on the knife when there is no disturbance in the region D of the shock tube. The dotted line l' is the image of all light rays that in the transition zone have obtained a certain deflection ϕ (see fig. 8). The displacement δ in fig. 10 is proportional to ϕ. It is clear that the amount of light falling on the photomultiplier is proportional to y_o and that the lower part of l' is blocked out. Further, it is seen that $y_o = \delta \tan \beta$. Thus the sensitivity is determined directly by tan β. There is, however, a maximum for the

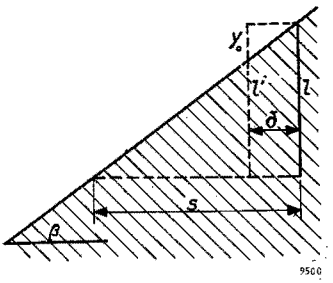

Fig. 10. The inclined knife-edge on which the light rays are focused as a straight line. The explanation of the symbols will be found on page 74.

angle β, given by the saturation of the system. Saturation means that some light is deflected so far that its image on the knife-edge is displaced over a distance δ that is greater than s. In that case there is, of course, no longer a definite relationship between the amount of light reaching the photomultiplier and the angle of deflection. The maximum deflection through the transition zone can be obtained from eq. (4.21). This is, for small values of z, equal to $b\kappa\Delta\rho/\lambda$. Then we get

$$s = \frac{b\kappa\Delta\rho}{\lambda} f_E, \tag{4.26}$$

where f_E is the focal length of lens E. From fig. 6 we see that

$$l = 2 f_E \alpha . \tag{4.27}$$

The magnitude of the maximum value of β can be obtained from the equation

$$\tan \beta_{\max} = \frac{l}{s} . \tag{4.28}$$

By using eqs. (4.26), (4.27) and (4.28) we derive for tan β the following condition

$$\tan \beta_{\max} = \frac{2 a \lambda}{b \kappa \Delta \rho} . \tag{4.29}$$

In some of our experiments $\Delta\rho$ was about 1.92 kg/m^3 and λ about 0.4 mm; consequently we find $\beta_{\max} = 80°$. Since the sensitivity was high enough for our purpose, we took for our measurements $\beta = 70°$ in order to obtain an easier adjustment of the image on the knife-edge.

The sensitivity of this method depends directly on the brightness B and the width d of the source slit. This, of course, requires as bright and uniform a light source as possible to start with. Lamps affording a line source are therefore superior to other types. There is a practical maximum for d, which is set by the required accuracy of the measurements. A relatively wide slit provides some deviation of the parallel light rays and produces an apparent shock thickness due to optical effects. This feature can be minimized by careful alignment of the optical system, and the apparent projection, due to this effect, of the shock front was of the order of $\frac{d}{u} \times b = \frac{0.2}{2 \times 200} \times 18 = 0.009$ mm; this is only 2% of the relaxation distance λ, which is 0.5 mm.

The signal is amplified in the photomultiplier and oscilloscope by a factor n, which is limited by the noise levels. Hence the final sensitivity is proportional to the following product:

$$\frac{n d B \kappa \Delta \rho b \tan \beta}{\lambda} .$$

If in this expression we substitute the value of tan $\beta_{\max}$, we find that the sensitivity is proportional to

$$n d B \alpha .$$

Thus we see that theoretically the sensitivity depends neither on the breadth of the shock tube nor on the density increase $\Delta\rho$, nor even on the relaxation distance λ, provided only that the knife-edge can be properly adjusted to $\beta_{\max}$. In principle the method will therefore retain its high sensitivity also for weak shocks.

When using carbon dioxide as our test gas we obtain traces of the kind shown in fig. 11. In the first part of the curve, AB, the signal rises as a straight line.

At the end of this part, indicated by B, we often found, especially at low densities, a discontinuity in the slope of the profile. We therefore incline to the opinion that the first part of the signal up to B, indicated by ζ, represents the curvature of the shock front. The upper part, indicated by $\Delta\rho_{signal}$ represents the density increase (behind the shock front) due to vibrational excitation. A justification for the above statements will be given in the next section.

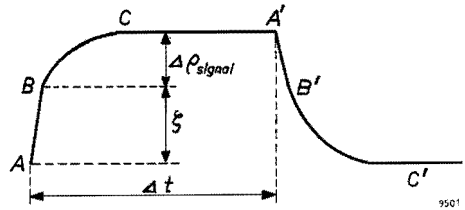

Fig. 11. A sketch of an oscillogram obtained with CO_2 as the test gas as described on page 76.

From the trace on the oscilloscope screen it is also possible to determine the Mach number of the shock. At the point A' of the trace, where the signal falls, the discontinuity in slope indicates that the shock front has left the light beam. Evidently the parts AC and $A'C'$ of the trace represent both the curvature effect and the density variation over the transition zone. The time required by the shock front to traverse the light beam is equal to Δt. In that time the front has moved over a distance m, equal to the slit width of 4 mm on the window. The shock velocity u_0 is equal to $m/\Delta t$. Thus the Mach number M_o of the shock is given by

$$M_o = \frac{m}{\Delta t\, c_o}, \tag{4.30}$$

where c_o is the velocity of sound in the test gas before the shock front.

4.5. Curvature effect of the shock front

Owing to the curvature of the shock front, part of the parallel light rays will cross the discontinuity surface and will consequently be refracted according Snell's law of refraction. In this section we shall therefore study the refraction of the light rays passing through the discontinuity of the shock front.

The first step in the treatment of this problem is to find an expression for the density distribution in the shock front.

As our observations are carried out over less than half the height of the shock tube and as the thickness of the boundary layer, which interacts with the shock front, is very small compared with the two dimensions of the cross-section of the tube, it may be reasonable to consider this problem only in the two dimensions of breadth and length of the shock tube.

For a two-dimensional oblique shock front the discontinuity conditions can be derived from the principles of the conservation of mass, momentum and energy, in about the same way as for the case of the straight shock front. The velocity components of the oblique shock are indicated in fig. 12.

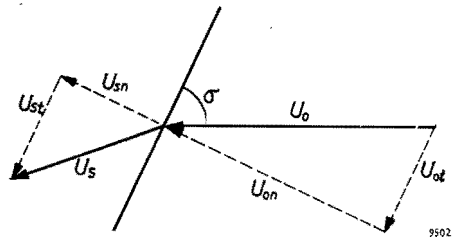

Fig. 12. The velocity components across an oblique shock (which represents an element of the curved shock front).

Mass: $$\rho_o u_{on} = \rho_s u_{sn}. \tag{4.31}$$

Momentum perpendicular to the surface:

$$\rho_o u_{on}^2 + p_o = \rho_s u_{sn}^2 + p_s. \tag{4.32}$$

Momentum parallel to the surface:

$$\rho_o u_{on} u_{ot} = \rho_s u_{sn} u_{st}. \tag{4.33}$$

Energy equation:

$$\frac{\gamma}{\gamma-1} RT_o + \tfrac{1}{2}(u_{on}^2 + u_{ot}^2) = \frac{\gamma}{\gamma-1} RT_s + \tfrac{1}{2}(u_{sn}^2 + u_{st}^2). \tag{4.34}$$

From eqs. (4.31) and (4.33) we find

$$u_{ot} = u_{st}.$$

By substituting this result in eq. (4.34) we get

$$RT_s = RT_o + \frac{\gamma-1}{2\gamma}(u_{on}^2 - u_{sn}^2).$$

This result when substituted in eq. (4.32) gives

$$\rho_o [u_{on}^2 + RT_o] = \rho_s [u_{sn}^2 + RT_o + \frac{\gamma-1}{2\gamma}(u_{on}^2 - u_{sn}^2)]. \tag{4.35}$$

Next we wish to express these quantities in terms of the shock strength parameter ε. From eqs. (4.3), (4.5) and (4.8) we derive

$$T_o = \frac{(1+\varepsilon)(1-\gamma\varepsilon)}{\gamma R} v_o^2.$$

The velocity components u_{on} and u_{sn} are given by

$$u_{on} = v_o (1 + \varepsilon) \sin \sigma$$

and

$$u_{sn} = v_o (1 + \varepsilon) \frac{\rho_o}{\rho_s} \sin \sigma.$$

If we substitute these expressions in eq. (4.35) we arrive at the density distribution along the shock front:

$$\rho_s = \rho_o \frac{1 + \varepsilon}{1 - \varepsilon + [2(1 - \gamma\varepsilon)/(\gamma + 1)] \cot^2 \sigma}. \tag{4.36}$$

When the light rays reach the discontinuity surface they will be refracted according to Snell's law. The refractive index μ is given by $\mu = 1 + \kappa\rho$. For low densities $\kappa\rho$ is of the order of 10^{-4}.

According to Snell's law

$$\frac{\sin \sigma'}{\sin \sigma} = \frac{1 + \kappa\rho_o}{1 + \kappa\rho_s}. \tag{4.37}$$

The angle of deflection of the light rays is given by ω, where

$$\omega = \sigma - \sigma'.$$

Eq. (4.37) reduces to

$$\cos \omega - \cot \sigma \sin \omega = 1 - \kappa (\rho_s - \rho_o). \tag{4.38}$$

The angle ω is very small, so that

$$\cos \omega \approx 1 \quad \text{and} \quad \sin \omega \approx \omega.$$

Along the shock front we have

$$\cot \sigma = \frac{\mathrm{d}x_s}{\mathrm{d}y_s}.$$

By substituting eq. (4.36) in eq. (4.38) we obtain

$$\omega = \kappa\rho_o \frac{2\varepsilon - [2(1 - \gamma\varepsilon)/(1 + \gamma)] \cot^2 \sigma}{1 - \varepsilon + [2(1 - \gamma\varepsilon)/(1 + \gamma)] \cot^2 \sigma} \frac{\mathrm{d}y_s}{\mathrm{d}x_s}. \tag{4.39}$$

After refraction at the shock front, the light rays are further deflected by the density gradient in the transition zone. However, this part of the deflection is generally less than 15% of the refraction across the shock front. Therefore, since we only study the qualitative effect of the curvature of the shock front on the method of recording, we shall only consider the refraction across the shock front.

The amount of light falling on the photomultiplier is proportional to ω.

Further, we call the part of the signal related to this curvature effect ζ. It is given by

$$\zeta = C \int_{x_{s,\min}}^{x_{s,\max}} \omega \mathrm{d}x \,. \tag{4.40}$$

Next we use the y-coördinate of the shock front and we find, by substituting eq. (4.39) in eq. (4.40),

$$\zeta = C\kappa\rho_o \int_{y_{s,\min}}^{y_{s,\max}} \frac{2\varepsilon - [2(1-\gamma\varepsilon)/(1+\gamma)]\cot^2\sigma}{1-\varepsilon+[2(1-\gamma\varepsilon)/(1+\gamma)]\cot^2\sigma}\,\mathrm{d}y_s \,.$$

The value of $\cot\sigma$ along the shock front can be obtained from eq. (4.17). It turns out that the factor $[2(1-\gamma\varepsilon)/(1+\gamma)]\cot^2\sigma$ is very small and approaches 2ε for very small values of y_s. Consequently, this factor may be neglected. The upper limit is given by half the breadth of the shock tube. We find

$$\zeta = C\kappa\rho_o \frac{2\varepsilon}{1-\varepsilon} \int_0^{b/2} \mathrm{d}y \,.$$

By using eq. (4.6) we finally obtain

$$\zeta = C\mathrm{b}\,\kappa\rho_s \frac{\varepsilon}{1+\varepsilon} \,.$$

Now, by comparing ζ with the magnitude of the signal that represents the total density increase (behind the shock front) due to vibrational excitation, as derived in eq. (4.24), we find

$$\frac{\Delta\rho_{signal}}{\zeta} = \frac{\Delta\rho}{\{\varepsilon/(1+\varepsilon)\}\,\rho_s} \,.$$

Fortunately, this ratio does not depend on the parameter B_s of the shock front (eq. 4.17), so that the result of this analysis is independent of the uncertainty concerning the shock front profile, provided that the shock front can be represented by a parabolic function. The above ratio is only a function of the Mach number. When using CO_2 we find, for $M_o = 3$,

$$\zeta = 1.2\,\Delta\rho_{signal} \,.$$

This result is in substantial agreement with the oscillographic observations of a shock wave in CO_2, as was pointed out in the preceding section.

4.6. Discussion

As the theoretical analysis of our method of shock-tube measurements is fully borne out by experimental observations, we feel that this method has been developed sufficiently to provide a faithful representation of the density pattern produced by vibrational excitation behind a shock wave. The technique, however, requires a great deal of attention being given to the proper optical alignment of the Schlieren system, to ensure that the light is of uniform intensity and that the light rays are parallel to the shock front. This is done by using helium as a test gas. Since helium is a monatomic gas and since the Mach numbers involved are low, relaxation phenomena need not be considered. Therefore, the only signal to be expected is related to the curvature effect of the shock front along the wall. The length of this effect can be minimized by making the light rays accurately parallel to the shock front. The minimum length of the curvature effect in helium is about 0.15 mm.

In attempting to understand this effect better we worked out a series of runs with Mach numbers between 1.5 and 2.5. In spite of the high sensitivity we could not correlate this effect with the Mach number. It seems to be more or less independent of the initial density of the gas, and also of the shock strength.

CHAPTER 5

EXPERIMENTAL RESULTS BEARING ON THE VIBRATIONAL EXCITATION OF CARBON DIOXIDE [33])

5.1. Introduction

The main purpose of our experiment was to try to establish the process in which translational and rotational energy is transferred to the vibrational degrees of freedom. This was done by using the shock wave technique described in chapter 4. This process, in which energy is supplied, by means of several elastic and inelastic collisions, to the various modes of vibration, can be studied in our experiment by measuring the density profile behind the shock wave as described in chapter 4.

We have already seen that for shock waves translational and rotational motion can be described by external degrees of freedom. Therefore we consider that the attainment of the final state takes place in two stages. In the first, or intermediate, stage just behind the shock front, the vibrational temperature is still equal to the gas temperature in front of the shock wave, while the translational and rotational temperature is that corresponding to the shocked gas without vibrational degrees of freedom; the latter temperature lies, for shock waves that are not too weak, above the final equilibrium value. In the second stage, which takes place in what has previously been called the transition zone, the vibrational energy, the pressure and the density increase and the temperature decreases, while at the same time the gas flow decelerates, until the equilibrium conditions of the gas are reached. This stage affords an opportunity to study the desired energy-transfer process. In such experimental study we neglect the energy associated with the asymmetric vibration, because this energy, at temperatures below 1000 °K, is less than 8 % of the vibrational energy of the other modes.

Since we are interested in the vibrational energy and since the density increase and the velocity of the shock wave are the only two quantities that are measured directly in our experiment, we want to express the vibrational energy in terms of the density variation. This can be done by using the conservation equations. From the measured density profile we shall then arrive at an energy profile expressed as a function of time.

In chapter 3 we calculated theoretically the probabilities of exciting the vibrations of carbon dioxide molecules through collisions. These calculations pointed to a direct excitation of the bending mode and an excitation in series of the valence mode, as described by eqs. (3.41c) and (3.71). The energy profile being known from the experiment, we can obtain the rate of energy transfer for any given time. If we now use the two predicted relaxation equations we can obtain the individual energy profiles of the two bending modes and of the

valence mode. In this way we may verify the theoretical predictions that have been worked out in chapter 3.

5.2. Formulae to obtain the vibrational energy and translational temperature as a function of time

It is convenient to consider the total energy E of the molecules as being made up of three parts:

$$E = E_{ex} + E_1 + E_2.$$

The first term, E_{ex} represents the energy of the external degrees of freedom (translation and rotation). E_1 and E_2 are the energies of respectively the symmetric valence and the bending vibrations. We can similarly write for the specific heats

$$\bar{C}_P = C_P + C_{vib}$$

and

$$\bar{C}_V = C_V + C_{vib},$$

where

$\bar{C}_P$ = specific heat at constant pressure,
C_P = specific heat of the external degrees of freedom at constant pressure,
$\bar{C}_V$ = specific heat at constant volume,
C_V = specific heat of the external degrees of freedom at constant volume,
C_{vib} = specific heat of the vibrational degrees of freedom.

With this notation the difference of the two specific heats becomes independent of C_{vib}, i.e. the vibrational energy now has no direct bearing on the work done in thermal expansion of the gas. The external degrees are fully excited even at room temperature to $\frac{1}{2} R$ per degree of freedom. The vibrational heat capacity C_{vib}, however, depends both on temperature and frequency. There are 5 external degrees of freedom, so we find $C_V = \frac{5}{2} R$. The gas densities in our experiments are low. Therefore they may be assumed to obey the equation of state of an ideal gas:

$$p = \rho RT. \tag{5.1}$$

Consequently we can derive $\bar{C}_P - \bar{C}_V = C_P - C_V = R$.

It is seen in fig. 13 that the variations of E_1 and E_2 with temperature are considerable. A relatively large part of the energy supplied from outside will go into the vibrations. The variations in the corresponding vibrational heat capacities are also large in the temperature region in which we are interested. It is therefore not possible to linearize the energy equations by taking C_{vib} as constant. Before expressing E_1 and E_2 in terms of the density variation, let us for convenience introduce some definitions. The equilibrium state of the gas

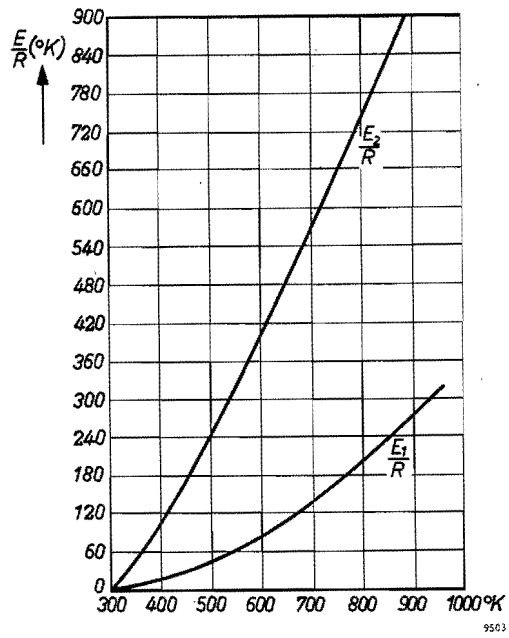

Fig. 13. Vibrational energy of the sum of the bending modes (E_2), and of the valence mode (E_1), relative to their values at room temperature.

before the passing of the shock wave is indicated with the subscript o and the state just behind the shock front, where translation and rotation are the first to reach equilibrium, with the subscript s. We indicate the variable state at any place behind the shock front with the subscript e. Since the translational and rotational modes are fully excited, it is clear that state s is reached in a process with constant specific heat. Therefore all the quantities in this state can be simply obtained from the Rankine-Hugoniot equations with $C_P/C_V = 1.4$. This is done by using the Mach number measured for the shock wave [34]). Knowing state s, we obtain the variable state e by applying the conservation equations relating to these states (we neglect friction effects and heat transfer with the wall over the small relaxation distance).

$$\text{Mass} \quad : \rho_o u_o = \rho_s u_s = \rho_e u_e = Q_m \tag{5.2}$$

$$\text{Momentum}: p_s + \rho_s u_s^2 = p_e + \rho_e u^2_e \tag{5.3}$$

$$\text{Energy} \quad : \tfrac{1}{2} u_s^2 + C_P T_s = \tfrac{1}{2} u_e^2 + C_P T_e + E_1 + E_2 \tag{5.4}$$

For the sake of simplicity we have taken the vibrational energy relative to its energy in state o. These equations are considered in a coördinate system moving with the shock front, so that the flow is reduced to a steady flow. From equations (5.1)-(5.4) we obtain for T_e, and for the sum of $E_1 + E_2$, the following relationships:

$$\frac{E_1+E_2}{R}=\frac{C_P}{R}\,T_s\left(1-\frac{\rho_s}{\rho_e}\right)+\frac{Q_m{}^2}{2\rho_s{}^2R}\left\{1-\left(\frac{\rho_s}{\rho_e}\right)^2\right\}-\frac{C_P}{R}\,\frac{Q_m{}^2}{R\rho_s{}^2}\left\{\frac{\rho_s}{\rho_e}-\left(\frac{\rho_s}{\rho_e}\right)^2\right\} \tag{5.5}$$

and

$$T_e=\frac{\rho_s}{\rho_e}\,T_s+\frac{Q_m{}^2}{R\rho_s{}^2}\left\{\frac{\rho_s}{\rho_e}-\left(\frac{\rho_s}{\rho_e}\right)^2\right\}. \tag{5.6}$$

The final equilibrium states of E_1 and E_2 are related to T_e by

$$E_1=RT_e\,\frac{h\nu_1/\mathrm{k}T_e}{\exp\,(h\nu_1/\mathrm{k}T_e)-1} \tag{5.7a}$$

and

$$E_2=2RT_e\,\frac{h\nu_2/\mathrm{k}T_e}{\exp\,(h\nu_2/\mathrm{k}T_e)-1}\,. \tag{5.7b}$$

The final equilibrium state will be obtained when ρ_e reaches its maximum value, called $\rho_{e,\max}$, so that eqs. (5.5), (5.6), (5.7a) and (5.7b) are satisfied. After we have found $\rho_{e,\max}$ in this way, we calculate $\Delta\rho_{\max}$ ($=\rho_{e,\max}-\rho_s$). This part is represented by BC on the oscillogram shown in fig. 11.

By comparing the maximum density increase on the oscillogram, $\Delta\rho_{signal}$, with the calculated one, $\Delta\rho_{\max}$, we find the scale factor of the measured profile. Hence we shall obtain values of $\Delta\rho$ at intermediate time intervals, so that we can work out $\rho_e=\rho_s+\Delta\rho$. For most calculations we used about 10 intermediate time intervals between the shock front and final equilibrium. To improve the accuracy of the measurements we made an optical enlargement of the transparency obtained from the oscilloscope, the magnification factor being 10.

Next we have to consider the time scale in our observations of the density. It is clear from the description of the experimental set-up that we are measuring the density profile behind the shock wave (whose velocity is u_o with respect to the gas in the initial state). If we consider the shock wave to be stationary, so that the gas in the initial state is imagined to travel towards the shock front with a velocity u_o, then we are in fact measuring the density profile at a speed of u_o. We want, however, to measure the time of the energy-transferring process in a coördinate system that is moving with the mean speed of the particles. This means that the actual time t is equal to $\int_0^{t'} u_o/u_e\,\mathrm{d}t'$, where t' is the recorded time; if $t'=0$, then the particles are at the shock front. Using eq. (5.2) we obtain

$$t=\int_0^{t'}\rho_e/\rho_o\,\mathrm{d}t'\,. \tag{5.8}$$

When by means of eqs. (5.5) and (5.8) we have arrived at the desired total energy

profile as a function of time, we can apply the predicted relaxation equations of (3.41c) and (3.71):

$$\frac{d(E_1 + E_2)}{dt} = \frac{1}{\tau_2} \{E_2(T_e) - E_2\} \tag{5.9}$$

$$\frac{dE_1}{dt} = \frac{1}{\tau_{12}} \{E_1(T_2) - E_1\} \tag{5.10}$$

the value of dE_3/dt being neglected on account of its small magnitude. Here $E_1(T_2)$ means the energy of the valence mode at the temperature of the bending modes, and $E_2(T_e)$ is the energy of the bending modes at temperature T_e.

Similarly by using eqs. (5.6) and (5.8) we obtain the translational temperature profile as a function of t.

5.3. Experimental results

With the aid of the derived equation we shall now calculate the individual energies E_1 and E_2. In eq. (5.10) dE_1/dt represents the rate at which energy is transferred to the valence modes. At $t = 0$, the vibrational modes are assumed to be in equilibrium, so that we obtain from eq. (5.10) $\left(\frac{dE_1}{dt}\right)_{t=0} = 0$.

For $t = 0$ we can calculate the energy $E_2(T_e)$ and measure the slope of the energy profile. E_2, which has been taken relative to its value at room temperature, is zero. For simplicity we shall divide the measured rate of energy transfer by the gas pressure. In this way, and by using eq. (5.9) we calculate τ_2 for atmospheric pressure as a function of the translational temperature. By making a series of runs with different Mach numbers we obtained the relaxation time τ_2 in the temperature range 440-816 °K. These values are found in table V and plotted in fig. 14; they are necessary for the calculation of the individual energy profiles.

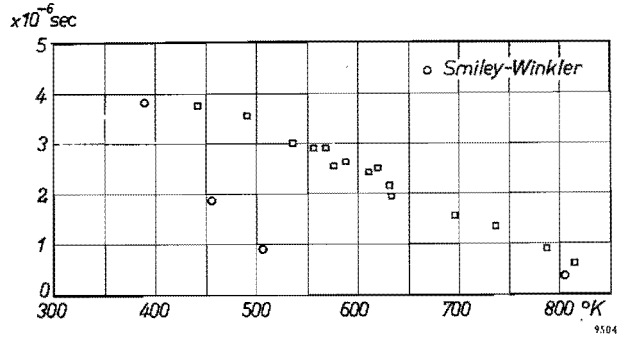

Fig. 14. Vibrational relaxation times of the bending modes as a function of the translational temperature.

Qualitatively, the present data compare quite well with those obtained by Smiley and Winkler [35]), who consider one relaxation time associated with the total vibrational energy. They found the density profile behind the shock wave by using the Mach-Zehnder interferometer.

TABLE V

M_o	p_o	T_s	$\rho_s/\rho_{e,\max}$	E_1/R	E_2/R	$\tau_2 \times 10^6$
1.75	0.967	441	0.868	17	122	3.74
1.96	0.766	490	0.847	25	168	3.36
2.13	0.466	533	0.828	34	208	3
2.23	0.526	556	0.823	40	233	2.9
2.27	0.55	568	0.816	45	254	2.9
2.29	0.260	574	0.813	48	267	2.55
2.31	0.408	588	0.809	51	276	2.63
2.42	0.379	618	0.798	56	294	2.43
2.42	0.450	618	0.798	56	294	2.50
2.46	0.277	630	0.795	58	308	2.13
2.46	0.340	630	0.795	58	308	1.94
2.68	0.258	697	0.781	78	374	1.52
2.83	0.287	734	0.767	89	415	1.36
2.95	0.132	786	0.754	105	469	0.93
3.04	0.195	816	0.748	116	500	0.64

Next we consider just one calculated energy profile, of which we know $E_1 + E_2$ and T_e at any instant. We measure at each point the rate of energy transfer and calculate $E_2(T_e)$. Then by using eq. (5.9) we obtain the value of E_2 at any instant, and from the sum we obtain also E_1. This procedure will be shown in the following two examples:

I. $\quad p_o = 100$ mm Hg; $\quad T_o = 300$ °K $\quad$ and $\quad M_o = 2.95$.

The Rankine-Hugeniot relationship gives

$$p_s = 1.31 \text{ kg/cm}^2; \quad \rho_s = 0.91 \text{ kg/m}^3; \quad T_s = 786 \text{ °K}.$$

We can satisfy eqs. (5.5), (5.6), (5.7a) and (5.7b) by substituting $\rho_s/\rho_e = 0.754$ and finding at thermal equilibrium $T_e = 636$ °K, $\dfrac{E_1 + E_2}{R} = 574$ °K. Furthermore we find $\rho_{e,\max} = 1.207$ and $\Delta\rho_{\max} = 0.297$ kg/m^3.

From the density profile we obtain 12 time intervals, and in table VI we have calculated the desired quantities. The energy profiles are shown in figs. 15 and 16.

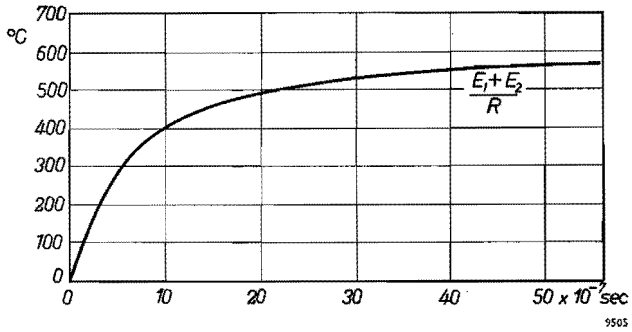

Fig. 15. The energy profile behind a shock wave, with $M_0 = 2.95$.

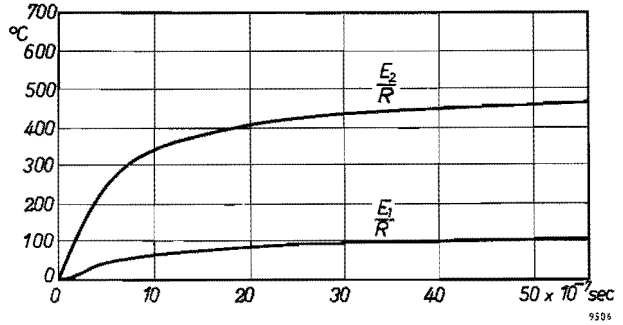

Fig. 16. The separate energy profiles of bending and valence modes behind a shock wave having a Mach number $M_0 = 2.95$.

TABLE VI

$10^7 t'$	$\Delta\rho$	ρ_s/ρ_e	$10^7 t$	T_e	$\frac{E_1+E_2}{R}$	$10^6 \frac{d}{dt}\left(\frac{E_1+E_2}{R}\right)$	$10^6 \tau_2$	$\frac{E_2(T_e)}{R}$	E_2/R	E_1/R
0	0	1	0	786	0	785	0.93	730	0	0
1	0.119	0.884	4.1	719	262	272	1.45	612	218	44
2	0.183	0.833	8.5	687	382	138	1.7	556	328	54
3	0.218	0.807	13.2	671	445	86	1.85	530	370	75
4	0.238	0.793	17.9	661	479	57	1.98	511	399	80
5	0.253	0.782	22.7	655	505	42	2.0	501	416	89
6	0.262	0.775	27.5	650	524	30	2.05	492	431	93
7	0.271	0.77	32.5	646	538	20	2.1	484	442	96
8	0.278	0.765	37.4	643	551	15	2.1	481	451	100
9	0.285	0.761	42.4	640	562	9	2.14	476	459	103
10	0.291	0.757	47.4	638	568	6	2.14	472	460	108
11	0.295	0.755	52.4	636	573	2	2.14	470	463	110
12	0.297	0.754	57.4	636	574	0	2.14	469	469	105

II. $p_0 = 148$ mm Hg; $T_o = 300$ °K and $M_o = 3.04$

$$p_s = 2.00 \text{ kg/cm}^2; \quad \rho_s = 1.363 \text{ kg/m}^3; \quad T_s = 816 \text{ °K}$$

We can satisfy eqs. (5.5), (5.6), (5.7a) and (5.7b) by substituting $\frac{\rho_s}{\rho_e} = 0.748$ and finding at thermal equilibrium $T_e = 655$ °K; $\frac{E_1 + E_2}{R} = 616$ °K. We also find $\rho_{e,\max} = 1.822$ and $\Delta\rho_{\max} = 0.459$ kg/m³. Next we obtained 8 time intervals from the density profile and calculated the desired quantities, which are set out in table VII. The energy profiles are shown in figs. 17 and 18.

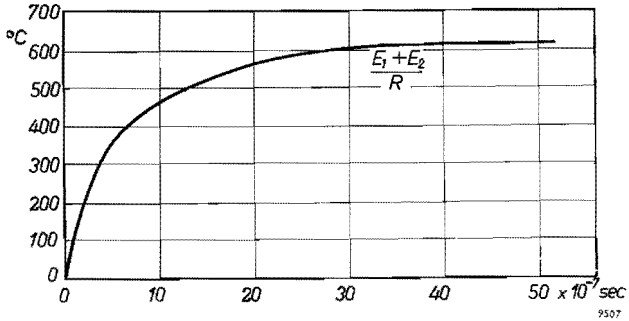

Fig. 17. The energy profile behind a shock wave, with $M_0 = 3.04$.

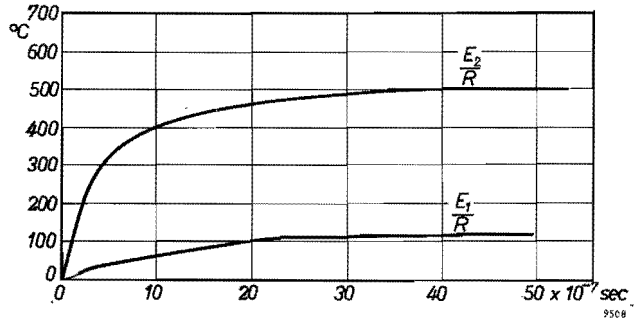

Fig. 18. The separate energy profiles of bending and valence modes behind a shock wave having a Mach number $M_0 = 3.04$.

The calculated values for E_1 and E_2 in tables VI and VII give us further information about the second relaxation equation.

TABLE VII

$10^6 t'$	$\Delta\rho$	ρ_s/ρ_e	$10^7 t$	T_e	$\frac{E_1+E_2}{R}$	$10^6 \frac{\mathrm{d}}{\mathrm{d}t}\left(\frac{E_1+E_2}{R}\right)$	$10^6 \tau_2$	$\frac{E_2(T_e)}{R}$	E_2/R	E_1/R
0	0	1	0	816	0	1190	0.64	783	0	0
0.5	0.16	0.895	2.1	754	245	398	1.17	673	211	34
1.5	0.28	0.830	6.6	711	406	150	1.55	596	363	43
2.5	0.34	0.80	11.3	692	481	85	1.7	563	419	62
3.5	0.386	0.780	16.2	677	534	51	1.85	539	444	90
4.5	0.420	0.765	21.2	667	572	32	1.90	523	463	109
5.5	0.448	0.754	26.3	659	599	10	1.95	509	488	111
6.5	0.456	0.751	31.5	656	611	2.5	2.0	504	499	112
7.5	0.459	0.749	36.5	655.5	614	1	2.0	502	500	114
8.5	0.460	0.748	41.5	655	616	0	2.0	500	500	116

5.4. Discussion

It is clear that the value of E_2 calculated from the measured derivative of the energy profile cannot be very accurate, because many observations and measurements are involved. Moreover the valence energy is much smaller than the bending energy, and by obtaining the former value from the sum, its relative uncertainty should be large. In spite of these experimental uncertainties we found in most calculations $E_1(T_2) > E_1$. Furthermore we generally saw that E_1 closely approached $E_1(T_2)$. On account of these uncertainties it was not possible to obtain reliable values for τ_{12}. However, we may conclude that the experimental results are in fair agreement with the theoretical predictions and that the second relaxation time of the indirect excitation is at least one order of magnitude smaller than the relaxation time of the direct excitation. In other words, the exchange of energy between the valence and the bending modes takes place very rapidly, compared with the exchange between bending and translational energy. This might be an explanation for the fact that many investigators could not find a second relaxation time in their observations of absorption and dispersion in ultrasonics.

The temperature range in which we have made our observations is limited by the following two considerations. For lower temperatures the valence mode is only weakly excited, so that the valence energy is relatively small compared with the bending energy. The specific heat at room temperature is for the valence mode 0.07 R and for the bending mode 0.9 R. Therefore these small valence energies cannot be found by our method. An upper limit of the temperature range is set by the fact that we always have to eliminate from the density profile the first steep part due to viscous effects at the wall of the shock tube. The higher

the temperatures, the smaller the relaxation distance; consequently we found it more difficult to separate these two parts.

Finally we will make some remarks on the purity of the gas. For our experimental observations we have used extra dry CO_2, supplied by the Southern Oxygen Company, with a purity of 99.84 %. It contained 0.03 % O_2 and 0.1 % N_2. The water content was stated as 20 parts per million. The leakage rate of the shock tube was less than 0.001 mm Hg per minute. The shock tube was usually fired within one minute after filling. Since the usual pressure of CO_2 was 100 to 700 mm before arrival of the shock, the total impurity level can have been increased by only 0.001 %. Moreover, it is most unlikely that these 10 parts per million consisted entirely of water, the only impurity known to have a large effect on the relaxation times.

APPENDIX I

Asymptotic value of f_{lk_o}

The general solution describing an incoming and an elastically scattered wave is of the form

$$R_{k_o} = \sum_l P_l(\cos\theta)\frac{1}{r} f_{lk_o}(r), \tag{I.1}$$

where f_{lk_o} is a bounded solution of eq. (3.7a).

Since the interaction potential tends to zero sufficiently rapidly as r tends to infinity, the bounded solution must at infinity have the form

$$f_{lk_o} \underset{r\to\infty}{\to} D_l \sin(k_o r - \tfrac{1}{2} l\pi + \delta_{lk_o}), \tag{I.2}$$

where D_l is an arbitrary constant and δ_{lk_o} is a phase shift. The term $\frac{1}{2} l\pi$ is added so that δ_{lk_o} vanishes if the interaction potential is zero.

The constant factor D_l in (I.2) must now be chosen so that R_{k_o} shall have the asymptotic form of

$$e^{ik_o z} + \frac{1}{r} g_o(\theta) e^{ik_o r}$$

In other words, D_l must be chosen so that

$$\sum_l P_l(\cos\theta)\frac{1}{r} f_{lk_o} - e^{ik_o z} \tag{I.3}$$

will represent the outgoing wave only.

We require an expansion of $e^{ik_o z} = e^{ik_o r\cos\theta}$ in Legendre polynomials

$$e^{ik_o r\cos\theta} = \sum_l (2l+1)\, i^l \left(\frac{\pi}{2k_o r}\right)^{1/2} J_{l+\frac{1}{2}}(k_o r)\, P_l(\cos\theta).$$

The Bessel function has the asymptotic form

$$J_{l+\frac{1}{2}}(k_o r) \underset{r\to\infty}{\to} \left(\frac{2}{\pi k_o r}\right)^{1/2} \sin(k_o r - \tfrac{1}{2} l\pi).$$

Substituting this result in (I.3) we find the asymptotic form of the elastic scattered wave as

$$\sum_l P_l(\cos\theta)\frac{1}{r}\left\{ D_l \sin(k_o r - \tfrac{1}{2} l\pi + \delta_{lk_o}) - (2l+1)\, i^l \frac{1}{k_o} \sin(k_o r - \tfrac{1}{2} l\pi)\right\}.$$

The two terms within the long brackets may be written as

$$\frac{1}{2i}\left[\left\{ D_l e^{i\delta_{lk_o}} - (2l+1) i^l \frac{1}{k_o}\right\} e^{i(k_o r - \frac{1}{2} l\pi)} - \left\{ D_l e^{-i\delta_{lk_o}} - (2l+1) i^l \frac{1}{k_o}\right\} e^{-i(k_o r - \frac{1}{2} l\pi)}\right].$$

This result, however, must represent an outgoing wave only. Therefore the second term must vanish. We find

$$D_l = \frac{1}{k_o}(2l+1)\, i^l\, e^{i\delta_{lk_o}}.$$

Substituting this in eq. (I.2), we find the asymptotic value of f_{lk_o} as

$$f_{lk_o} \underset{r\to\infty}{\longrightarrow} \frac{1}{k_o}(2l+1)\, i^l\, e^{i\delta_{lk_o}} \sin(k_o r - \tfrac{1}{2} l\pi + \delta_{lk_o}).$$

APPENDIX II

Maxwell-Boltzmann distribution for the valence vibrations

We wish to consider the distribution of the energy levels of excited symmetrical valence vibrations initially in equilibrium.

If we consider the first excitation process of the ν_1 vibration we find that the relaxation equation, in terms of the distribution of the energy levels, can be written as

$$\frac{dq_n}{dt} = \frac{1}{35} N_o P_e^2 \Big\{ q_{n-1} B_{n-1,n}^2 \sum_{m=0}^{\infty} \bar{q}_m C_{m,m-2}^2 + \bar{q}_{n+1} B_{n+1,n}^2 \sum_{m=0}^{\infty} q_m C_{m,m+2}^2 - q_n B_{n,n+1}^2 \sum_{m=0}^{\infty} \bar{q}_m C_{m,m-2}^2 - q_n B_{n,n-1}^2 \sum_{m=0}^{\infty} \bar{q}_m C_{m,m+2}^2 \Big\}, \quad \text{(II.1)}$$

where $\bar{q}_m$ is the fraction of modes with energy state m. The terms on the right-hand side are respectively: the number of molecules excited from state $(n-1)$ to state n, the number of molecules de-excited from state $(n+1)$ to state n, the number of molecules excited from state n to state $(n+1)$ and the number of molecules de-excited from the state n to state $(n-1)$.

Since the bending vibrations may be considered to have a Maxwell-Boltzmann energy distribution, we derive, by using eqs. (3.59a) and (3.59b):

$$\sum_{m=0}^{\infty} \bar{q}_m C_{m,m-2}^2 = C_{0,2}^2 \{\exp(h\nu_2/kT_2) - 1\}^{-2}$$

and

$$\sum_{m=0}^{\infty} \bar{q}_m C_{m,m+2}^2 = C_{0,2}^2 \{\exp(h\nu_2/kT_2) - 1\}^{-2} \exp(2h\nu_2/kT_2).$$

Furthermore we use eqs. (3.58a) and (3.58b) and find for eq. (II.1)

$$\frac{dq_n}{dt} = \frac{1}{35} N_o P_e^2 B_{0,1}^2 C_{0,2}^2 \exp(2h\nu_2/kT_2) \{\exp(h\nu_2/kT_2) - 1\}^{-2} [n \exp(-2h\nu_2/kT_2) q_{n-1} + (n+1) q_{n+1} - \{n + (n+1)\exp(-2h\nu_2/kT_2)\} q_n], \quad \text{(II.2)}$$

If we now substitute $2\nu_2 = \nu_1$ and, for the sake of simplicity, replace the first factor on the right-hand side of eq. (II.2) by Z, we obtain

$$\frac{dq_n}{dt} = Z\,[n \exp(-\theta_1)\, q_{n-1} + (n+1)\, q_{n+1} - \{n + (n+1) \exp(-\theta_1)\} q_n], \quad \text{(II.3)}$$

where $\theta_1 = h\nu_1/kT_2$.

If we next consider the other nine excitation processes for the symmetrical valence vibration we find, apart from a numerical factor, the same relaxation equation for the distribution of the energy levels.

When the integer n increases from zero to infinity, eq. (II.3) forms a set of differential difference equations describing the relaxation of the symmetrical valence vibrations.

The exact solution of equations of the type of eq. (II.3) has been obtained by Montroll and Shuler [22]) and is written in terms of a generating function:

$$G(z,t) = \sum_{n=0}^{\infty} z^n\, q_n(t)\,.$$

If the initial energies have a Maxwell-Boltzmann distribution, the generating function becomes

$$G(z,t) = \frac{(1 - e^{\theta_1})(1 - e^{-\theta_o})}{[(e^{-\tau} - e^{\theta_1}) + e^{(\theta_1 - \theta_o)}(1 - e^{-\tau})] + z\,[(1 - e^{-\tau}) - e^{-\theta_o}(1 - e^{(\theta_1 - \tau)})]}, \quad \text{(II.4)}$$

where $\tau = Zt(1 - e^{-\theta_1})$, and $\theta_o = h\nu_1/kT_o$ is associated with the temperature corresponding to the initial distribution.

From this generating function we obtain

$$q_n(t) = [1 - \exp(-\Theta)] \exp(-n\Theta)\,,$$

where

$$\Theta = \log\left\{\frac{e^{-\tau}(1 - e^{(\theta_1 - \theta_o)}) - e^{\theta_1}(1 - e^{-\theta_o})}{e^{-\tau}(1 - e^{(\theta_1 - \theta_o)}) - (1 - e^{-\theta_o})}\right\}.$$

In other words, the initial distribution of the symmetrical valence vibrations relaxes to a final energy distribution via a sequence of energy distributions, all of which obey a Maxwell-Boltzmann function. The effective temperature will change from T_o to T_2, the effective temperature of the bending vibration.

In a similar way we can prove that also during the excitation of the asymmetric valence vibrations the corresponding Maxwell-Boltzmann distributions persist.

REFERENCES

1) Landau, L., and Teller, E., Phys. Z. Sowjetunion, **10**, 34, 1936.
2) Tisza, L., Phys. Rev. **61**, 531, 1942.
3) Broer, L. J. F., Appl. sci. Res. **A5**, 55, 1954.
4) Zener, C., Phys. Rev. **38**, 277, 1931.
5) Herzfeld, K. F. and Litovitz, T. A., Absorption and Dispersion of Ultrasonic Waves Academic Press, New York, 1959.
6) Slawsky, Z. I., Schwartz, R. N. and Herzfeld, K. F., J. chem. Phys. **20**, 1591, 1952.
7) Schwartz, R. N. and Herzfeld, K. F., J. chem. Phys. **22**, 767, 1954.
8) Jackson, J. M. and Mott, N. F., Proc. Roy. Soc. London **A137**, 703, 1932.
9) Fricke, E. F., J. acoust. Soc. Amer. **15**, 22, 1943.
10) Pielemeier, W. H., J. acoust. Soc. Amer. **15**, 22, 1943.
11) Vigoureux, P., Ultrasonics, John Wiley and Sons, Inc., New York, 1951, p. 78.
12) Shields, F. D., J. acoust. Soc. Amer. **29**, 450, 1957.
13) Gutowski, F. A., J. acoust. Soc. Amer. **28**, 478, 1956.
14) Henderson, M. C. and Klose, J. Z., J. acoust. Soc. Amer. **31**, 29, 1959.
15) Dennison, D. M., Rev. mod. Phys. **3**, 280, 1931.
16) Schiff, L. I., Quantum Mechanics, Mc.Graw-Hill, New York, 1955.
17) Mott, N. F. and Massey, H. S., The Theory of Atomic Collisions, University Press Cambridge, England, 1952.
18) Bird, R. B., Hirschfelder, J. O. and Curtiss, C. K., Molecular Theory of Gases and Liquids.
19) Rossini, F. D., ed., Thermodynamics and Physics of Matter, Section H, Princeton Univ. Press, Princeton, New Yersey, 1955.
20) de Wette, F. W. and Slawsky, Z. I., Physica, **20**, 1169, 1954.
21) Jackson, J. M. and Howarth, A., Proc. Roy. Soc. **A152**, 515, 1935.
22) Montroll, E. W. and Shuler, K. E., J. chem. Phys. **26**, 454, 1957.
23) Witteman, W. J., J. chem. Phys. **35**, 1, 1961.
24) Bleakney, W., Weimer, D. K. and Fletcher, C. H., Rev. sci. Instr. **20**, 807, 1949.
25) Resler, E. L., Lin, S. C. and Kantrowitz, A., J. appl. Phys. **23**, 1390, 1952.
26) Courant, R. and Friedrichs, K. O., Supersonic Flow and Shock Waves, Interscience, New York, 1948.
27) Broer, L. J. F., Ned. Tijdschr. Natuurk. **20**, 205, 1954.
28) Broer, L. J. F., Appl. sci. Res. **A2**, 447, 1951.
29) Resler, Jr., E. L. and Scheibe, M., J. acoust. Soc. Amer. **27**, 932, 1955.
30) Witteman, W. J., Rev. sci. Instr. **32**, 292, 1961.
31) Hartunian, R. A., Phys. of Fluids, **4**, 1059, 1961.
32) Duff, R. E., Phys. of Fluids, **2**, 207, 1959.
33) Witteman, W. J., J. chem. Phys., **37**, 655, 1962.
34) Keenan, J. H. and Kay, J., Gas Tables, John Wiley and Sons, Inc., New York, 1948.
35) Smiley, E. F. and Winkler, E. H., J. chem. Phys. **22**, 2018, 1954.

SAMENVATTING

Wanneer aan een gas warmte wordt toegevoegd, zal deze warmte aanvankelijk alleen door de translatie en rotatie van de moleculen worden opgenomen. De translatie-energie is nu niet in evenwicht met de vibratie-energie van het gas. Dit evenwicht wordt hersteld tijdens moleculaire botsingen, wanneer energie tussen de verschillende vrijheidsgraden wordt uitgewisseld. De wijze waarop nu de moleculaire vibraties van koolzuurgas worden aangeslagen wordt hier behandeld. De thermische beweging van twee botsende moleculen wordt quantum-mechanisch behandeld, waarbij we gebruik maken van de methode van de gestoorde golven. Het blijkt dat tijdens het aanslaan van de buigingstrilling er een directe energie-uitwisseling met de translatie is, terwijl bij het aanslaan van de symmetrische en asymmetrische valentietrilling er een energie-uitwisseling tussen de vibraties onderling is.

De energie-overdracht tussen de verschillende vibraties zal niet uitsluitend binnen het molecule plaatsvinden, want er bestaan ook mogelijkheden dat dit kan gebeuren tussen verschillende moleculen. We vinden tien mogelijkheden voor de energie-overdracht aan de symmetrische valentietrilling en acht mogelijkheden voor de asymmetrische valentietrilling.

Nadat het aantal effectieve botsingen dat een molecule per seconde ondergaat is berekend, worden vervolgens de drie relaxatievergelijkingen voor de vibraties opgesteld. De bijbehorende relaxatietijden zijn berekend. Voor temperaturen beneden de 600 °K blijken de berekende en overeenkomstige experimentele relaxatietijden voor de buigingstrilling minder dan een factor twee te schelen. Dit is, gezien de beperkte kennis van de intermoleculaire potentiaal en andere benaderingen die in de berekeningen moesten worden gebruikt, een vrij goede overeenstemming.

Het blijkt, dat de op deze wijze gevonden relaxatievergelijkingen voor de vier vibratievrijheidsgraden van eenvoudige gedaante zijn. Zij bestaan slechts uit termen van de nulde en eerste orde, onafhankelijk van de energiesprong die de vibraties ondergaan. Tevens is hierbij gevonden, dat tijdens deze relaxaties de energie van iedere vibratie blijft voldoen aan de Maxwell-Boltzmann verdeling, waarbij de effektieve temperatuur variëert.

Experimenteel is deze energie-overdracht bestudeerd met behulp van schokgolven. De dichtheidsveranderingen achter het schokfront die het gevolg zijn van relaxaties zijn met de geïntegreerde Schlieren-methode gemeten. Deze optische methode is zodanig ontwikkeld dat de dichtheidsverandering over een bepaalde afstand nu direkt wordt gemeten. Uit de gevonden dichtheidsverandering kan het verloop van de vibratie-energie als functie van tijd en translatietemperatuur worden bepaald.

In het temperatuurgebied van 440 °K tot 816 °K bevestigen de gevonden resultaten een directe energie-overdracht tussen buigingstrilling en translatie en

een onderlinge uitwisseling van energie tussen buigings- en valentietrilling. De gemeten relaxatietijden voor de directe energie-overdracht variëren van 3.75 μ sec bij 440 °K tot 0.64 μsec bij 816 °K. De invloed van eventuele verontreinigingen, door het lekken van de schokbuis ontstaan, kan verwaarloosd worden.

De temperatuur van de gemeten energie voor de buigingstrilling ligt juist boven de overeenkomstige temperatuur van de energie voor de valentietrilling, hetgeen betekent dat de relaxatietijd voor het indirecte relaxatieproces minstens een factor 10 kleiner is dan de relaxatietijd van het directe relaxatieproces.

Wilhelmus Jacobus Witteman, geboren 12 december 1933, bezocht gedurende de jaren 1947-1952 de R.K. H.B.S. afd. B van het St.Janscollege te 's-Gravenhage. Hij liet zich in september 1952 aan de T.H. te Delft inschrijven. In april 1958 verkreeg hij het diploma van werktuigkundig ingenieur. Daarna was hij eerst als Fellow en later als Research Associate verbonden aan het Institute for Fluid Dynamics and Applied Mathematics van de University of Maryland (U.S.A.). Sinds januari 1961 is hij werkzaam op het Natuurkundig Laboratorium van de N.V. Philips' Gloeilampenfabrieken te Eindhoven.

STELLINGEN

I

Bij drie-atomige gassen met lineaire moleculen vindt de energie-overdracht tussen translatie en vibratie plaats via de slapste vibratie van het molecule.

Dit proefschrift, hoofdstuk III.

II

Het relaxatieproces voor de energie van een willekeurige vibratie van een drie-atomig gas met lineaire moleculen kan worden beschreven met de eenvoudige relatie

$$\frac{dE}{dt} = \frac{1}{\tau}\{E' - E\},$$

waarbij E' de energie van deze vibratie voorstelt bij een temperatuur die bepaald wordt door de vrijheidsgraden die aan deze vibratie energie overdragen.

Vergelijk dit proefschrift, hoofsdtuk III.

III

In de door Herzfeld gegeven quantum—mechanische berekening voor de gelijktijdige rotatie- en vibratie-overgangen van twee-atomige gassen wordt de foutieve veronderstelling gemaakt dat de diagonaal matrix elementen voor verschillende waarschijnlijkheidstoestanden aan elkaar gelijk zijn.

Karl F. Herzfeld and Theodore A. Litovitz, Absorption and Dispersion of Ultrasonic Waves, pag. 303 e.v. Academic Press New York and London (1959).

IV

Met behulp van de z.g. Schlieren methode kan langs optische weg de dichtheidsgradiënt van gasstromingen gemeten worden. Het is echter mogelijk om met deze methode bij niet stationnaire, één-dimensionale stromingen ook de grootte van de dichtheidsverandering over een bepaald gebied te meten.

Vergelijk dit proefschrift, hoofdstuk IV.

V

Het is bekend dat de toelaatbare axiale belasting van een rond staafje hardmetaal aanzienlijk verhoogd kan worden als dit hardmetaal voorzien is van krimpringen. De hoogst mogelijke krimpdruk wordt niet bepaald door de toelaatbare tangentiaalspanning in de krimpringen, zoals Christiansen, Kistler

en Gogarty menen, maar veel meer door de toelaatbare radiaalspanningen in de krimpringen.

E. B. Christiansen, S. S. Kistler and W. B. Gogarty, Rev. Sc. Instr. **32**, 775 (1961).

VI

Voor het bereiken van super hoge drukken is zowel de calibratie als de spanningstoestand van de gebruikte materialen bij de cilindervormige segmentenapparatuur gunstiger dan bij een tetraedrische apparatuur.

H. T. Hall, Rev. Sc. Instr., **29**, 267 (1958).

VII

De door Kao gegeven afleiding voor de mechanische krachten die in diëlectrische materialen kunnen ontstaan als gevolg van de electrische veldsterkte houdt geen rekening met de drukafhankelijkheid van de dielectrische constante.

K. C. Kao, Br. J. Appl. Phys. **12**, 629, (1961).

VIII

De wijze waarop Henderson en Klose gezocht hebben naar de aanwezigheid van meer dan een relaxatietijd voor de vibratie-energie van koolzuurgas sluit de mogelijkheid voor een energie-overdracht in serie uit.

M. C. Henderson and J. Z. Klose, J. Acoust. Soc. Amer., **31**, 29, (1959).

IX

Voor het fabriceren langs hydrothermale weg van grote synthetische kwartskristallen zonder barsten is het gewenst de entkristallen in een omgeving met voldoend kleine temperatuurgradiënt te plaatsen.

X

Een fundamentele vereenvoudiging van het systeem van aanslag regeling der inkomstenbelasting naar Amerikaans voorbeeld, inhoudende dat de belastingplichtigen in beginsel zelf hun belastingschuld vaststellen en dat de fiscus zich beperkt tot repressieve contrôle verdient veel aanbeveling.

Vergelijk pleidooi van de algemene vergadering van vereniging van inspecteurs van 's rijks belastingen 1962.
Weekblad voor fiscaal recht No 4608, 9 juni 1962.

XI

In tegenstelling tot sommige adviezen is het voor bestuurders van automobielen met voorwielaandrijving raadzaam om bij het begin van slip in bochten zoveel gas te geven dat het voertuig geen snelheid verliest.

Autokampioen, no 40, okt. 1962.

Dissertatie W. J. Witteman,
5 maart 1963.